

**INVESTIGATING  
THE ADHESIVE STRENGTH AND MORPHOLOGY OF  
POLYELECTROLYTE MULTILAYERS  
BY ATOMIC FORCE MICROSCOPY**

by  
Sena Ada  
A Thesis

Submitted to the Faculty of the  
WORCESTER POLYTECHNIC INSTITUTE  
in partial fulfillment of the requirements  
for the Degree of Master of Science  
in  
Chemical Engineering

---

August 25<sup>th</sup>, 2010

Approved:

---

Terri A. Camesano, Ph.D., Research Advisor  
Professor of Chemical Engineering  
Worcester Polytechnic Institute

---

David DiBiasio, Ph.D., Department Head  
Associate Professor of Chemical Engineering  
Worcester Polytechnic Institute

# Contents

---

## Contents

Contents.....	ii
List of Tables .....	v
List of Figures .....	vi
Acknowledgements .....	x
<b>1. Introduction .....</b>	<b>1</b>
<b>2. Literature Review .....</b>	<b>3</b>
2.1. The Polyelectrolyte Layer-by-Layer Assembly Technique: An overview of the field.....	3
2.2. Polyelectrolyte Multilayer (PEM) Thin Films .....	8
2.3. Interactions between PEM Covered Surfaces .....	10
<b>3. Chapter I : The Effect of Salt Type and Concentration on the Adhesive Strength and Morphology of Polyelectrolyte Multilayers .....</b>	<b>14</b>
3.1. Introduction .....	14
3.2. Materials and methods .....	16
3.2.1. Materials .....	16
3.2.2. Polyelectrolyte Film Formation .....	17
3.2.3. Adhesion Force Measurements .....	18
3.2.4. Roughness Measurements .....	19
3.3. Results and Discussion .....	20
3.3.1. Adhesive Strength of the PEM Thin Films .....	20
3.3.2. Roughness and Morphology of the PEM Thin Films .....	27
3.3.3. Relating Adhesive Strength and Roughness of the PEM Thin Films .....	31
3.4. Conclusions .....	32
<b>4. Chapter II : The Effect of Various Probes on the Adhesion Force Measurements .....</b>	<b>34</b>
4.1. Introduction .....	34
4.2. Experimental Section .....	36

# Contents

---

4.2.1. Formation of the PEM Thin Films .....	36
4.2.2. AFM Probes and Force Measurements .....	37
4.3. Results and Discussion .....	38
4.3.1. Probe Effect on the adhesion forces of PEI(PAA <sub>5</sub> PAH <sub>5</sub> ) .....	38
4.3.2. Probe Effect on the adhesion forces of PEI(PSS <sub>6</sub> PAH <sub>6</sub> ) .....	49
4.4. Conclusions .....	57
<b>5. Chapter III : Comparison of Adhesive Strength of Thin Films prepared via Different Techniques.....</b>	<b>58</b>
5.1. Introduction .....	58
5.2. Experimental Section .....	60
5.2.1. Materials .....	60
5.2.2. Layer-by-Layer Deposition Method .....	60
5.2.3. Grafting Method .....	61
5.2.4. AFM Force Measurements .....	61
5.3. Results and Discussion .....	63
5.3.1. Adhesive strength of thin films prepared by the LbL deposition method.....	63
5.3.2. Adhesive strength of thin films prepared by the grafting method .....	67
5.4. Conclusions .....	74
<b>6. Chapter IV : The Effect of Relative Humidity on the Adhesion Force Measurements .....</b>	<b>75</b>
6.1. Introduction .....	75
6.2. Experimental Section .....	76
6.2.1. Preparation of Samples .....	76
6.2.2. AFM Force Measurements .....	76
6.3. Results and Discussion .....	77
6.3.1. Effect of humidity on the adhesion forces of clean glass slides .....	77
6.3.2. Effect of humidity on the adhesion forces of PEI(PSS/PAH) .....	85
6.4. Conclusions .....	87
<b>7. Conclusions and Future Work .....</b>	<b>88</b>

# Contents

---

<b>8. References .....</b>	<b>92</b>
<b>9. Appendices .....</b>	<b>102</b>
Appendix A: Support File for Chapter I .....	102
Appendix B: Support File for Chapter II .....	104

## List of Tables

---

### List of Tables

<b>Table 3.1</b> Roughness (nm) of the PEM thin films as a function of salt type and concentration.....	28
<b>Table 4.1</b> Comparison of mean and normalized adhesion forces obtained with various probes .....	46
<b>Table 4.2</b> Comparison of mean and normalized adhesion force values obtained with various probes .....	56
<b>Table 5.1</b> Comparison of mean adhesion forces for the samples .....	67
<b>Table 5.2</b> Grafted thin films prepared with a different choice of PGMA grafting time and a polyelectrolyte for the subsequent grafting .....	68
<b>Table 5.3</b> Comparison of mean adhesion forces for PGMA series .....	72
<b>Table 6.1</b> Mean adhesion forces for PEI(PSS/PAH) at different humidity levels .....	86

## List of Figures

---

### List of Figures

<b>Figure 2.1</b> Number of publications on LbL self assembly in the first decade after it was developed by Decher et.al <sup>8,9</sup> .....	4
<b>Figure 2.2</b> Schematic of the Layer-by-Layer Deposition Process <sup>2</sup> .....	6
<b>Figure 2.3</b> Comparison of dipping (left) versus spray (right) methods <sup>20</sup> .....	7
<b>Figure 3.1</b> Structural formulas of the polyelectrolytes used in this study .....	17
<b>Figure 3.2</b> Adhesion forces as a function of salt type and concentration. The reported adhesion values are the average of fifty measurements between the PEM and a colloidal silica probe. Measurements were made in air at 45 % relative humidity .....	22
<b>Figure 3.3</b> Adhesion force distribution for PEI(PSS <sub>5</sub> PAH <sub>5</sub> ) as a function of salt type effect at an ionic strength of a) 0.5 M, and b) 1.0 M .....	24
<b>Figure 3.4</b> Adhesion force distribution for PEI(PSS <sub>5</sub> PAH <sub>5</sub> ) as a function of salt type effect at an ionic strength of a) 0.5 M, and b) 1.0 M .....	24
<b>Figure 3.5</b> AFM images of PEI(PSS <sub>5</sub> PAH <sub>5</sub> ) at an ionic strength of 0.5 M NaBr (top) and 1.0 M NaBr (bottom) The bars represent z-scale .....	30
<b>Figure 3.6</b> Adhesion forces versus RMS roughness for all systems .....	31
<b>Figure 4.1</b> Typical force-separation curve shown for the clarity of discussed terms such as range and magnitude of pull-off force and tip-sample separation .....	39
<b>Figure 4.2</b> Force-separation curves for PEI(PAA <sub>5</sub> PAH <sub>5</sub> ) prepared at 0.5 M NaCl. The measurements were collected at 45% RH with a colloidal silica probe. Ten force curves, five being from the same spot, were represented upon retraction .....	40
<b>Figure 4.3</b> Force-separation curves for PEI(PAA <sub>5</sub> PAH <sub>5</sub> ) prepared at 0.5 M NaCl. The measurements were collected at 45% RH with a colloidal silica probe functionalized with COOH surface chemistry. Ten force curves, five being from the same spot, were represented upon retraction .....	41
<b>Figure 4.4</b> Force-separation curves for PEI(PAA <sub>5</sub> PAH <sub>5</sub> ) prepared at 0.5 M NaCl. The measurements were collected at 45% RH with a PEI-PSS deposited colloidal silica probe. Ten force curves, five being from the same spot, were represented upon retraction .....	43

## List of Figures

---

<b>Figure 4.5</b> Probe effect on the approach curves for PEI(PAA <sub>5</sub> PAH <sub>5</sub> ) is represented with ten force curves for each probe, five being from the same spot, were represented. The measurements were collected at 45% RH .....	44
<b>Figure 4.6</b> Probe effect on the adhesion force distribution values for PEI(PAA <sub>5</sub> PAH <sub>5</sub> ). Each color stands for one type of probe. The measurements were collected at 45% RH.....	45
<b>Figure 4.7</b> Force-separation curves for PEI(PSS <sub>6</sub> PAH <sub>6</sub> ) prepared at 0.5 M NaCl. The measurements were collected at 45% RH with a colloidal silica probe. Ten force curves, five being from the same spot, were represented upon retraction .....	50
<b>Figure 4.8</b> Force-separation curves for PEI(PSS <sub>6</sub> PAH <sub>6</sub> ) prepared at 0.5 M NaCl. The measurements were collected at 45% RH with a colloidal silica probe functionalized with COOH surface chemistry. Ten force curves, five being from the same spot, were represented upon retraction .....	51
<b>Figure 4.9</b> Force-separation curves for PEI(PSS <sub>6</sub> PAH <sub>6</sub> ) prepared at 0.5 M NaCl. The measurements were collected at 45% RH with a PEI-PSS deposited colloidal silica probe. Ten force curves, five being from the same spot, were represented upon retraction .....	52
<b>Figure 4.10</b> Probe effect on the approach curves for PEI(PSS <sub>6</sub> PAH <sub>6</sub> ) is represented with ten force curves for each probe, five being from the same spot, were represented. The measurements were collected at 45% RH .....	53
<b>Figure 4.11</b> Probe effect on the adhesion force distribution values for PEI(PSS <sub>6</sub> PAH <sub>6</sub> ). The measurements were collected at 45% RH .....	54
<b>Figure 5.1</b> Comparison of typical force-separation curves of a)PEI-PGA-PAH, b)PDADMAC-PSS-PAH, c)PDADMAC <sub>5</sub> PAA <sub>5</sub> .....	64
<b>Figure 5.2</b> Adhesion force distribution for samples PEI-PGA-PAH, PDADMAC-PSS-PAH, and PDADMAC <sub>5</sub> PAA <sub>5</sub> . Fifty measurements were collected for each sample at 45% RH using a functionalized colloidal silica probe .....	65
<b>Figure 5.3</b> Comparison of typical force-separation curves of a) PEM thin film [PEI(PSS <sub>5</sub> PAH <sub>5</sub> ), 1.0 M NaCl], with problematic curves observed for PGMA series, b) PGMA 2 .....	70
<b>Figure 5.4</b> Adhesion force distribution for samples PGMA 1 through PGMA 6. Fifty measurements were collected for each sample at 45% RH using AFM and functionalized colloidal silica probe .....	71

## List of Figures

---

- Figure 6.1** Adhesion force distribution for a clean glass slide at 24% RH. Twenty-five force measurements were collected per experiment .....78
- Figure 6.2** Adhesion force distribution for a clean glass slide at 45% RH. Twenty-five force measurements were collected per experiment .....79
- Figure 6.3** Adhesion force distribution for a clean glass slide at 50% RH. Twenty-five force measurements were collected per experiment .....80
- Figure 6.4** Retraction curves of a clean glass slide at 24% RH. Ten out of twenty-five force measurements from each set of experiment were selected and compared by their retraction part. From one to ten, each force curve was represented with a different color. The order of representation of each color was same for each set of experiment, resulting the same color to be used three times .....82
- Figure 6.5** Retraction curves of a clean glass slide at 45% RH. Ten out of twenty-five force measurements from each set of experiment were selected and compared by their retraction part. From one to ten, each force curve was represented with a different color. The order of representation of each color was same for each set of experiment, resulting the same color to be used three times .....83
- Figure 6.6** Retraction curves of a clean glass slide at 50% RH. Ten out of twenty-five force measurements from each set of experiment were selected and compared by their retraction part. From one to ten, each force curve was represented with a different color. The order of representation of each color was same for each set of experiment, resulting the same color to be used three times .....84
- Figure 6.7** Adhesion force distribution for PEI(PSS<sub>20</sub>PAH<sub>20</sub>), PEI(PSS<sub>40</sub>PAH<sub>40</sub>), and PEI(PSS<sub>60</sub>PAH<sub>60</sub>) at a)28% RH, and b)42% RH. Each color represents different sample. Twenty-five measurements were obtained for each sample .....86
- Figure 9.1** Typical force-separation curves for PEI(PSS<sub>5</sub>PAH<sub>5</sub>) prepared at 0.5 M NaBr ionic strength a) retraction curves, b) approach curves .....102
- Figure 9.2** Force versus separation data for all the samples .....103
- Figure 9.3** Force-separation curves for PEI(PAA<sub>5</sub>PAH<sub>5</sub>) prepared at 0.5 M NaCl. The measurements were collected at 45% RH with a colloidal silica probe functionalized with COOH surface chemistry. This figure is zoomed-in version of Figure 4.3. Ten force curves, five being from the same spot, were represented upon retraction .....104

## List of Figures

---

**Figure 9.4** Force-separation curves for PEI(PSS<sub>6</sub>PAH<sub>6</sub>) prepared at 0.5 M NaCl. The measurements were collected at 45% RH with a colloidal silica probe functionalized with COOH surface chemistry. This figure is zoomed-in version of Figure 4.8. Ten force curves, five being from the same spot, were represented upon retraction .....105

## Acknowledgements

---

### Acknowledgements

I would like to express my great gratitude to my advisor Professor Terri A. Camesano for giving me the opportunity to work in her lab. I consider myself fortunate to have had such a rarely amiable and understanding advisor. Her guidance and support throughout this research were invaluable and meaningful to me. Thank you, Terri, for also giving me the opportunity to present our work at the conferences in New York, Hartford, San Francisco and Boston where I had great experiences.

I would also like to thank to our collaborators from Natick Soldier Research, Development and Engineering Center. Thank you, Ramanathan Nagarajan, it wouldn't be possible to complete this work without the helpful and fruitful discussions I had with you. Thank you, Stephanie A. Marcott, for your patience in answering all my questions.

I also give thanks to my labmates Kathleen Wang, Sophia D'Angelo, Ivan Enchev Ivanov, Yuxian Zhang, Paola Pinzon-Arango, Angela Tao, and former lab-mate Joshua Strauss.

I also want to give special thanks for the people who supported me during the last two years at WPI: Deniz and Cengiz Karakoyunlu, Ferit O. Akgul, the Ayturk family, the Akdemir family, the Padir family, J.R Courtman, Susan Eisnor, and Roland Nentwich. I was so lucky to have had your great friendship during my time at WPI.

I would like to acknowledge two special professors in the department of Chemical Engineering, Hacettepe University, Turkey. Thank you, Professor Serdar S. Celebi, for believing in me and making my dream possible: getting my Masters degree in USA. Thank you, Professor Erdogan A. Alper, for your advice and referral to WPI.

## Acknowledgements

---

I would like to dedicate this work to my beloved family. My parents Sevgi and Suleyman Ada, and my siblings Sibel and Sertan Ada: You are the most important reasons for happiness and success in my life. Without your encouragement, trust and love, I wouldn't be able to pursue my degree in USA.

Finally, I would like to thank to Brad Carleen for his support and patience in the past two years. Thanks for everything you have made for me; the life would be unbearably difficult and colorless without you.

## 1. Introduction

Polyelectrolyte multilayer (PEM) thin films prepared via Layer-by-Layer (LbL) deposition technique are of special interest in this research. The purpose of this study is to replace the current mechanical closure systems based on hook and loop type fasteners (i.e. Velcro) with PEM thin films. PEMs via LbL deposition technique have attracted attention since Decher and coworkers<sup>1, 2</sup> first introduced them in the early 1990s. The technique is simple, cheap, versatile and environmental friendly; as a consequence a variety of thin films can be easily fabricated. By proposing PEMs as non-mechanical and nanoscopic molecular closures, we aim to obtain hermetic sealing, good adhesive strength, and peel off ease.

We studied the adhesive forces of PEM thin films using atomic force microscopy (AFM) and colloidal silica probes. We performed the force measurements in air at a controlled humidity level. Each chapter discusses parameters that are important in the determination of adhesive strength.

In Chapter I, we investigated the effect of salt concentration and type on the adhesion forces, morphology, and roughness of the resulting PEM thin films. We conducted AFM measurements and imaging in air at ~45% relative humidity. PEI(PSS<sub>5</sub>PAH<sub>5</sub>) and PEI(PSS<sub>10</sub>PAH<sub>10</sub>) PEMs prepared from NaF, NaCl, and NaBr salts at 0.5 M and 1.0 M ionic strengths were studied. We hypothesized that the parameters used during the PEM construction were important to tune the properties of the resulting thin films.

In Chapter II, we studied the effect of probe chemistry on the adhesive forces of PEM thin films, namely PEI(PAA<sub>5</sub>PAH<sub>5</sub>) and PEI(PSS<sub>6</sub>PAH<sub>6</sub>). The interactions between a PEM-

## Introduction

---

covered surface and a probe of interest were investigated in a systematic way. The probes were a colloidal silica probe (unmodified), a colloidal silica probe functionalized with COOH surface chemistry, and a colloidal silica probe coated with PEI-PSS. While an unmodified colloidal silica probe was used for the quantification of interaction forces on the PEMs, modified colloidal silica probes were used to simulate PEM-PEM interactions.

In Chapter III, we expanded the scope of research using samples prepared by LbL deposition and grafting methods. For this reason, we used different types and combinations of polyelectrolytes than we studied in previous chapters. We performed AFM force measurements with a colloidal silica probe functionalized with COOH at 45% RH. The adhesive strengths of LbL deposited PEMs and grafted films were compared.

In Chapter IV, we aimed at showing the effect of relative humidity (RH) on the adhesion forces. This chapter provides validation as to why we performed adhesion force measurements at ~45% RH. It was important to determine the working conditions and be systematic while conducting AFM force measurements in air since capillary force effects and static charging can be significant at certain RH values. Clean glass slides were used and force measurements were made at different humidity levels; both adhesion force distribution and retraction curves helped to determine the best RH conditions. In addition, PEI(PSS<sub>x</sub>PAH<sub>x</sub>) PEMs, where x was varied as 20, 40, and 60, were also studied at different humidity levels and a comparison was made.

## 2. Literature Review

### 2.1. The Polyelectrolyte Layer-by-Layer Assembly Technique: An overview of the field

The modification of surfaces is of great interest for controlling the adhesion between substrates. Surface modification of substrates can be utilized through several methods. Layer-by-Layer (LbL) deposition method is one of the most promising and versatile methods. Thin films prepared via LbL method have overcome Langmuir-Blodgett (LB) films<sup>3</sup>: LB technique has some limitations such as substrate size, film quality and stability. Furthermore this technique requires special equipment. As an alternative to the LB technique, chemisorption from solution is also not a great technique, since both of those methods are limited to certain class of molecules.

In 1966, Iler<sup>4</sup> proposed the layer-by-layer deposition of charged colloids to build-up multilayer films. This pioneering work led to the development of the research field of polyelectrolyte multilayer thin films. However, due to a lack of sensitive surface characterization techniques, the detailed study of such assemblies could not be done and the technique was neglected. In the beginning of 1990s, Decher and coworkers<sup>1, 5</sup> demonstrated the feasibility of the layer-by-layer deposition of charged amphiphiles and polyelectrolytes, which led to thin polyelectrolyte multilayer (PEM) films. Since then, the technique progressed rapidly<sup>6-8</sup> (Figure 2.1).

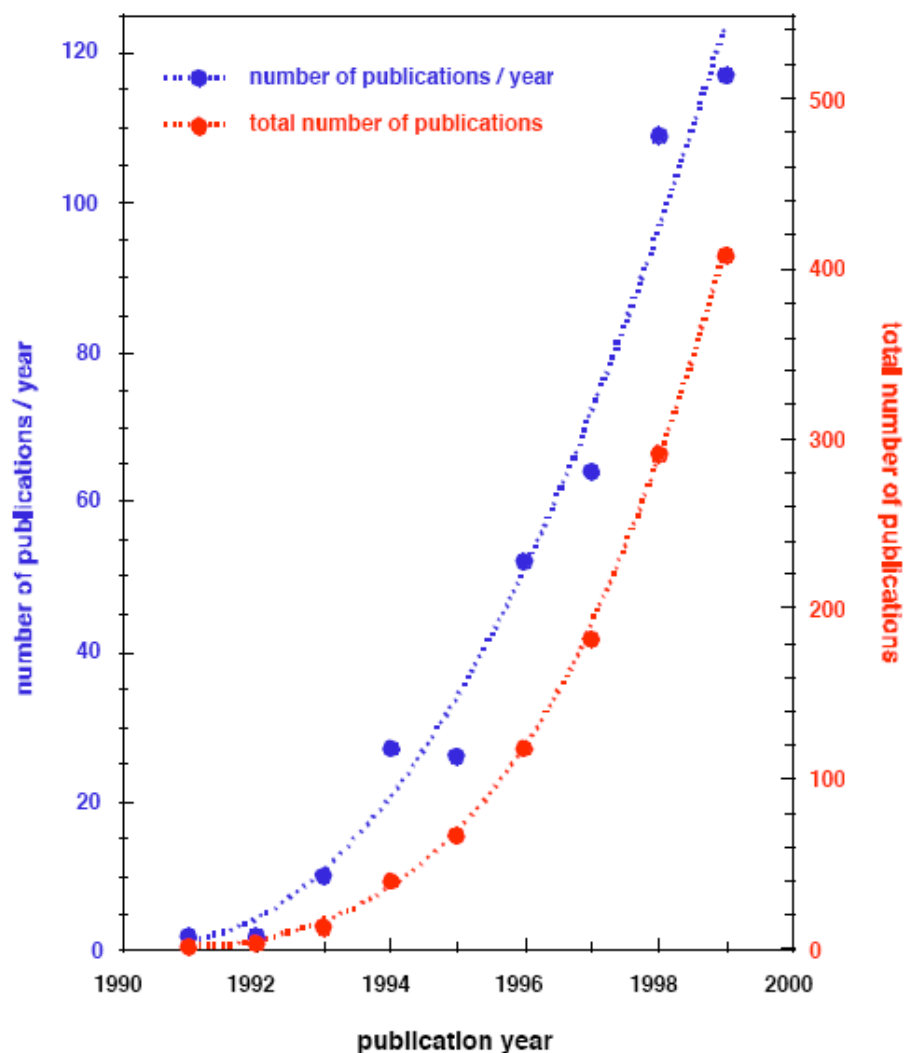


**Figure 2.1** Number of publications on LbL self assembly in the first decade after it was developed by Decher et.al.<sup>8,9</sup>

Figure 2.1 demonstrates how the field rapidly expanded in the first decade. It was not surprising to observe this rapid progress in the field considering the simplicity and versatility of the technique. Schlenoff<sup>10</sup> has recently written a perspective for the future of this field and has had a very important remark: the field is mushrooming rather than maturing due to the

## Literature Review

---

incorporation of various materials such as dendrimers, colloids, carbon nanotubes, and viruses in the construction of multilayers.

Polyelectrolytes (PEs) are the most widely studied materials in the LbL method. They are commonly used as additives to control colloidal stability and adhesive properties of surfaces.<sup>11</sup> An example for the latter case can be found in the application of paper making, as cationic polyelectrolytes help increase the dry strength of paper, serving as retention aids.<sup>12</sup>

Other materials can be used for creating LbL self assembly structures, including colloidal particles,<sup>13</sup> biopolymers<sup>14, 15</sup> (such as peptides, proteins, etc.), carbon nanotubes,<sup>16</sup> and microgels.<sup>17</sup> By incorporating a variety of materials into the fabrication of thin films via LbL technique, highly tuned films with controllable composition, structure, and thickness can be created. Another advantage of the LbL method is that the shape of the substrate does not matter. Thin films can be built-up on colloidal particles<sup>18, 19</sup> as well as flat substrates.<sup>1</sup>

A depiction of the LbL method on the glass substrate can be seen in Figure 2.2. Polyelectrolyte multilayers (PEMs) are fabricated via LbL deposition method which is the immersion of a substrate into oppositely charged polyelectrolyte solutions alternatingly. Between each PE deposition layer, a rinsing step takes place, which helps remove weakly bounded polyelectrolytes on the surface. Rinsing is also important to prevent the contamination of the subsequent PE solution by adhered PEs from the previous PE solution. Usually, after each rinsing step, drying is also applied prior to the subsequent PE formation on the surface.

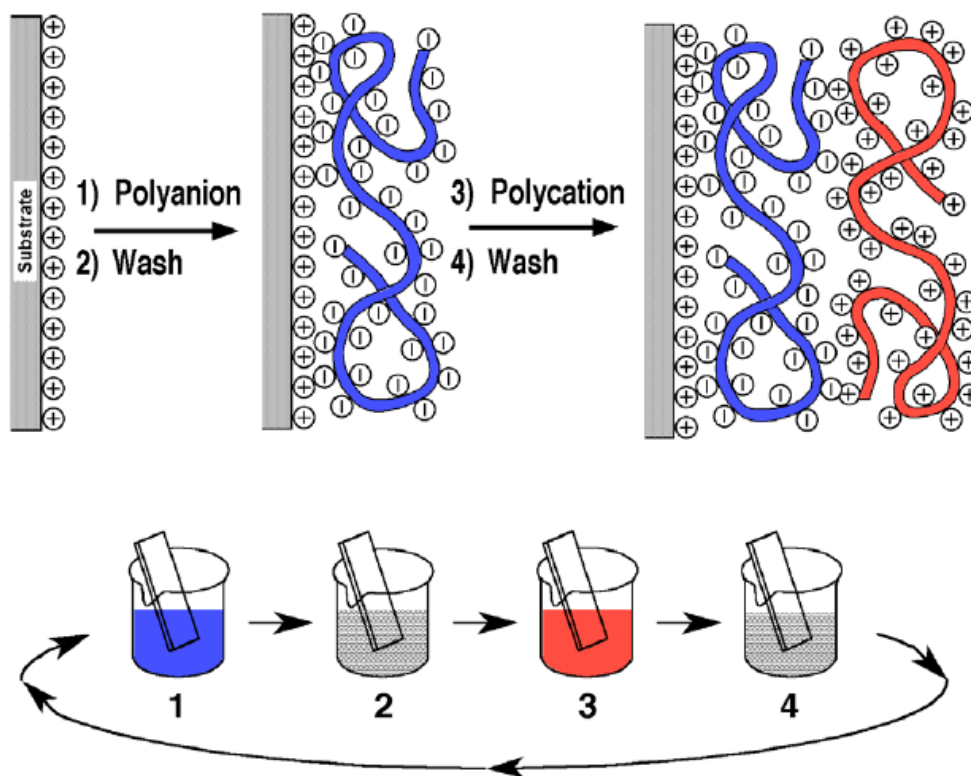


**Figure 2.2** Schematic of the Layer-by-Layer Deposition Process.<sup>2</sup> a) The molecular representation shows how polyanion and polycation are adsorbed on the positively charged substrate. Blue is used for polyanion chains while red is used for polycation chains. b) Immersion of positively charged substrate into polyanion and polycation solutions, respectively, with an intermittent rinsing step.

PEMs are fabricated by dipping, either manually or with an automated device. Nowadays, the studies with spray deposition are of great interest since the fabrication of thin films in this technique is much faster compared to those made by dipping (Figure 2.3).<sup>20-22</sup> The

## Literature Review

studies are aimed at proving that PEM thin films are stable when they are prepared via spray deposition; as a consequence, spraying can replace dipping.

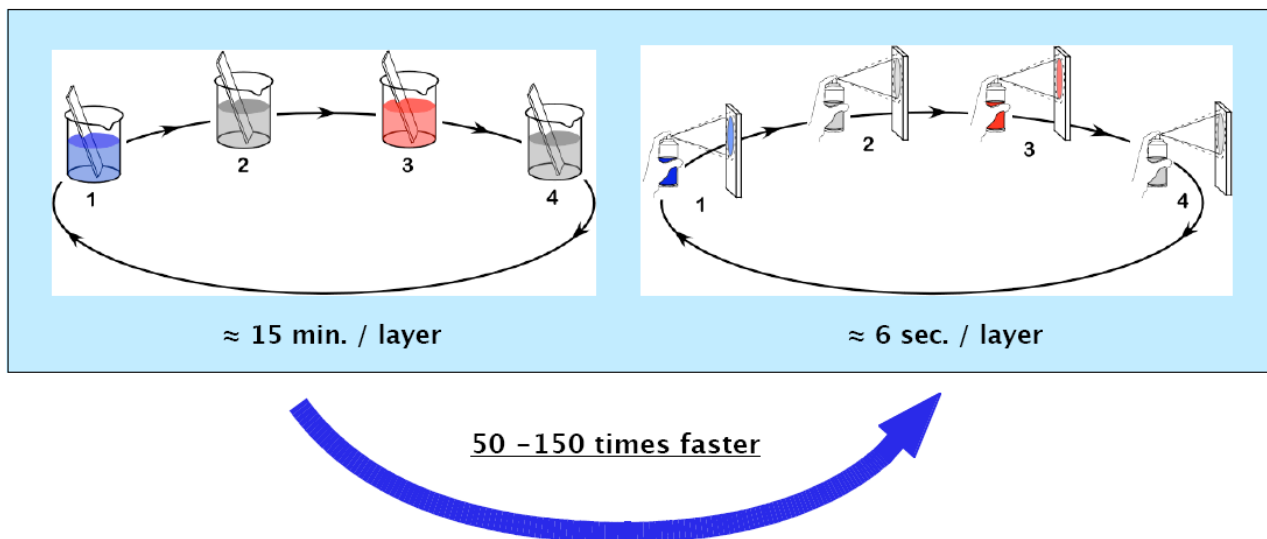


**Figure 2.3** Comparison of dipping (left) versus spray (right) methods.<sup>20</sup>

Since the polyelectrolyte layer-by-layer assembly technique is environmentally friendly, inexpensive, simple, and versatile due to adaptability to a large number of surfaces, it could be used in various fields. The technique has been extensively investigated for various applications in electrical,<sup>23, 24</sup> optical,<sup>25</sup> and biomedical devices.<sup>26, 27</sup> To name some examples, contact lenses,<sup>7</sup> sensors,<sup>28</sup> electrochromic films,<sup>29</sup> conductive layers,<sup>30</sup> and non-linear optical devices<sup>31</sup> can be given. As it is obvious, the technique can be used on both surface modification and fabrication of thin film devices.

### 2.2. Polyelectrolyte Multilayer (PEM) Thin Films

PEM thin films have been studied by several techniques such as ellipsometry, X-ray reflectivity, quartz-crystal microbalance (QCM), atomic force microscopy (AFM), and surface force apparatus (SFA), etc.<sup>7, 32-35</sup>

The parameters used during the build-up process are very important and they can be used to tune the properties of the desired film. The choice of polycation/polyanion pair, pH of the solution,<sup>32, 36-38</sup> ionic strength,<sup>33, 39, 40</sup> solvent quality,<sup>33, 41</sup> molecular weight of polyelectrolytes,<sup>35, 36</sup> and dipping time<sup>42</sup> are among those several parameters that govern the properties of PEMs. The conformation of the polyelectrolyte chains in solution is assumed to be preserved during the PEM formation and this conformation determines the internal structure of the deposited multilayer. For instance, when the PE solutions are prepared at high salt concentrations, thicker and rougher films are obtained, which is the result of coiled conformation of PE chains at this high ionic strength.<sup>37</sup> A detailed review can be found elsewhere that discusses the internal structure and dynamics of PEMs as well as their functional properties.<sup>43</sup>

The heterogeneity of the substrate plays an important role in the PEM deposition. Trybala et al.<sup>39</sup> studied the deposition of PSS/PAH on various substrates. For this reason, polished and unpolished silica, polished and electrochemically passivated titanium, polished and unpolished surgical stainless steel were used. They concluded that relatively higher amount of polymers adsorbed at heterogeneous surfaces.

The properties of the PEMs are dependent on the substrate features at the very first deposition layers. Above a minimal number of layers, which are called ‘precursor’ layers, the properties of the system are independent of the underlying substrate and governed by the choice

## Literature Review

---

of polycation/polyanion pair, as well as the deposition conditions. At the precursor layer regime, the properties of the system such as thickness and roughness are different than the so called 'true multilayer regime'. This fact was shown by several researchers.<sup>35, 44</sup> M. Kolasinska et al.<sup>35</sup> showed that the increase of PAH/PSS film thickness with the number of deposition layers were smaller for the first six layers than the layers comprising the rest of the system. While the thickness per layer for the first six layers was 0.5 nm, it was 1.1 nm for the subsequent layers. This result was in agreement with the zone model proposed by Ladam et al.,<sup>44</sup> in which the multilayer structure is divided into three zones. The first zone is adjacent to the substrate where thinner layers are observed. The second zone is the real bulk film and the third one is closest to the air.

Furthermore, several researchers conducted studies on poly (ethyleneimine) (PEI), which is the most studied polyelectrolyte (PE) as a precursor layer.<sup>35, 39, 45</sup> PEI serves as an anchoring layer and helps to obtain homogenous and smoother films. Of special importance, PEI is also intensively used in pharmaceutical formulations, personal care products, household and industrial detergents.<sup>46</sup> The effect of PEI on the built up of PEMs was shown in one of the studies where the multilayers prepared with PEI as the first layer were much less rough than those having the same number of layers but without an anchoring layer.<sup>35</sup> In addition, Bosio et al.<sup>45</sup> showed that without a PEI precursor layer, the adhesion forces between the surfaces were affected by the heterogeneity of the substrate in the very first layer depositions.

The effect of PEI as a precursor layer was also shown on the tapping mode AFM images.<sup>45</sup> When only two layers of PAH/PSS was deposited without PEI, some holes were observed in the size of around 300-400 nm which was about 10 times larger than the typical contact radius of a colloidal probe. The holes disappeared when the more layers were deposited

and no holes existed if PEI-precoated surfaces were used for the deposition treatment. Furthermore, the films without PEI were significantly rougher than the films with PEI-precoated. The root mean square (rms) of a film (four layers) with PEI was ~ 0.5 nm while it was ~3.0 nm for the same film without PEI.

### **2.3. Interactions between PEM Covered Surfaces**

The majority of studies on the adhesive forces of PEMs were conducted using the surface force apparatus (SFA) and atomic force microscopy (AFM). One of the first studies on the interactions between polyelectrolyte coated surfaces was carried out by Lowack and Helm using SFA.<sup>40</sup> One can find an information on the current understanding of interactions between surfaces coated with polyelectrolytes in a review, where various surface force techniques were reported.<sup>47</sup>

AFM is a powerful technique for probing the interactions between various surfaces. From the force-distance curves, the pull-off force or called adhesion force is obtained which gives information about the adhesive strength.<sup>48</sup> Furthermore, colloidal probes are ideal candidates to be used with AFM to investigate the molecular interactions. The principles of the colloidal probe technique with an overview on the adhesion force measurements can be found elsewhere.<sup>49</sup> By this technique, the interactions between a bare or modified colloidal probe and a planar surface can be studied. The importance of modified colloidal probes comes from the fact that those are helpful on the investigations where i.e. polymer coated surfaces are of interest. It is also worth to

## Literature Review

---

note some comprehensive overviews by Drelich et al.,<sup>50</sup> Capella et al.,<sup>48</sup> and Butt et al.<sup>51</sup> on the adhesion force measurements with AFM.

In the literature, the studies on the interactions between PE coated surfaces can be grouped as symmetrical and asymmetrical systems. The interactions between identical charges are named as symmetrical, such as the studies of Bosio et al.<sup>45</sup> and Johansson et al.<sup>52</sup> On the other hand, the study of Gong et al.<sup>53</sup> is an example of an asymmetrical system where the interactions between oppositely charged surfaces were probed. Some of the studies will be briefly overviewed here.

Johansson et al.<sup>52</sup> studied the symmetrical system formed from PAH and PAA on silica surfaces and mica, at a low ionic strength (0.01 M NaCl). They investigated the effect of molecular weight and contact time, using SFA and AFM under both dry and wet conditions. From the AFM measurements in a liquid cell, they observed greater pull-off force adhesion when PAH was formed on the outermost layer. The same phenomenon was also shown in a study conducted by Notley et al.<sup>34</sup> In addition, when low molecular weight ( $LM_w$ ) polyelectrolyte combinations were used, the pull-off forces were greater than those for high molecular weight ( $HM_w$ ) combinations. This observation was a contrary to what Creton et al.<sup>54</sup> suggested. However, Johansson et al.<sup>52</sup> made a strong interpretation on this result. Higher pull-off forces in the case of  $LM_w$  polyelectrolyte combinations were attributed to the higher mobility of chain ends, which would diffuse across the interface and form entanglements; and also to the increased contact area due to the compression of easily deformable  $LM_w$  PEMs at a given load. The pull-off force for ( $PAH_6PAA_5$ ) formed from  $LM_w$  polyelectrolytes was 6 mN/m at a contact time of 5 s while it was 3.5 mN/m for the  $HM_w$  combination at the same conditions. From the SFA measurements, they found that the adhesion forces between two bare mica substrates under dry

## Literature Review

---

conditions were decreased when the mica was coated with PEMs. At 100% relative humidity (RH), the adhesive strength was higher for the PEM covered surfaces compared to those obtained under dry conditions, and a rapid decrease in adhesion forces was observed when the wet conditions were used.

Another study on symmetrical systems was conducted by Notley et al.<sup>34</sup> who studied the interactions between PAH/PAA pair using QCM-D and AFM. They investigated the pH effect on the growth behavior of PEMs deposited at 0.01 M NaCl ionic strength on two silica surfaces; silicon wafer and colloidal silica probe. They investigated the pull-off forces under wet conditions and they found that the pull-off force was greater when PAH was adsorbed on the outermost layer. They interpreted this result as PAH being less rigid and easily penetrating across the interface which in turn leads to an increased adhesion between the PEMs. The normalized pull-off force values were approximately 2.2 mN/m for PAH<sub>6</sub>PAA<sub>6</sub> and 3.8 mN/m for PAH<sub>6</sub>PAA<sub>5</sub>. The stronger adhesive pull-off force stemmed from the more conformable and looser structure of the multilayer when PAH was deposited on the outermost layer.

On the other hand, Gong et al.<sup>53</sup> studied an asymmetrical system. The interactions between a glass sphere and PEMs formed from PSS/PAH and DNA/PAH on the glass substrates were investigated using AFM in liquid. This study differed from the other studies where the interactions between two PEM covered surfaces were investigated. When PAH was deposited on the outermost layer, they did not observe any adhesion force between the glass sphere and the negatively charged PEM surface. They observed strong adhesion forces when PAH served as an outermost layer due to the interactions between the oppositely charged surfaces and possible entanglements of the polyelectrolyte chains that form a bridge between the glass particle and multilayer. The magnitude of the pull-off forces was lower for PSS/PAH than those for

## Literature Review

---

DNA/PAH. For PEI(PSS<sub>5</sub>PAH<sub>5</sub>), the pull-off force was roughly 0.18 mN/m while it turned out to be roughly 5.0 mN/m when PSS was replaced by DNA. The difference on the magnitude of adhesion forces was related to different surface morphologies of the resulted films and bridging of the polyelectrolyte chains. Moreover, the pull-off forces differed qualitatively, too; they obtained multiple adhesion peaks, which they referred to as the so called 'sawtooth pattern', for PSS/PAH, and a larger single adhesion peak for DNA/PAH.

Adhesion forces are strongly dependent on environmental conditions. The adhesive strength obtained in a liquid environment or in air can differ. Studies in air must be performed carefully due to the existence of capillary forces. Even though capillary effects become strong at higher humidity levels, one should be always careful about adjusting the humidity in the work environment. For instance, at too low RH, static charging can also be a problem.

### 3. Chapter I: The Effect of Salt Type and Concentration on the Adhesive Strength and Morphology of Polyelectrolyte Multilayers

#### 3.1. Introduction

Polyelectrolyte multilayer (PEM) thin films have attracted attention since they were introduced by Decher et al.<sup>1, 2</sup> in the early 1990s. These films are prepared by so called layer-by-layer (LbL) deposition, which is the consecutive immersion of the substrate into oppositely charged polyelectrolyte solutions. The LbL deposition technique is an efficient method for surface modification and obtaining multilayered thin films with a controllable thickness at the angstrom level. The technique and its applications have been extensively investigated.<sup>7, 28, 55</sup>

For the LbL deposition technique, any charged surface can be used as a substrate. A wide variety of substrates were used such as SiO<sub>2</sub>, quartz, glass, titanium plates, charged colloids, and polymers. Different from the conventional substrates that are inorganic, it is possible to find studies on a variety of polymers such as poly (propylene), poly (styrene), etc.<sup>56</sup> Chen and McCarthy<sup>57</sup> applied LbL deposition on chemically modified and unmodified PET substrates, such as on neutral (PET), negatively (PET-CO<sub>2</sub><sup>-</sup>) and positively charged (PET-NH<sub>3</sub><sup>+</sup>) substrates .

The parameters that govern the properties of the PEMs are the choices of polycation/polyanion pair, ionic strength,<sup>33, 39, 40</sup> solvent quality,<sup>33, 41</sup> molecular weight of polyelectrolytes,<sup>35, 36</sup> pH of the solution,<sup>32, 36-38</sup> and dipping time.<sup>42</sup> The conformation of the polyelectrolyte chains in solution is assumed to be preserved during the PEM formation and this

conformation determines the internal structure of the deposited multilayer. From this point of view, the parameters used during the build-up process can be used to tune the properties of the desired film. A detailed review can be found elsewhere that discusses the internal structure and dynamics of PEMs as well as their functional properties.<sup>43</sup>

The deposition of the first layer is very important during PEM formation. Due to the heterogeneities of the substrate, the properties of the film are affected, where the film can be treated independent of the substrate only after a certain numbers of the deposition layers or by a certain choice of the first deposition layer. Poly (ethyleneimine) (PEI) is the most studied polyelectrolyte (PE) as a precursor layer<sup>35, 45</sup>, which helps to obtain homogenous and smoother films starting from the first layer. Bosio et al.<sup>45</sup> showed that not only morphology and thickness are altered, also adhesion between the surfaces are affected in the prior to ‘true’ multilayer regime. Without a PEI precursor layer, the adhesion forces were influenced by the heterogeneity of the substrate, such that even between same charged PEs, a strong adhesion was observed. The adhesion disappeared with the addition of layers when the ‘true’ multilayer regime was reached.

Thus far, the interactions between PEM covered substrates and a colloidal particle or two PEM covered surfaces were investigated with the surface force apparatus (SFA) and atomic force microscopy (AFM). One of the first studies on the interactions between polyelectrolyte coated surfaces were carried out by Lowack and Helm using SFA.<sup>40</sup> In the present study, we used AFM and colloidal probe microscopy. The principles of the colloidal probe technique with an overview of adhesion force measurements can be found elsewhere.<sup>49</sup> The studies investigating the interactions and adhesive properties of the thin films have mainly used silicon wafer, glass, or mica as a substrate. In this work, poly (ethylene terephthalate) (PET) which is a thermoplastic

was used as a substrate, different from conventional inorganic supports. PET has been previously used as a substrate on which the LbL technique was investigated.<sup>56, 57</sup>

There are numerous studies on the self-assembly and growth mechanism of polyelectrolytes, whereas studies on the interactions between polyelectrolyte coated surfaces are scarce. Bosio et al.<sup>45</sup> (2004) and Gong et al.<sup>53</sup> (2005) have also pointed out this gap in their studies. The present study attempts to fill this gap using AFM and colloidal probe microscopy. We prepared the thin films of PEI(PSS/PAH) at 5 and 10 bilayers with NaCl, NaBr and NaF salts at 0.5 M and 1.0 M concentrations, for the purpose of investigating the role of salt type and ionic strength on the adhesion properties, morphology and roughness of these films. The interactions between positively charged outermost layer of PEMs and negatively charged probes were studied. While force measurements and roughness measurements gave quantitative results, imaging of the samples indicated some information about the morphology.

## 3.2. Materials and methods

### 3.2.1. Materials

For the preparation of PEM thin films, poly(ethyleneimine) (PEI, 50 % w/v,  $M_w$  of 600-1000 kg/mol) and poly(allylamine hydrochloride) (PAH,  $M_w \sim 70$  kg/mol) as polycations and poly(sodium 4-styrenesulfonate) (PSS, 30 % w/v,  $M_w \sim 200$  kg/mol) as a polyanion were used (Figure 3.1). The salts used during the build up process were NaCl (purity  $\geq 99.0$  %), NaF ( $M_w$  of 41.99 g/mol), and NaBr ( $M_w$  of 102.89 g/mol). All the polyelectrolytes and salts were purchased from Sigma-Aldrich, except NaBr from J.T. Baker. MilliQ reversed osmosis water (purity 18.2

ohms.cm) was used during multilayer deposition. Poly(ethylene terephthalate) (PET) film (Melinex S/142 Gauge) was used as the substrate, purchased from DuPont Teijin Films.

Two different types of AFM probes were used for the purposes of adhesion force measurements and imaging. Colloidal silicon AFM probes (1  $\mu\text{m}$   $\text{SiO}_2$  particles) functionalized with COOH surface chemistry, spring constant of 14 N/m, were purchased from Novascan Technologies, Inc. Regular silicon cantilevers (Asylum Research, manufacturer Olympus®) with a spring constant of 42 N/m were used for only imaging while the colloidal probes were used for adhesion force measurements.

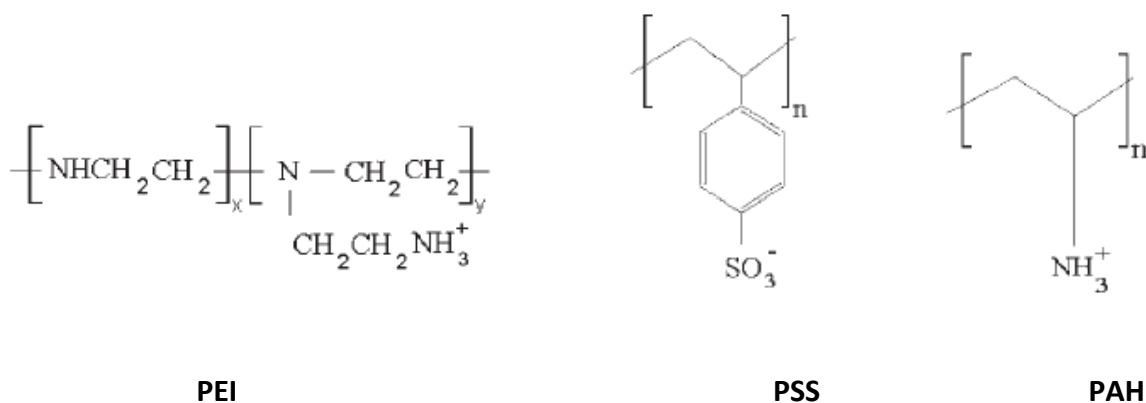


**Figure 3.1** Structural formulas of the polyelectrolytes used in this study.

### 3.2.2. Polyelectrolyte Film Formation

The LbL deposition technique was applied to prepare the PEM thin films. HMS™ Series Programmable Slide Container (Carl Zeiss, Inc.) was used for dipping. Prior to multilayer deposition, PET films were air plasma-treated (PDC-32G, Harrick Plasma Cleaner) for 20 minutes to improve surface coverage and enhance adhesion between surfaces. The preparation of

films was initiated by immersing the substrate into PEI solution followed by consecutive adsorption of oppositely charged polyions from their solutions (30 minutes each). The concentration of PE solutions was  $1 \text{ mg mL}^{-1}$ , containing  $0.5 \text{ M NaCl}$ .<sup>53</sup> Between each deposition layer, the films were rinsed twice with water for 2 minutes each and later dried in air for 10 minutes. The washing steps are helpful to stabilize the weakly adsorbed polymer layer.<sup>2</sup> The repetition of deposition of PEs was continued until the desired number of layers was obtained. For the investigation of salt type effect, PE solutions were prepared with either NaF or NaCl or NaBr at ionic strengths of  $0.5 \text{ M}$  and  $1.0 \text{ M}$ .

### 3.2.3. Adhesion Force Measurements

Adhesion forces were quantified with an AFM, NanoScope IIIa (Dimension 3100, Veeco Metrology Inc., Santa Barbara, CA), by using intermittent contact mode in air. Fifty force measurements were taken from each sample. For increased accuracy, five repeat measurements were taken from each location. By moving the cantilever to ten different locations on the sample in both x and y directions, fifty measurements were obtained. The raw force curves were processed with the assistance of self-written MATLAB® and Microsoft Excel scripts. Humidity control played an important role in these experiments because the measurements were taken in air. For all the experiments, the relative humidity (RH) was set to  $\sim 45\% \text{ RH}$  where it is safe to be away from capillary force effects.<sup>58, 59</sup>

### 3.2.4. Roughness Measurements

Sample morphology and roughness were investigated via another AFM, (MFP-3D™, Asylum Research, Santa Barbara, CA), by using intermittent contact mode in air. The images were taken with a scan size of 5 μm × 5 μm. The scan rate was kept constant at 1.0 Hz. A high resolution of 512 × 512 data points was acquired. All the images were flattened by applying a 1<sup>st</sup> order flattening. The roughness was analyzed on at least two independent samples with 5 equally divided areas on each (having the number of measurements to be at least 10). A box size of 1 μm × 1 μm was used to quantify the roughness. Standard deviation values were obtained from all the measurements.

The root-mean-square (rms) of the films was calculated using the Igor Pro 6 software, according to:

$$\text{rms of Y values} = \left( \sqrt{\frac{1}{V_{\text{npnts}}} \sum Y_i^2} \right) \quad (3.1)$$

where  $Y_i$  is the height value and  $V_{\text{npnts}}$  is the number of points for the defined area.

## 3.3. Results and Discussion

### 3.3.1. Adhesive Strength of the PEM Thin Films

In our study, the adhesion forces between oppositely charged surfaces were investigated by colloidal probe technique via AFM. A colloidal probe functionalized with a negative surface chemistry was used to quantify the interactions between the probe and the positively charged PEM in the outermost layer. To the best of our knowledge, this is the first study investigating the role of salt type and ionic strength on the adhesive strength of PEM covered PET substrates.

The studies investigating the interactions between charged surfaces can be grouped as symmetrical (same charged surfaces) and asymmetrical (oppositely charged surfaces) systems. Bosio et al.<sup>45</sup> and Johansson et al.<sup>52</sup> studied symmetrical systems comprised of PSS/PAH and PAH/PAA, respectively. Our system is asymmetrical because the interactions between the surfaces of interest are oppositely charged.

Independent of the deposition number, salt type and ionic strength, we observed only one single sharp peak for the pull-off force upon the retraction curves (Figure 9.1). This result is in agreement with an earlier study<sup>53</sup> where the interactions between a glass sphere and positively charged multilayer formed from DNA/PAH were investigated and only a large single adhesion peak was observed. In that same study,<sup>53</sup> when DNA was replaced by PSS, the behavior of the adhesion peaks changed from a single adhesion to multiple adhesions. The ‘sawtooth pattern’, as this was called, was attributed to bridging between the negatively charged glass sphere and positively charged polymer. The difference between those adhesion peak behaviors were attributed to the bridging and structure and morphology of the multilayers. Single adhesion was

observed likely due to the entanglement of PAH/DNA chains that caused partial detachment of adsorbed DNA layers, considering the pull-off force range and contour lengths of polyelectrolytes. Although our system is very similar to theirs, the discrepancy between the adhesion peak behaviors could be related to the conditions under which the AFM force measurements were made. Their results show the interactions between oppositely charged surfaces in an aqueous environment while our experiments investigated the interactions under ambient conditions at a controlled humidity level. Pericet-Camara et al.<sup>60</sup> also showed multiple adhesion events in an experiment conducted in an aqueous environment, namely in KCl solution.

Figure 9.1 shows typical force-distance curves obtained for PEI(PSS<sub>5</sub>PAH<sub>5</sub>) prepared at 0.5 M NaBr ionic strength as a representative of all systems. Although fifty force cycles were taken for each sample, only ten are shown. Different colors refer to different locations on the sample and one out of the five replicate force measurements from the same spot. We consistently observed a single adhesion peak in the retraction curves, without any exception. Upon the approach, we did not observe any long-range attraction. For both the retraction and approach curves, we had some perturbations due to the noise effect related to AFM.

Our objective was to determine the role of various salts and ionic strength on the adhesion properties of the samples as well as to find the best sample(s) that would show the greatest adhesive strength.

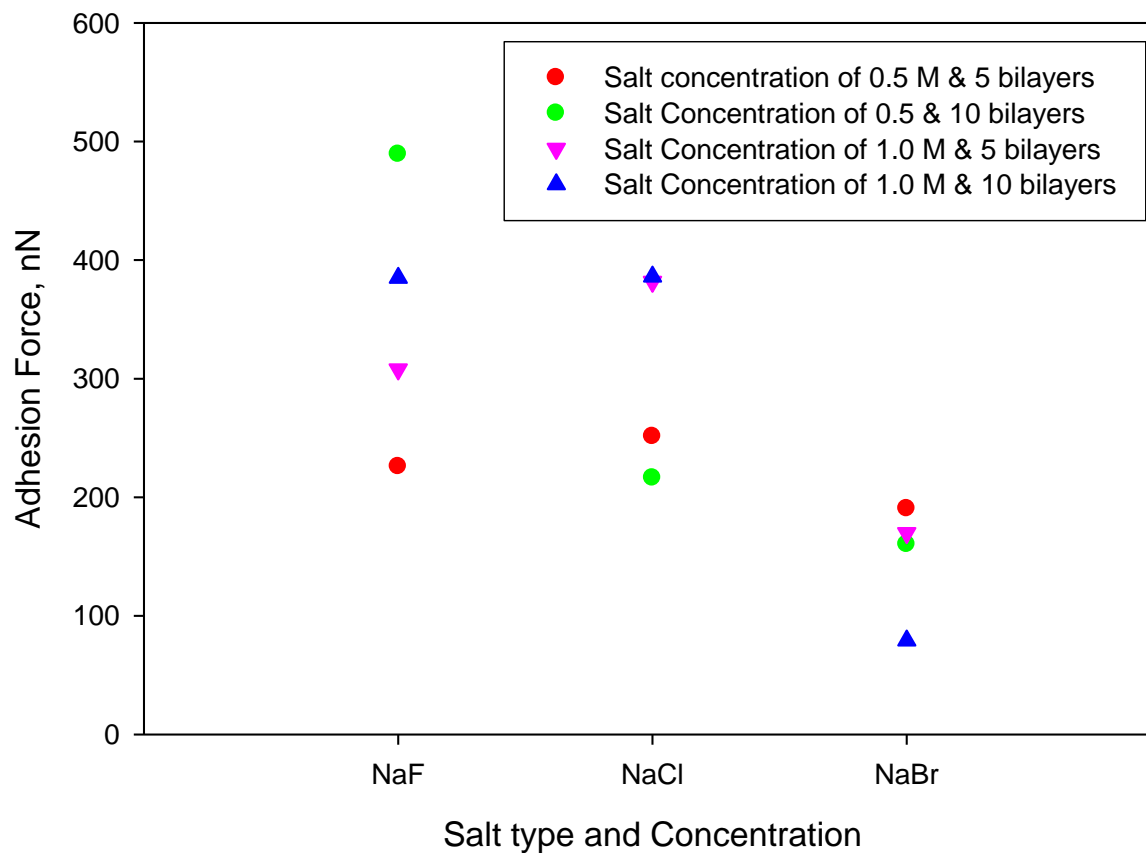
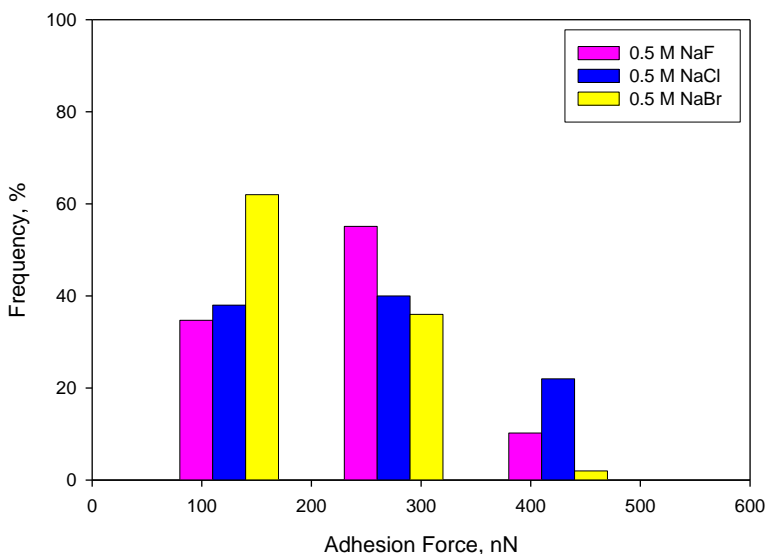


**Figure 3.2** Adhesion forces as a function of salt type and concentration. The reported adhesion values are the average of fifty measurements between the PEM and a colloidal silica probe. Measurements were made in air at 45 % relative humidity.

Figure 3.2 shows the average adhesion forces as a function of salt type and concentration at 5 and 10 bilayers of prepared PEM thin films. The adhesive strength of these thin films is in the range of approximately 80-490 nN. The adhesion values in a range of 0-200 nN were observed for samples prepared from only NaBr salt, comprising 33.33 % of overall adhesion

(avg) force data. The samples prepared from NaCl and NaF salts showed higher adhesion forces and they were in the range of 200-400 nN. The adhesion force contribution of these salts to the overall data was 58.33 %. The highest adhesion force was obtained as 489.12 nN for a sample, having the 8.33 % contribution to the overall adhesion force data. The role of ionic strength as an increase on adhesion forces was pronounced when NaCl and NaF salts were used at the multilayer build-up process, except for 10 bilayers of NaF. Furthermore, the effect of increasing the deposition number on the adhesion forces was pronounced especially on the samples prepared from NaF salt. On the other hand, any treatment such as increase on deposition number or salt concentration did not help improving the adhesive strength of samples prepared from NaBr salt. Regardless of the deposition number and ionic strength, the poorest adhesive properties were obtained for this salt.

a)



b)

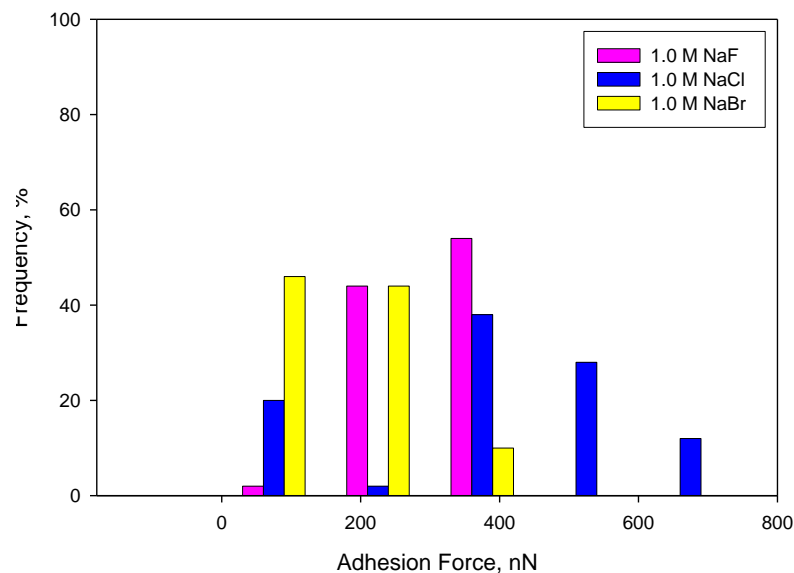
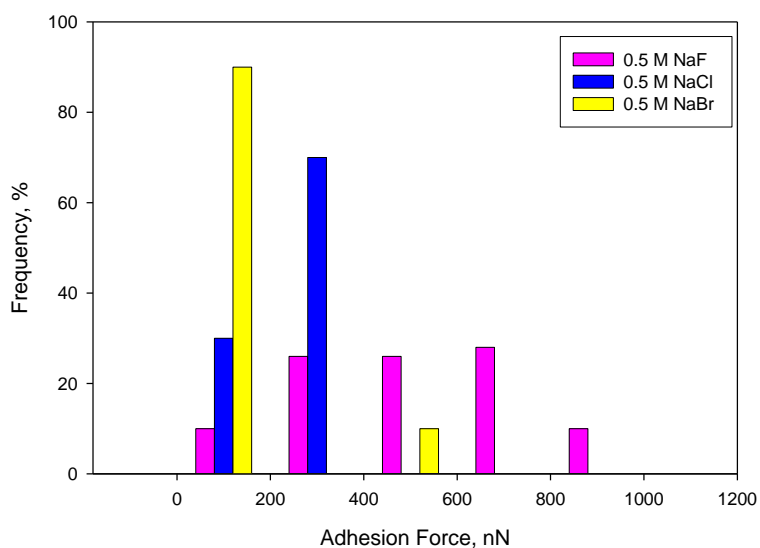


**Figure 3.3** Adhesion force distribution for PEI(PSS<sub>5</sub>PAH<sub>5</sub>) as a function of salt type effect at an ionic strength of a) 0.5 M, and b) 1.0 M.

a)



b)

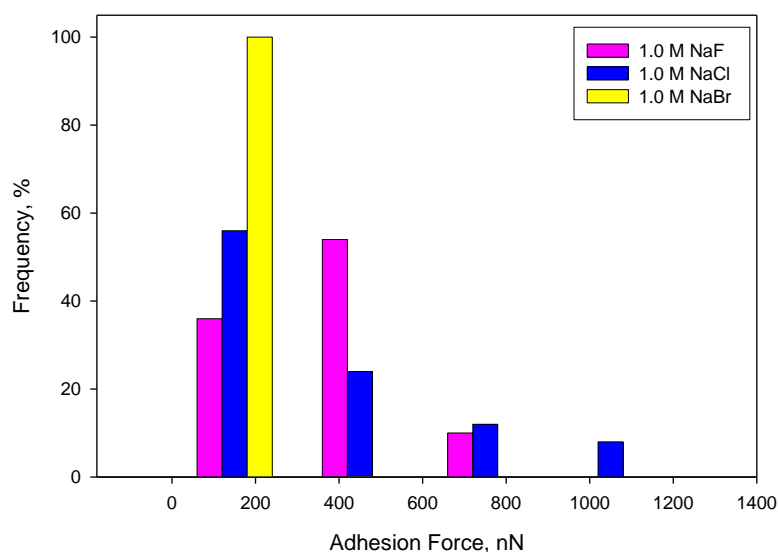


**Figure 3.4** Adhesion force distribution for PEI(PSS<sub>5</sub>PAH<sub>5</sub>) as a function of salt type effect at an ionic strength of a) 0.5 M, and b) 1.0 M.

The discussion held for average adhesion forces requires further analysis of the data. For this reason, the adhesion force distribution plots were created for all the samples. The narrowest adhesion force range at lower values obtained for NaBr salt confirms why the poorest adhesive strength was observed for the films prepared from this salt (Figures 3.3 and 3.4). In addition, the broader adhesion force distribution for NaCl and NaF is indicative of the greater adhesive strength. The adhesion forces for 1.0 M NaCl (5 and 10 bilayers, Figures 3.3 and 3.4) and 0.5 M NaF (10 bilayers, Figure 3.4) range up to 700 nN, 900 nN and 1100 nN, respectively (Figure 3.4). Furthermore, when the force-separation data for all the samples were put into one plot, it was observed that most of the data accumulated at the range of ~ 25-500 nN while the whole range was approximately 25-1000 nN (Figure 9.2). In Figure 9.2, each color represents different case, such as different deposition number with a chosen salt type and concentration. The contributions from the higher adhesion values, 500 nN to 1000 nN, should have made a difference for some samples, which outstand as showing the greatest adhesive strength. Confirmed from both the average adhesion values and the distribution plots, those samples were the ones prepared from 1.0 M NaCl (5 and 10 bilayers) and 0.5 M NaF (10 bilayers).

To compare our adhesion forces with the ones from literature, all the average values were divided by the probe radius. Our normalized adhesion forces are much greater than those reported in the literature. While our results are on the order of 100s of mN/m (the lowest 158.1 mN/m, the highest 978.24 mN/m), the reported values are much lower for similar studies. Johansson et al.<sup>52</sup> showed that the pull-off force for PAH<sub>6</sub>PAA<sub>5</sub> formed from LM<sub>w</sub> polyelectrolytes was 6 mN/m at a contact time of 5 s while it was 3.5 mN/m for the HM<sub>w</sub> combination at the same conditions. In another study, Notley et al.<sup>34</sup> obtained approximately 2.2 mN/m for PAH<sub>6</sub>PAA<sub>6</sub> and 3.8 mN/m for PAH<sub>6</sub>PAA<sub>5</sub>. In a similar study to ours, Gong et al.<sup>53</sup>

showed that the pull-off force obtained for PEI(PSS<sub>5</sub>PAH<sub>5</sub>) was roughly 0.18 mN/m while it turned out to be roughly 5.0 mN/m when PSS was replaced by DNA.

There are several possible reasons. First, it should be noted that the contact time at the measurements were held constant. One of the possible scenarios could be based on the ‘screening effect’ of charges when the ionic strength was high. At higher salt concentrations, polyelectrolytes tend to form coiled structures due to the reduced interactions along the PE chains. As a consequence, greater pull-off force is required to snap away from the surface and to break the stronger interactions between the coiled structure of PEM and the probe. The second possible scenario could be any excess charge at the PEM surface bridging with the probe surface. Under high salt concentration, one can expect to have more PAH or PSS monomers that are not polyion paired and cause residual charges. This observation was discussed in a study where the presence of uncompensated polyion charges was probably the main cause for the oscillations in the solvent fraction.<sup>61</sup>

The modeling of the forces is not in the scope of this work; however, one can assume that the contributions from van der Waals attraction could be higher in air than those in water. Claesson et al.<sup>11</sup> obtained significantly greater pull-off forces for polymer coated mica surfaces in air (1000 mN/m) while the same system in water showed much lower values (2-5 mN/m). The strong pull-off force for polymer coated mica surfaces in air is reasonable when the interactions between highly energetic mica surfaces are considered (800-1200 mN/m).<sup>11</sup> Similarly, in another study, the interactions between PEM covered mica surfaces obtained from the SFA measurements in wet conditions were significantly lower (1.9 mN/m) than those in dry conditions (100 mN/m) and PEM coverage decreased the adhesion force between bare mica surfaces (1500 mN/m).<sup>52</sup> Therefore, it should not be surprising to obtain greater adhesive

strength in our system compared to the reported values in water. Although we made some conclusions about the differences on the adhesive strength of the samples prepared at various salt types and concentrations, the reasons for observing such differences when the salt type was changed are not clear yet.

### 3.3.2. Roughness and Morphology of the PEM Thin Films

Furthermore, we performed AFM imaging on the same samples. The ionic strength of the polyelectrolyte solution is important since the thickness and roughness of the resulted films are affected. Several researchers have observed this fact which was attributed to the conformational changes of the PE chains in their aqueous solutions. At high ionic strengths, the chains can form a more coiled conformation since the electric charges are screened along these PE chains.<sup>39</sup> As well as increasing ionic strength effect, decreasing degree of polymer charge also leads to more coiled conformation of PE chains which is the result of reduced electrostatic repulsions along these chains. As a conclusion, thicker and rougher films are obtained.<sup>37</sup> Despite some exceptions, we also observed much rougher films when the ionic strength was increased (Table 3.1). The images taken for 5 bilayers with a NaBr salt at different ionic strengths demonstrate this observation (Figure 3.5). With an increase in ionic strength, much taller features on a comparatively larger area were observed. The ionic strength affects also the morphology of the films. McAloney et al.<sup>62</sup> found that the morphology of the films was different at low and high salt concentrations (NaCl, 0.0001 M to 1.0 M) for PDDA/PSS films at 10 bilayer. At high salt concentrations, they observed vermiculate structures in these films which were stable even in high temperatures and existed in wet conditions.

The films prepared from PEI(PSS/PAH) with different deposition number, salt type and concentration are relatively smooth compared to other studies which used other PEs. McAloney et al.<sup>62</sup> obtained much rougher films of (PDDA/PSS)<sub>10</sub> when the salt concentration was increased from 0.5 M (rms, ~13 nm) to 1.0 M (rms, ~21 nm). For our films, the range of the rms values is approximately 3-6 nm. On the other hand, Gong et al.<sup>53</sup> showed much smoother films comprised by PSS/PAH up to 5 bilayers. They did not observe any dependence of deposition number on the rms values, which were in the same order of for bare glass substrates (rms, ~ 1 nm). Despite the same parameters used in the LbL deposition technique (0.5 M NaCl, 1.0 g/l PE concentration), the discrepancy between their results and ours might stem from the scan size (1  $\mu\text{m} \times 1 \mu\text{m}$ ) of the images that were used for roughness analysis and the substrate (glass).

**Table 3.1** Roughness (nm) of the PEM thin films as a function of salt type and concentration.

		0.5 M NaF	0.5 M NaCl	0.5 M NaBr	1.0 M NaF	1.0 M NaCl	1.0 M NaBr
PEI(PSS <sub>5</sub> PAH <sub>5</sub> )	avg	5.01	5.53	4.55	8.50	6.09	5.39
	stdev	1.69	1.73	1.73	1.92	2.89	2.41
PEI(PSS <sub>10</sub> PAH <sub>10</sub> )	avg	6.74	3.48	4.40	2.97	3.64	7.34
	stdev	3.02	1.21	2.22	1.20	1.74	2.22

In contrast to what was shown by Wong et al.,<sup>37</sup> we could not make any generalization on the roughness values of different types of salt. They obtained thicker and rougher films for PSS/PDADMAC system, in the order of  $\text{F}^- < \text{Cl}^- < \text{Br}^-$ . They interpreted the results as  $\text{Br}^-$  being a

---

much bigger ion and having larger polarizability ( $\sim 12.2 \cdot 10^{-6} \text{ m}^3/\text{mol}$ ) compared to  $\text{F}^-$  ion ( $\sim 2.3 \cdot 10^{-6} \text{ m}^3/\text{mol}$ ). They also claimed that PDADMAC ions could interact more strongly with  $\text{Br}^-$  than with  $\text{F}^-$ , possibly by means of “bridging” or another way, since  $\text{Br}^-$  ion is surrounded by a thin, less-ordered hydration shell which makes it easy to adjust to the environment. Therefore, when  $\text{Br}^-$  ions were used, the screening effect was more effective along the charges of polycation chain that lead to stronger coiling of the chains and thicker films with rougher multilayers.<sup>37</sup> However, in our case, having a weak polycation (PAH) could have changed this scenario.

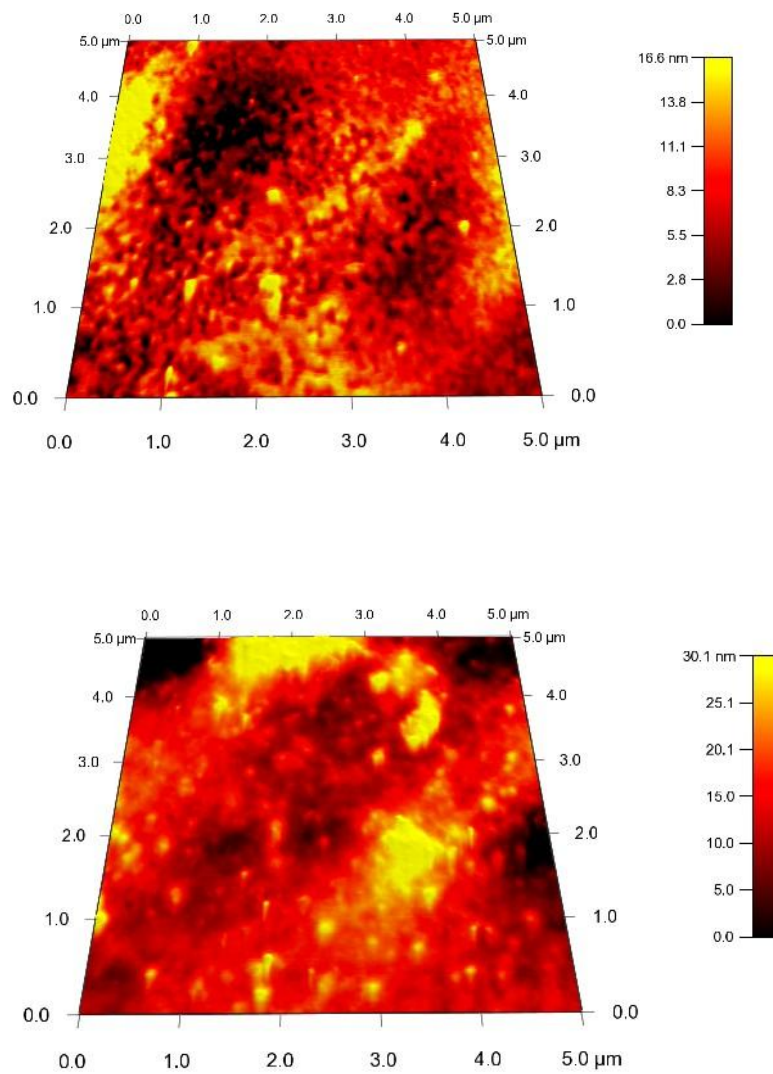


**Figure 3.5** AFM images of PEI(PSS<sub>5</sub>PAH<sub>5</sub>) at an ionic strength of 0.5 M NaBr (top) and 1.0 M NaBr (bottom). The bars represent z-scale.

### 3.3.3. Relating Adhesive Strength and Roughness of the PEM

#### Thin Films

Furthermore, we attempted to find some correlations between the adhesive and roughness properties of the PEM thin films.

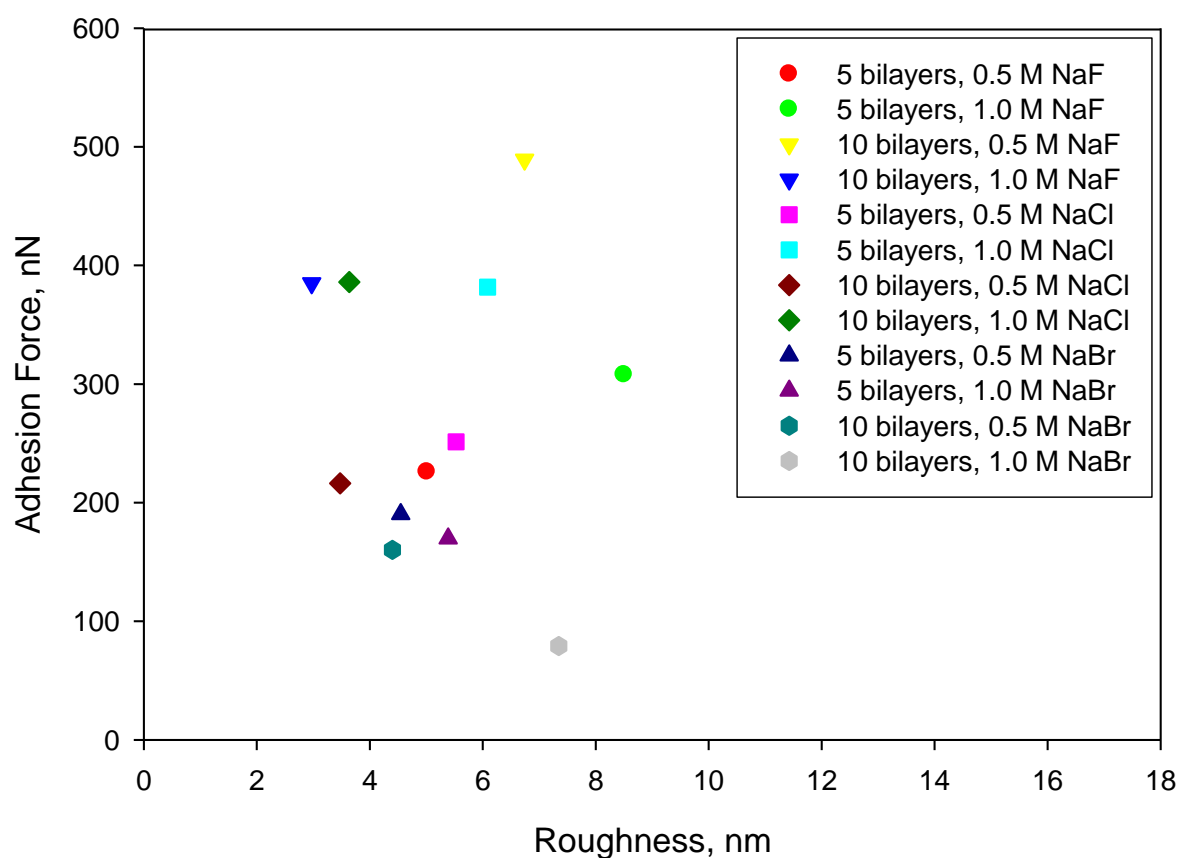


**Figure 3.6** Adhesion forces versus RMS roughness for all systems.

All the films are relatively smooth films. The highest adhesion force with a relatively rough surface was obtained for NaF salt at 0.5 M ionic strength and 10 bilayers (489.12 nN and 6.74 nm). The next highest adhesion forces were obtained at an ionic strength of 1.0 M NaCl and

NaF salts (386.01 nN, 385.02 nN, and 381.74 nN) where the roughness of these films varied between approximately 3-6 nm (Figure 3.6). These observations show that a film with good adhesive properties might have relatively smooth structure when another salt type was used. Although the adhesion forces are approximately the same for NaF and NaCl salts at 1.0 M ionic strength, the surface properties seem to differ when the deposition layer number is changed. One can decrease the roughness of the resulted films by depositing more PEMs while keeping the adhesive strength same. Furthermore, the lowest adhesion forces at medium roughness, except 7.34 nm, obtained in the case of NaBr salt.

All the observations reward for the applications of PEM thin films where smooth surfaces with good adhesive properties or vice versa are preferred. By changing the salt type, concentration and deposition number, the properties of the films could be tuned.

### 3.4. Conclusions

We have studied the role of salt type and concentration on the adhesive properties and morphology of PEI(PSS/PAH) thin films. AFM was used for both imaging and quantifying the adhesion forces of the prepared samples at 5<sup>th</sup> and 10<sup>th</sup> bilayers. We showed both the distribution and the average adhesion forces to explain the adhesive properties of the PEMs. The films prepared from NaCl and NaF at an ionic strength of 1.0 M were outstanding among all the samples by showing the greatest adhesive strength. Furthermore, the highest adhesion force was obtained as 489.12 nN (0.5 M NaF, 10 bilayers). The PEMs deposited in the case of NaBr salt exhibited the poorest adhesive strength and neither deposition number nor salt concentration helped to improve the adhesion properties. Moreover, the reasons for obtaining significantly

---

higher (normalized) adhesion forces compared to the reported values from literature were discussed stating some possible scenarios. Those results were attributed to the measurements taken in dry conditions and van der Waals force contribution in air as well as coiled structures of PEMs at high ionic strengths and any excess charge on the surface. Films with relatively smooth surfaces were obtained and the roughness of the films varied with a change on ionic strength and multilayer number. We proposed that by changing the salt type, concentration and deposition number, the thin films with the desired adhesive strength and morphology could be obtained.

---

## 4. Chapter II: The Effect of Various Probes on the Adhesion Force Measurements

### 4.1. Introduction

The interactions between polyelectrolyte multilayer (PEM) covered surfaces are of great interest. There are numerous studies about the growth and self-assembly of PEM thin films since the layer-by-layer (LbL) deposition technique was first introduced;<sup>1, 2</sup> however the little work about the interactions of polyelectrolyte coated surfaces is not satisfactory for the moment. Surface force apparatus (SFA) and atomic force microscopy (AFM) are the most common tools that have been used for the investigation of the interactions between the surfaces. One of the first studies on the matter of this subject was held by Lowack and Helm using SFA.<sup>40</sup> On the other hand, adhesive strength can also be quantified at macroscopic level, such as applying the peel-off test between the two surfaces.<sup>63, 64</sup>

Atomic force microscopy and colloidal probe technique have been used for the quantification of interaction forces between various surfaces. Colloidal probes with a diameter of 1  $\mu\text{m}$  to several microns are used either as bare or coated with various polymers.<sup>52, 58, 65</sup> From this point of view, colloidal probes bring versatility to the field by allowing various coatings on their sphere surfaces. As a consequence, the interactions between PEM covered surfaces can be probed by AFM at nanonewton to piconewton sensitivity.

The properties of the PEM thin films, prepared by layer-by-layer deposition technique, can be tuned simply by the choice of polycation/polyanion pair, molecular weight of the PEs,<sup>35,</sup>

<sup>36</sup> pH of the solution,<sup>32, 37, 38</sup> ionic strength,<sup>33, 39, 40</sup> and etc. The adhesion force, or so called pull-off force, between the polyelectrolyte coated surfaces does not depend only on the conformation of the polyelectrolytes that adsorbed on the sample, but it also depends on the environmental conditions where the force measurements are conducted. Specifically, the measurements in air can be affected by the relative humidity or the presence of organic vapors in the environment.<sup>66</sup> Therefore, it is important to understand the interactions between an AFM tip and a sample surface under different environmental conditions.

The studies on the interaction forces between two PEM covered surfaces or a PEM covered surface and a bare surface were held commonly in aqueous environments.<sup>34, 45, 52, 53, 60</sup> However, the studies carried out on the matter of this subject in air are scarce. In our previous study, we pointed out this gap and discussed in detail (Chapter I). The present work discusses the interactions between oppositely charged surfaces in air; one PEM-covered sample and a probe of interest. Three different probes were used to investigate the effect of various probes on the adhesion forces; namely as, a colloidal silica probe, a colloidal silica probe functionalized with either COOH surface chemistry or PEI/PSS coating. While a bare silica probe was used for the quantification of interaction forces on the PEMs, functionalized silica probes were used to simulate PEM-PEM interactions.

## 4.2. Experimental Section

### 4.2.1. Formation of the PEM Thin Films

Thin films of PEI(PAA<sub>5</sub>PAH<sub>5</sub>) and PEI(PSS<sub>6</sub>PAH<sub>6</sub>) were prepared using LbL deposition technique on PET (DuPont Teijin Films, Melinex S/142 Gauge) substrates. Poly(ethyleneimine) (PEI, 50 % w/v,  $M_w$  of 600-1000 kg/mol) and poly(allylamine hydrochloride) (PAH,  $M_w \sim 70$  kg/mol) as polycations and poly(sodium 4-styrenesulfonate) (PSS, 30 % w/v,  $M_w \sim 200$  kg/mol) and poly(acrylic acid) (PAA, 25 % w/v,  $M_w \sim 50$  kg/mol) as polyanions were used. PE solutions of concentration 1 mg/mL containing 0.5 M NaCl (purity  $\geq 99.0$  %) were prepared with milliQ reversed osmosis water (purity 18.2 ohms.cm). All the polyelectrolytes and salt were purchased from Sigma-Aldrich, except PAA from Polyscience Inc. The PEM thin films were built up automatically by using HMS<sup>TM</sup> Series Programmable Slide Container (Carl Zeiss, Inc.). First, PET substrates were exposed to air-plasma cleaning (PDC-32G, Harrick Plasma Cleaner) for 20 minutes to enhance adhesion between surfaces. LbL deposition of polyelectrolytes were initiated by immersing the substrate into PEI solution and continued by the consecutive adsorption of oppositely charged polyions from their solutions (30 minutes each). Post deposition a layer, the film was always rinsed twice with water for 2 minutes each and dried in air for 10 minutes. After this washing and drying steps, the procedure was continued till the desired number of layers was obtained.

### 4.2.2. AFM Probes and Force Measurements

For investigating the effect of various probes on the interactions between two surfaces, three different types of AFM probes were used. Colloidal silica probes (1  $\mu\text{m}$   $\text{SiO}_2$  particles) with a spring constant of 14 N/m were purchased from Novascan Technologies, Inc. in two forms: bare and functionalized with COOH surface chemistry. The third type of probe was prepared at the lab conditions using the LbL deposition method. A bare silica probe was coated with a monolayer of PEI (50 % w/v,  $M_w \sim 750$  kg/mol) and PSS (30 % w/v,  $M_w \sim 70$  kg/mol) by manually dipping the probe into the solutions. The rinsing and drying steps were applied as well. The spring constant of this PE coated probe was assumed to be the same as bare colloidal silica probes. The probes were cleaned prior to AFM measurements leaving under UV light overnight.

AFM, NanoScope IIIa (Dimension 3100, Veeco Metrology Inc., Santa Barbara, CA), was used for the quantification of adhesion forces. Twenty-five force measurements were collected for each sample in air at  $\sim 45\%$  relative humidity (RH) where it was safe to be away from the capillary force effects.<sup>58, 59</sup> The cantilever was moved to five different locations on the sample in both x and y directions, and five measurements were collected from each location. The raw force curves were processed with the assistance of self-written MATLAB® and Microsoft Excel scripts.

### 4.3. Results and Discussion

#### 4.3.1. Probe effect on the adhesion forces of PEI(PAA<sub>5</sub>PAH<sub>5</sub>)

The interactions between oppositely charged PEM thin films and probes of interest were investigated using AFM. The force measurements were made in air at a controlled humidity level (45% RH). For the ease of discussion of the various probes, each type of the probe will be named shortly. A colloidal silica probe will be referred to as a ‘bare probe’, while a colloidal silica probe functionalized with COOH surface chemistry will be referred to as a ‘functionalized probe’ and a PEI-PSS deposited colloidal silica probe will be referred to as a ‘PE coated probe’. Considering a series of probe measurements, starting from a bare probe to a functionalized probe and finally to a PE coated probe, we aimed to have the best representative system for the interactions between two PEM covered surfaces. In the present study, for the interactions between a PEM-covered substrate and a probe, the pull-off force as a magnitude and a range was of great interest (Figure 4.1). The magnitude of the pull-off force is simply the adhesive strength of the sample. The range of the pull-off force is the distance where the adhesion peak is observed and this range is important since it can give an idea about the molecular interactions. For instance, this range can give information about bridging between the polymer surface and probe based on the contour lengths of polymers.

For each probe, the pull-off forces were presented in force-separation curves. In each system, only one single sharp peak was observed upon retraction. Based on the probe, the strength of the interactions was different as it was seen in the magnitude of the pull-off forces. With a bare probe, very large adhesive forces were obtained (Figure 4.2). Although the tip-sample separation occurred at considerably short distances (~2 nm), the range where the pull-off

forces observed was large, being approximately 80-120 nm. Even though the tip-sample interactions were broken at shorter distances, the reason of having large pull-off force range can be related to bridging or interactions between the PE chain and the probe. In other words, upon snapping off the probe from the surface, the detachment of the PE chain still continues and this is what makes the variation on the pull-off force range. The pull-off force range increased with an increase in the magnitude of the pull-off force. We believe that this relation is important. However, the reason(s) for this relation are not clear yet.

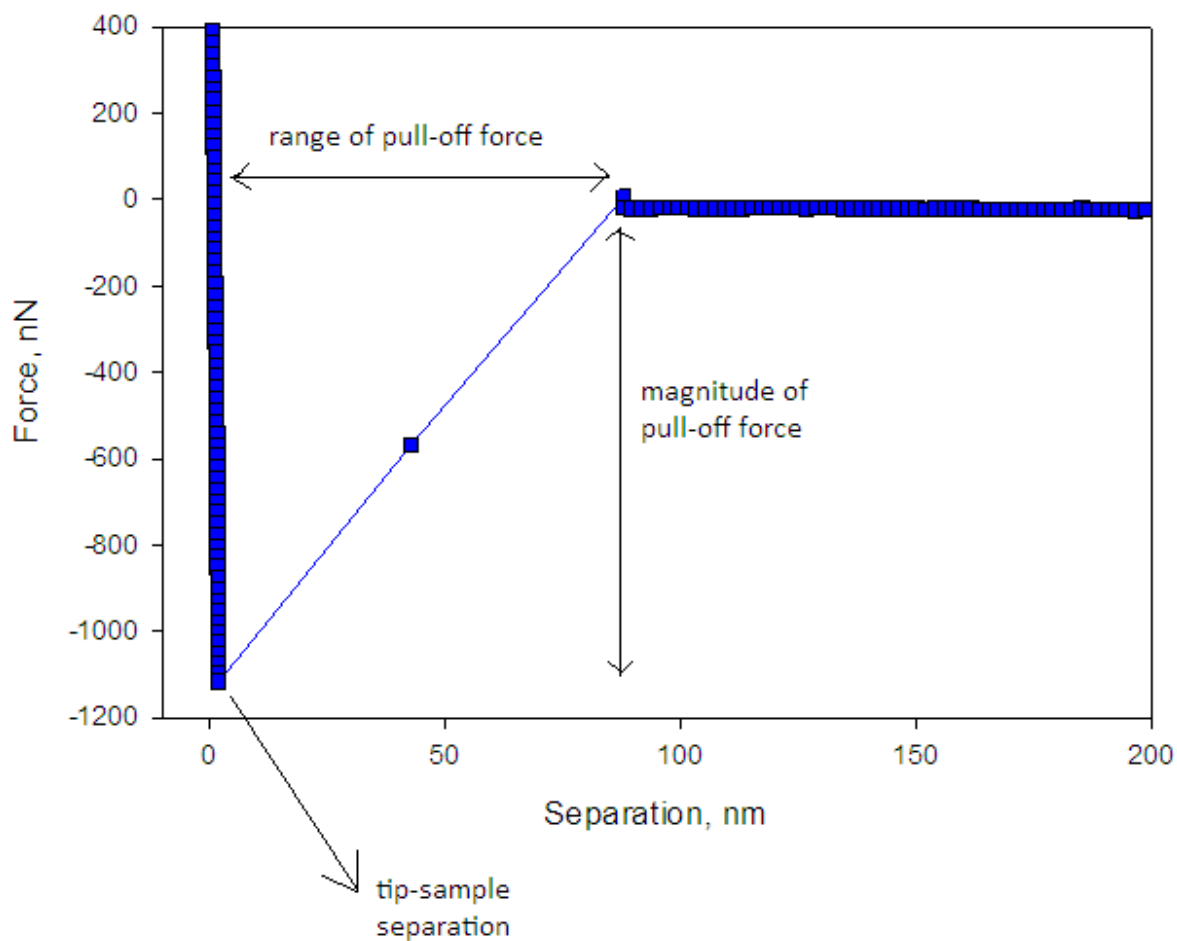


**Figure 4.1** A typical force-separation curve shown for the clarity of discussed terms such as range and magnitude of pull-off force and tip-sample separation.

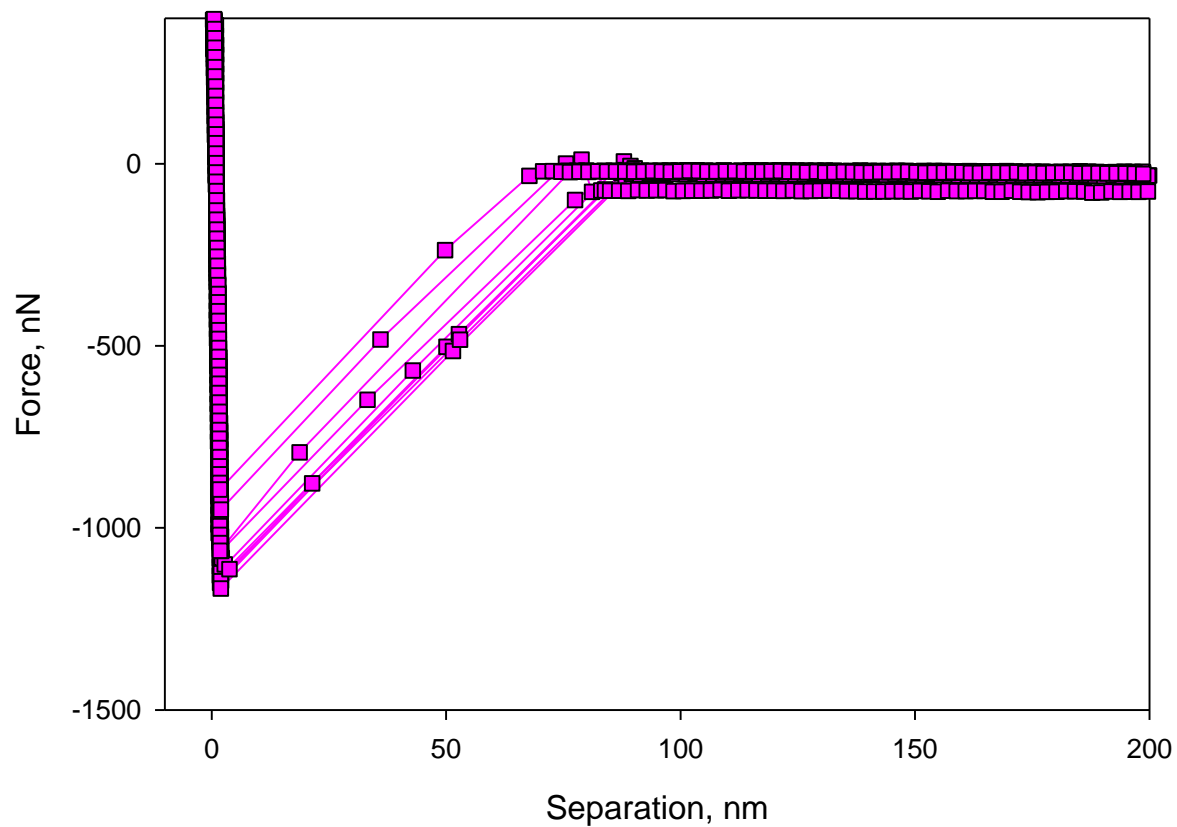


**Figure 4.2** Force-separation curves for PEI(PAA<sub>5</sub>PAH<sub>5</sub>) prepared at 0.5 M NaCl. The measurements were collected at 45% RH with a colloidal silica probe. Ten force curves, five being from the same spot, were represented upon retraction.

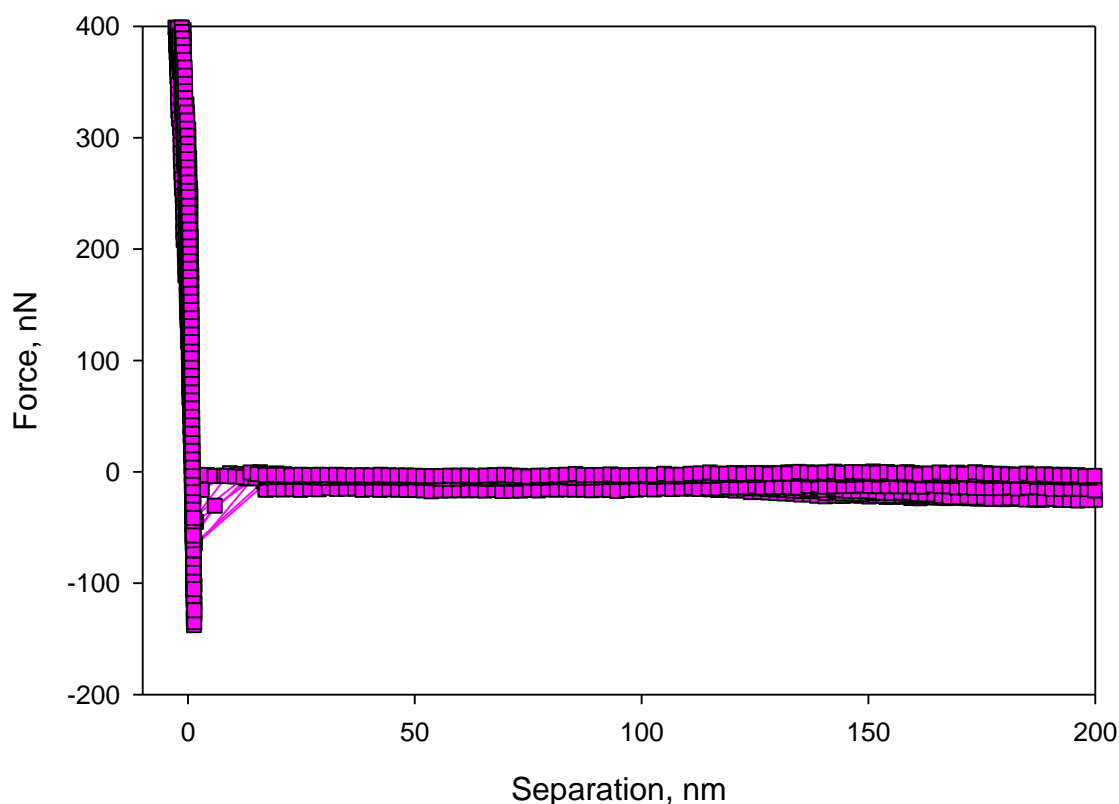


**Figure 4.3** Force-separation curves for PEI(PAA<sub>5</sub>PAH<sub>5</sub>) prepared at 0.5 M NaCl. The measurements were collected at 45% RH with a colloidal silica probe functionalized with COOH. Ten force curves, five being from the same spot, were represented upon retraction.

Another type of probe used in the present study was a functionalized probe. The adhesive strength obtained from the interactions of a functionalized probe and a PEM surface was very low (Figure 4.3). To be consistent on the comparisons of force-separation curves, the scale for both separation and force was kept same for all the systems. However, it was difficult to distinguish the adhesion peaks from the curves in this scale for a functionalized probe. For this reason, the figure was zoomed-in (Figure 9.3). Contrary to the pull-off force range obtained for

bare probe interactions, much smaller values were obtained (~7-15 nm). Even 40% of the data (25 force cycles) showed that this range was less than 1 nm which was very close to the tip-sample separation values. The interactions with a functionalized probe were not as strong as the ones observed with a bare probe.

Finally, two PEM-covered surfaces were investigated using a PE coated probe. Similar to the results obtained from a bare probe, relatively large adhesion forces were observed (Figure 4.4). Contrary to the pull-off force range from a functionalized probe, considerably larger range was obtained varying from 15 nm to 80 nm, but still smaller than a bare probe range. A remarkable and systematic trend was caught in the relation between the magnitude of pull-off forces and the range. In other words, at a certain adhesion force window, the pull-off force range was scaled to the corresponding adhesive strength and increased with an increase on adhesion force.

Furthermore, we investigated the behavior of approach curves (Figure 4.5). No long-range forces were observed upon approach for any type of the probes. For a functionalized probe, the approach curves could not be zeroed to the x-axis: This might be related to optical noise of the instrument (AFM).

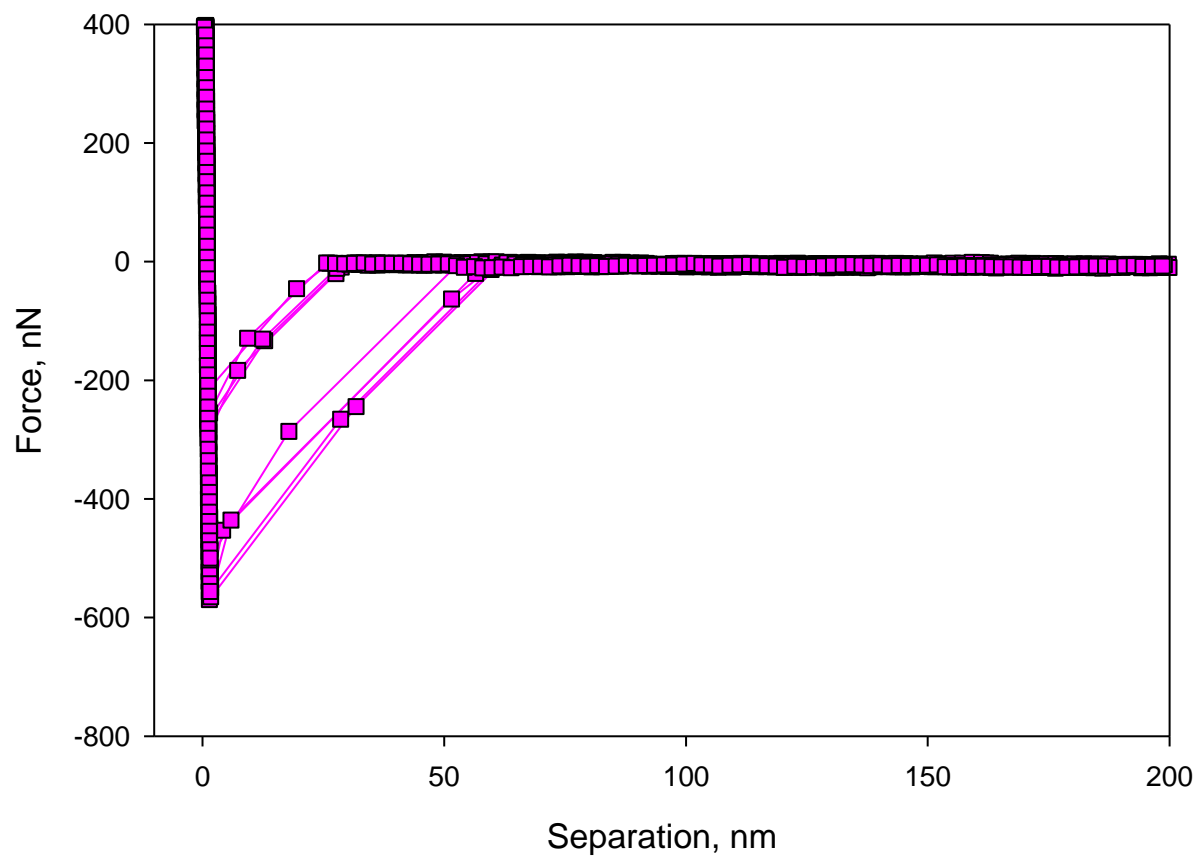


**Figure 4.4** Force-separation curves for PEI(PAA<sub>5</sub>PAH<sub>5</sub>) prepared at 0.5 M NaCl. The measurements were collected at 45% RH with a PEI-PSS deposited colloidal silica probe. Ten force curves, five being from the same spot, were represented upon retraction.

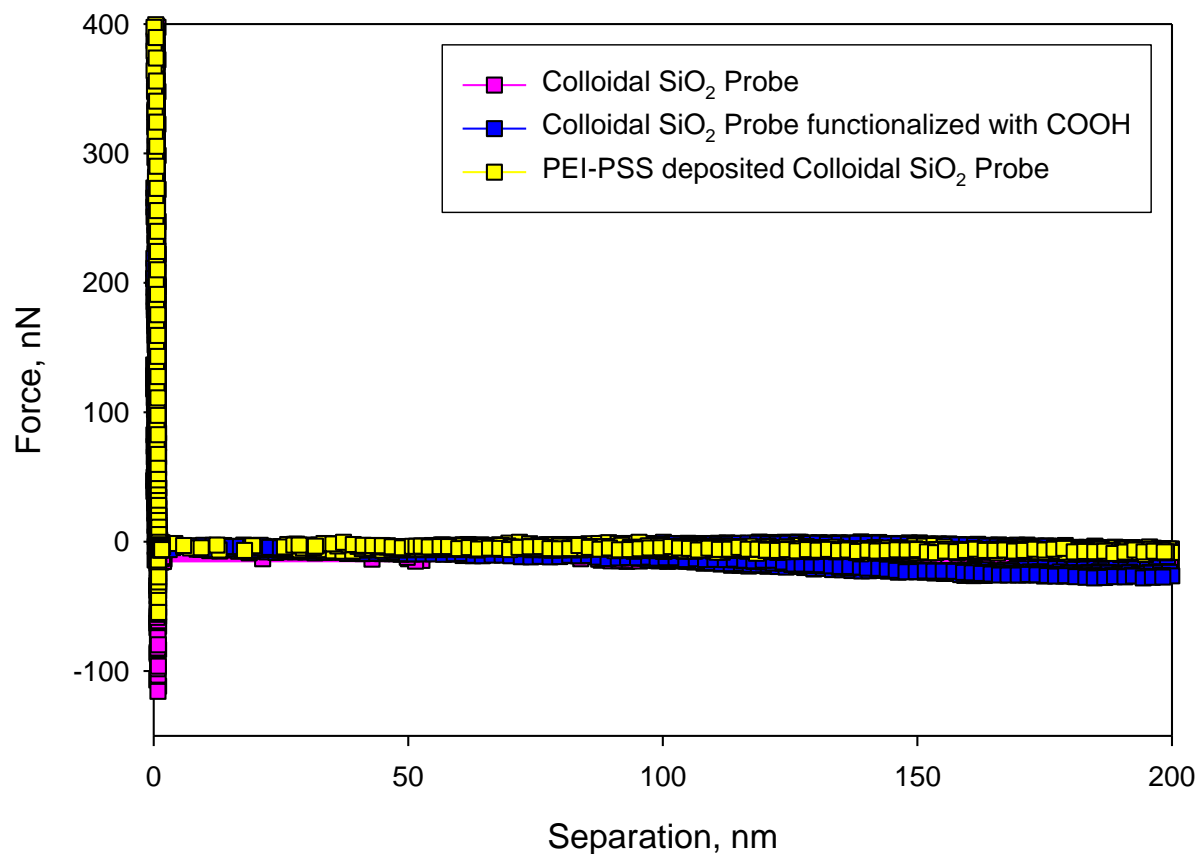


**Figure 4.5** Probe effect on the approach curves for PEI(PAA<sub>5</sub>PAH<sub>5</sub>) is represented with ten force curves for each probe, five being from the same spot, were represented. The measurements were collected at 45% RH.

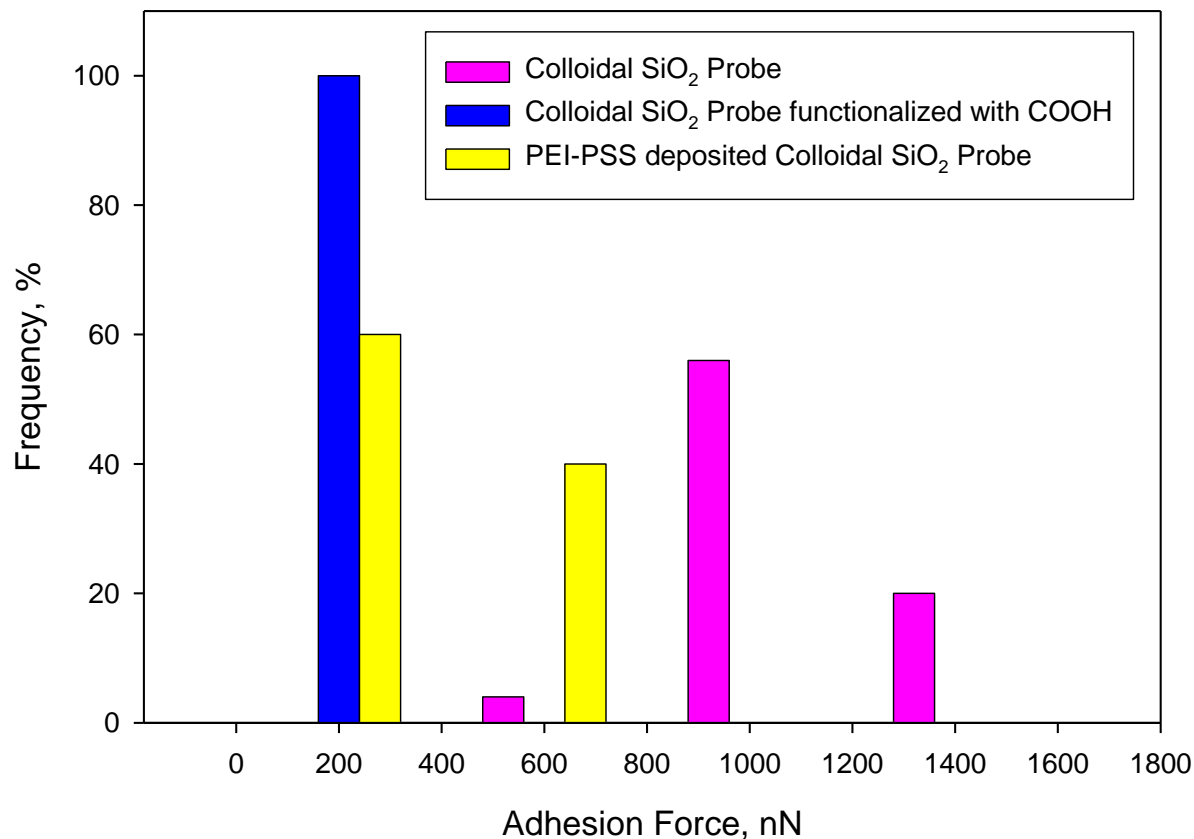


**Figure 4.6** Probe effect on the adhesion force distribution values for PEI(PAA<sub>5</sub>PAH<sub>5</sub>). Each color stands for one type of probe. The measurements were collected at 45% RH.

The adhesive strength of the sample was dependent on the interactions with different probes. A wide range of adhesion force distribution was obtained where each probe interaction resulted in a different adhesive force window (Figure 4.6). Even though each probe was negatively charged, different functional groups in each probe probably affected the interactions and caused differences on the adhesive strengths. The adhesion forces accumulated at a narrow range and lower values for a functionalized probe while relatively broader adhesion force

distribution at higher values were obtained for a silica probe and a PE coated probe. The majority of the adhesion forces obtained with a bare probe was around 1000 nN. For a PE coated probe, adhesion forces as high as 500 nN and 700 nN were obtained. On the other hand, the adhesion forces of a functionalized probe did not exceed 150 nN.

**Table 4.1** Comparison of mean and normalized adhesion forces obtained with various probes.

Type of probe	Bare probe		Functionalized probe		PE coated probe	
	mean	stdev	mean	stdev	mean	stdev
<b>Adhesion Force (nN)</b>	1104.88	256.50	70.73	36.15	372.61	220.26
<b>Normalized Mean Adhesion Force (mN/m)</b>	2209.76		141.46		745.22	

Furthermore, we normalized the mean adhesion forces to make a comparison within the present study and literature. The greatest adhesive strength was obtained when a bare probe was used (Table 4.1). On the other hand, the lowest adhesive strength was observed when a functionalized probe was used. Relatively higher adhesive strength was obtained with a PE coated probe. When these results were compared with similar studies, a substantial difference on the adhesive strengths was found. For instance, the symmetric systems where the interactions between the identical surfaces were studied revealed that the adhesive strength was only several mN/m. Both deposited at pH 7.5 but at different molecular weight combinations, the pull-off forces of 3.8 mN/m<sup>34</sup> and 3.5 mN/m<sup>52</sup> were obtained for PAH<sub>6</sub>PAA<sub>5</sub> in two similar studies. On the other hand, in the present study, the adhesive strength obtained from the interactions with a PE coated probe is much greater (745.22 mN/m) than those reported values. It should be noted

that the present study differs from those discussed studies in the number of PE layers deposited on the sample and the probe, in force measurement conditions and also in the type of charges that interact with.

The comparison of different probes showed that the lowest adhesion forces, confirmed from both mean and distribution values, were obtained with a functionalized probe. The lowest interactions can be explained by considering the discrepancy between the dispersion forces of functionalized and bare probes. Chen et. al.<sup>67</sup> conducted a study where the interactions of a COOH-terminated probe and various surfaces were investigated. In that study, they obtained relatively lower adhesion forces for the interactions between a COOH-terminated probe and CH<sub>3</sub> surface compared to the interactions between an unmodified Si<sub>3</sub>N<sub>4</sub> probe and the same sample surface. The observed phenomenon was attributed to the lower dispersion force of a COOH-terminated probe, 26.6 mJ/m<sup>2</sup>, compared to a fully hydroxylated SiO<sub>2</sub> probe's (as a model for the Si<sub>3</sub>N<sub>4</sub> probe), 29.4 mJ/m<sup>2</sup>.<sup>68</sup> The same observation was also made by Noy et al.<sup>69</sup> who obtained lower adhesion force between a COOH-terminated probe and a CH<sub>3</sub> self-assembled monolayer (SAM) surface measured in alcohol, than that between a CH<sub>3</sub>-terminated probe and a CH<sub>3</sub> SAM surface or a COOH-terminated probe and a COOH SAM surface. Considering all these observations, we speculate that the reason for having lower adhesion forces between a COOH-terminated probe and a PEM-covered sample in the present study could have stemmed from the lower dispersion force of the functionalized probe.

Relatively lower adhesion forces were observed for a PE coated probe compared to the ones from a bare probe, and this can be attributed to the single layer of PE deposited on the probe (regarding PEI deposition as a precursor layer and counting for only PSS while starting numbering). Johansson et al.<sup>52</sup> studied the interactions between identical surfaces formed from

PAA/PAH onto one flat and one spherical silica substrates in a liquid cell and observed an increase on the adhesion forces when the number of deposition steps is increased. The interaction forces after the first layer deposition were weaker, reaching as low as 0.8 mN/m, compared to 6 mN/m at the 11<sup>th</sup> layer. The same trend could be seen in other studies<sup>34, 53</sup> as well, where the interactions were monitored at each layer and an increase on the pull-off forces was obtained with further deposition steps. Therefore, we likely would have stronger interactions and greater adhesion forces if we had more layers deposited on the silica probe.

The pull-off force range was discussed by Gong et al.<sup>53</sup> in a similar study and this range was related to the contour length of each polyelectrolyte. For the interactions between PEI(PSS<sub>3</sub>PAH<sub>3</sub>) sample and a bare glass sphere investigated in liquid using AFM, they observed multiple adhesion peaks and a pull-off force range of (above 600 nm) greater than the sum of individual PE contour lengths (PAH, 187 nm and PSS, 91 nm). This so-called sawtooth pattern was attributed to a bridge formed by entangled PAH and PSS chains. In that same study, in the case of PEI(DNA<sub>3</sub>PAH<sub>3</sub>), their pull-off force range (~600 nm) well exceeded the contour length of PAH but not DNA's (~3  $\mu$ m). It was interpreted as the entanglement of PAH/DNA chains causing partial detachment of adsorbed DNA layers. However, the pull-off force range obtained in the present study for any sample-probe interactions was well below the established numbers from that study.<sup>53</sup> The contour length of PSS was recalculated (270 nm) since the molecular weight of this PE used in the present study was different than the one discussed above, using the bare chain cross section stated in another study.<sup>70</sup> However, the pull-off force ranges were always lower than the contour lengths of each PE chains. All in all, we observed a noteworthy relation between the pull-off force range (nm) and magnitude (nN). Greater adhesive strengths were observed at relatively large pull-off force ranges. Variation on the pull-off force range was

attributed to the interactions between a PE chain and a probe of interest where sometimes it seemed to be difficult to break the interaction even after snapping away from the surface.

### 4.3.2. Probe effect on the adhesion forces of PEI(PSS<sub>6</sub>PAH<sub>6</sub>)

The same series of probes were used for another sample, PEI(PSS<sub>6</sub>PAH<sub>6</sub>). The interactions between a PAH-terminated thin film and a probe of interest were investigated. One single sharp peak was observed for each type of probe interactions.

The adhesion forces obtained via the interactions with a bare probe were around 100 nN (Figure 4.7). The strength of the adhesion forces was substantially lower than those obtained for the previous sample, PEI(PAA<sub>5</sub>PAH<sub>5</sub>), with the same probe. The magnitude of the pull-off forces was lower and the range of the pull-off forces was also lower. The pull-off force range was around 16-30 nm.

With a functionalized probe, low pull-off forces around 60-70 nN were obtained. It was again difficult to distinguish the adhesion peaks in the retraction curves (Figure 4.8) and for clarity, the retraction curves were zoomed-in (Figure 9.4). Low adhesion forces with a very low pull-off force range around 1.0 nm were observed.

The adhesion forces obtained with a PE coated probe were larger than those functionalized and bare probes (Figure 4.9). The pull-off forces around 200-300 nN were observed with a pull-off force range of 20-25 nm. The largest pull-off force range was approximately 45 nm at the greatest adhesive strength. A systematic increase on both the magnitude and range of the pull-off forces was seen.

The tip-sample separation occurred around 1 nm for all the interactions investigated so far. This separation was greatly less than the pull-off force ranges for a bare probe and a PE coated probe while it was very close to the pull-off force range for a functionalized probe. Again, no long range forces were observed in the approach curves (Figure 4.10).

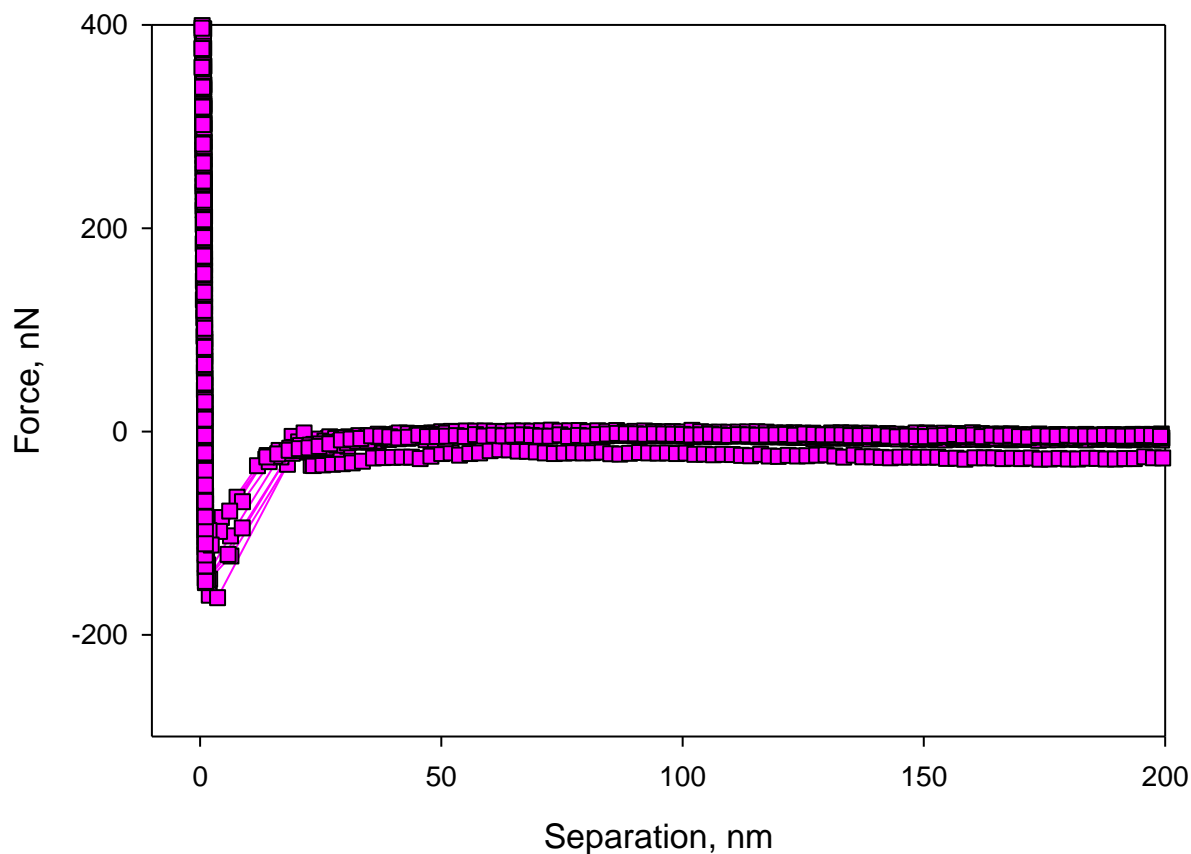


**Figure 4.7** Force-separation curves for PEI(PSS<sub>6</sub>PAH<sub>6</sub>) prepared at 0.5 M NaCl. The measurements were collected at 45% RH with a colloidal silica probe. Ten force curves, five being from the same spot, were represented upon retraction.

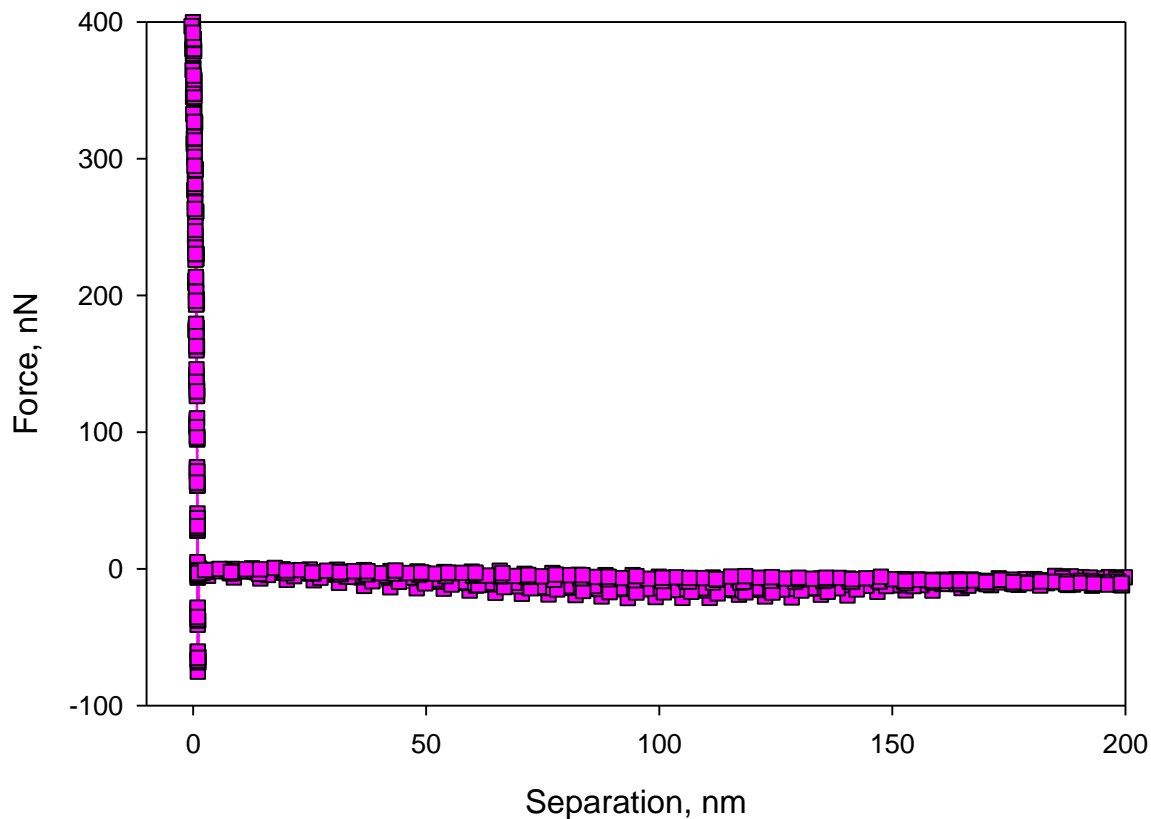


**Figure 4.8** Force-separation curves for PEI(PSS<sub>6</sub>PAH<sub>6</sub>) prepared at 0.5 M NaCl. The measurements were collected at 45% RH with a colloidal silica probe functionalized with COOH surface chemistry. Ten force curves, five being from the same spot, were represented upon retraction.

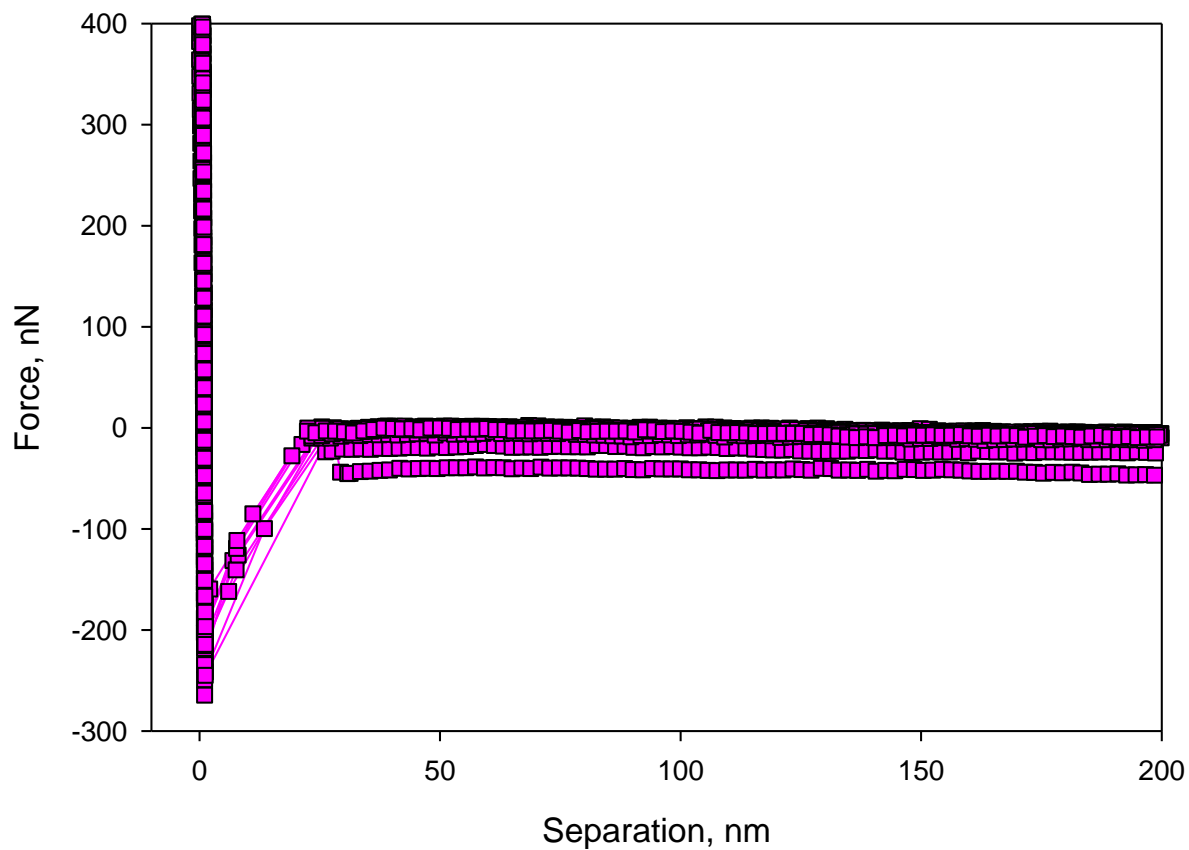


**Figure 4.9** Force-separation curves for PEI(PSS<sub>6</sub>PAH<sub>6</sub>) prepared at 0.5 M NaCl. The measurements were collected at 45% RH with a PEI-PSS deposited colloidal silica probe. Ten force curves, five being from the same spot, were represented upon retraction.

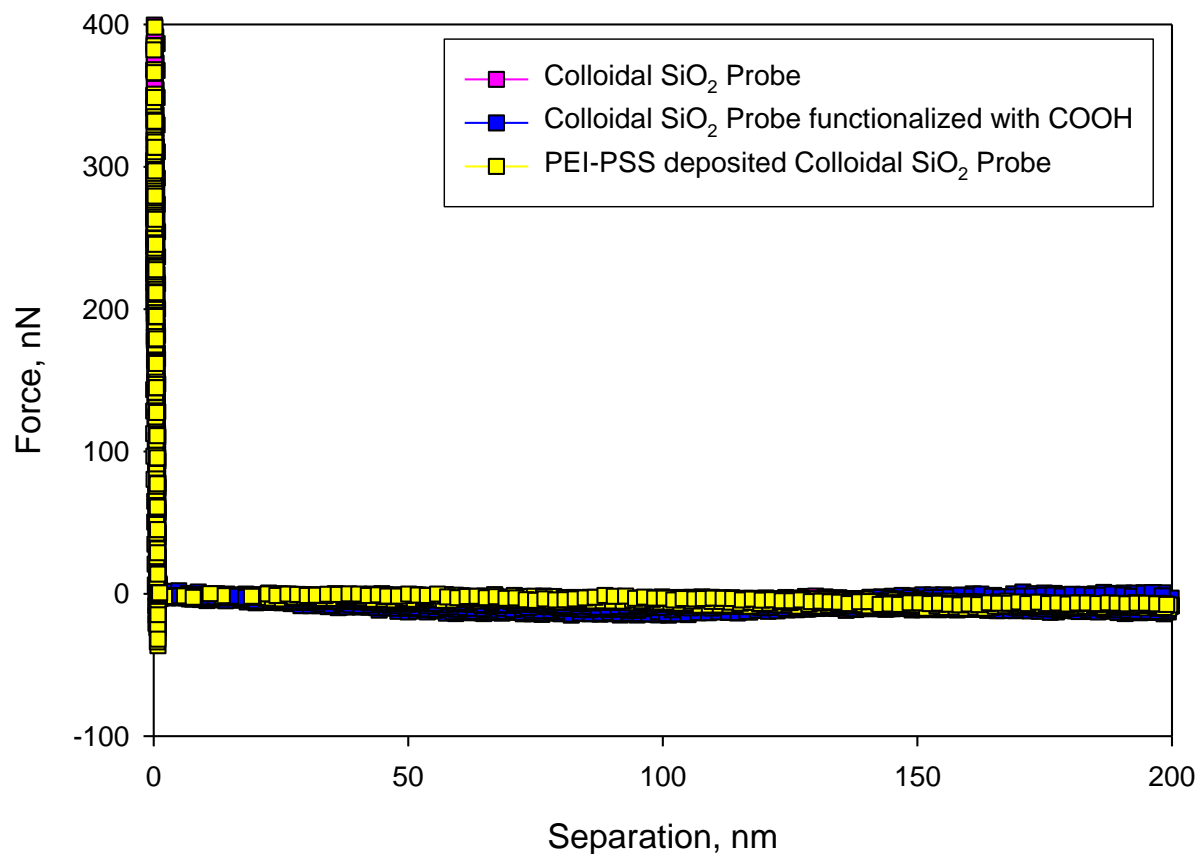


**Figure 4.10** Probe effect on the approach curves for PEI(PSS<sub>6</sub>PAH<sub>6</sub>) is represented with ten force curves for each probe, five being from the same spot, were represented. The measurements were collected at 45% RH.

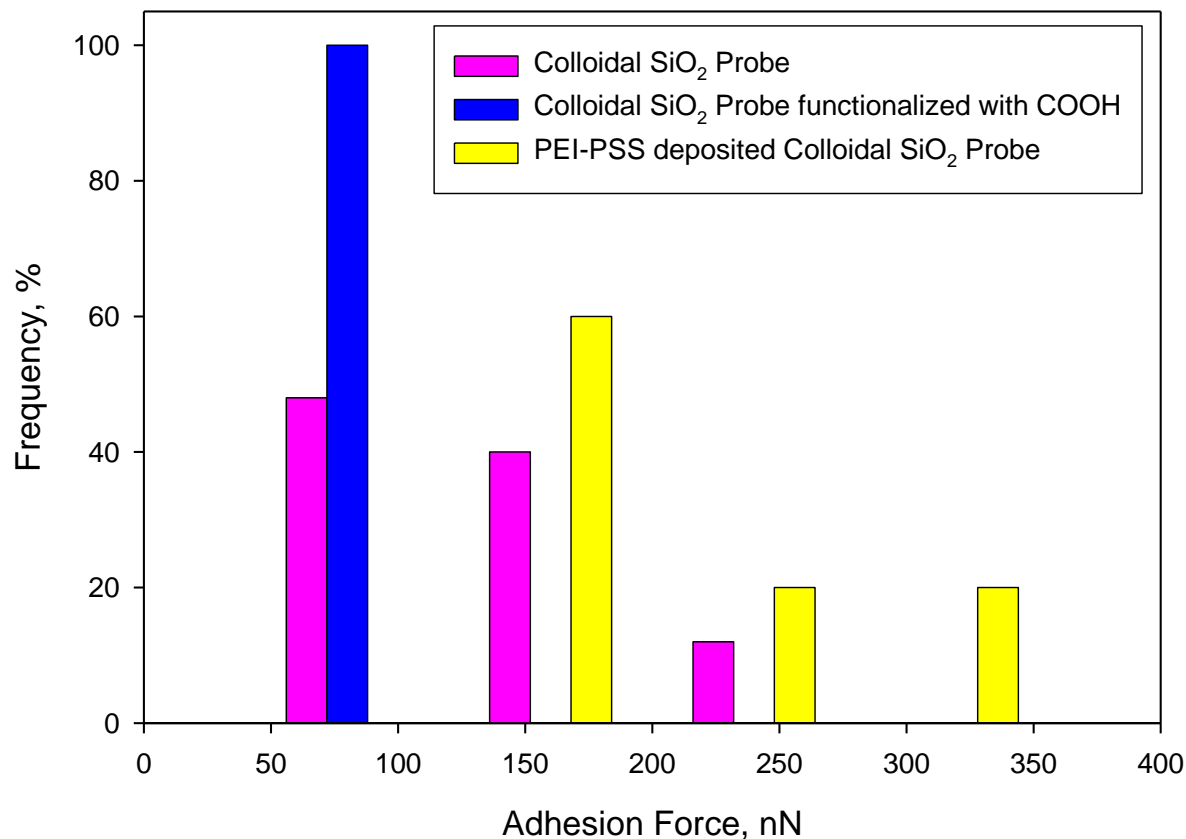


**Figure 4.11** Probe effect on the adhesion force distribution values for PEI(PSS<sub>6</sub>PAH<sub>6</sub>). The measurements were collected at 45% RH.

The adhesion force distribution for each probe was compared in Figure 4.11. Very narrow adhesion force distribution at around 70 nN was seen for a functionalized probe. Relatively broader distribution was obtained for both bare and PE coated probes. The adhesion forces for a PE coated probe were higher than those for a bare probe and this effect was also seen in the mean values (Table 4.2). Coating the probe with PE seemed to work well for this sample since the greatest adhesion force was obtained with a PE coated probe compared to the other

ones. Similarly what was concluded for PEI(PAA<sub>5</sub>PAH<sub>5</sub>), the lowest mean adhesion force was obtained for the interactions of a functionalized probe.

In summary, the mean adhesion forces for PEI(PSS<sub>6</sub>PAH<sub>6</sub>) are lower than those for PEI(PAA<sub>5</sub>PAH<sub>5</sub>) (Tables 4.1 and 4.2). For both samples, the interactions investigated between the two surfaces were same (a PAH-terminated sample and a probe of interest); however, we observed a substantial difference on the adhesive strengths when bare and PE coated probes were considered. On the other hand, close adhesive strengths were obtained for both samples when a functionalized probe was chosen for investigating the interactions. The discrepancy between the results of two samples may stem from the different properties of the resulting films. Two different polyanions were used for the preparation of those samples; while PSS was a strong polyanion, PAA was a weak polyanion. Strong polyelectrolytes are fully charged no matter what the pH of the solution is. However, weak polyelectrolytes strongly depend on the pH of the solution and the number of charges is different at various pH levels. Shiratori and Rubner studied<sup>71</sup> the thickness of PEMs formed from PAA and PAH at different pH levels and observed significant changes in the thickness over a very narrow pH range. Similarly, any change on the structure of the thin films could possibly affect the interactions with a probe [We did not monitor the pH of the solutions during the build-up of PEM thin films]. Another difference between the two samples is the number of deposition steps [PEI(PAA<sub>5</sub>PAH<sub>5</sub>) versus PEI(PSS<sub>6</sub>PAH<sub>6</sub>)]. Even though the multilayer number might have an effect on the adhesion forces, we do not believe that it affects the results this much significantly. We propose that it is more likely to be the choice of polyanion/polycation pair that played an important role in here.

**Table 4.2** Comparison of mean and normalized adhesion force values obtained with various probes

Type of probe	Bare probe		Functionalized probe		PE coated probe	
	mean	stdev	mean	stdev	mean	stdev
<b>Adhesion Force (nN)</b>	128.12	38.28	71.68	9.50	205.34	70.54
<b>Normalized Mean Adhesion Force (mN/m)</b>	256.24		143.36		410.68	

Finally, we present the adhesion forces in mean and normalized forms (Table 4.2). Normalized mean adhesion forces in the present study are significantly higher than those in a similar study.<sup>53</sup> The interactions between PEI(PSS<sub>5</sub>PAH<sub>5</sub>) sample and a bare glass sphere were investigated using AFM in liquid and the adhesive strength was ~0.15 mN/m. When we compared the adhesive strength obtained via a bare probe (256.24 mN/m) to that value, we noticed a substantial difference on the strengths for these very similar systems. One of the main reasons can be the larger contribution of van der Waals (vdW) forces in air than in liquid. Claesson et al.<sup>11</sup> also observed significantly greater adhesion forces in air than in water for the interactions of polyelectrolyte-coated surfaces (800 mN/m versus 2-5 mN/m). Another reason can be attributed to the size of probes. For the sample compared,<sup>53</sup> the probe diameter was 10  $\mu\text{m}$  which was larger than what we used in the present study. We believe that at larger probe sizes, the tip asperities can possibly reduce the contact area and poor interactions can be experienced. Thomas et al.<sup>72</sup> showed the dependence of surface energy for the interactions between two methyl-terminated SAMs on an Au probe and a planar Au substrate, with a varying probe radius from 50 nm to 60  $\mu\text{m}$ . They showed that the magnitude of the normalized adhesive interactions

decreased strongly for larger probe radii, after the tip radii exceeded ~400 nm. Therefore, we suggest that the different probe sizes in the present study and the compared study could have some effect on the discrepancy of the measured adhesive strengths.

#### 4.4. Conclusions

The interactions between oppositely charged surfaces of PEM-covered samples and various probes were investigated in air using AFM. The adhesive strengths of two samples, PEI(PAA<sub>5</sub>PAH<sub>5</sub>) and PEI(PSS<sub>6</sub>PAH<sub>6</sub>), were studied using 3 different colloidal probes both in unmodified and modified forms. The greatest adhesive force, 2209.76 mN/m, was obtained with a bare probe for PEI(PAA<sub>5</sub>PAH<sub>5</sub>). On the other hand, the lowest adhesive forces were obtained with a functionalized probe for both samples. This observation was attributed to the lower dispersion force of a functionalized probe compared to a bare probe's. The order of the adhesive strengths for PEI(PAA<sub>5</sub>PAH<sub>5</sub>) was such that bare probe > PE coated probe > functionalized probe, while this order changed (PE coated probe took the first place) when PEI(PSS<sub>6</sub>PAH<sub>6</sub>) was used. The adhesive strengths obtained for PEI(PAA<sub>5</sub>PAH<sub>5</sub>) were always greater than those of PEI(PSS<sub>6</sub>PAH<sub>6</sub>)'s. Even though the samples were terminated with the same PE, the differences on adhesive strengths might have stemmed from the structural differences or properties of the resulting films as a result of the choice of polycation/polyanion pairing. In addition, the adhesive strengths of the samples in the present study were significantly greater than the reported literature, which were possibly due to the force measurements in air and greater contribution of vdW forces in these conditions. Furthermore, a correlation between the pull-off force range (nm) and magnitude (nN) was made; greater adhesive strengths were always obtained at larger pull-off force ranges.

---

## 5. Chapter III: Comparison of Adhesive Strength of Thin Films prepared via Different Techniques

### 5.1. Introduction

The adhesive strength of thin films is of special interest in this study and atomic force microscopy (AFM) is a tool used for probing the interactions and quantifying the adhesion forces. Two different techniques were used for the fabrication of samples and a comparison of adhesive strengths was made.

Surface modification of substrates can be utilized through several different methods. Layer-by-layer (LbL) deposition method is in use and became one of the promising techniques since the pioneering work of Decher et al.<sup>1,2</sup> Thin films prepared via LbL method have overcome problems associated with Langmuir-Blodgett (LB) films<sup>3</sup> in many ways. Limitations of the LB technique include substrate size, film quality, and stability. Furthermore this technique requires special equipment. As an alternative to the LB technique, chemisorption can also be tried, but both techniques are limited to certain class of molecules. However, LbL assembly technique is versatile as a variety of materials for the fabrication of multilayered thin films can be used such as polymers, proteins, clay particles, colloids and etc. Another advantage of LbL deposition is that the technique is not limited to the shape of solid support. Thin films can be built-up on colloidal particles<sup>18,19</sup> as well as flat substrates.<sup>1</sup>

The use of polyelectrolytes (PEs) is common for forming multilayered structures. In the present study, poly(ethyleneimine) (PEI), poly(allylamine hydrochloride) (PAH), poly(sodium 4-

styrenesulfonate) (PSS), poly(acrylic acid) (PAA), and poly(diallyldimethylammonium) chloride (PDADMAC) were used at different combinations and deposited on poly(ethylene terephthalate) (PET) substrates. The use of these polyelectrolytes is quite common in the literature.

Another method for surface modification is grafting, which we also used. In both ‘grafting from’<sup>73</sup> and ‘grafting to’<sup>74, 75</sup> methods, a polymer brush<sup>76</sup> is created on the surface. Particularly for this study, poly(glycidyl methacrylate) (PGMA) was used as an anchoring layer<sup>63, 77</sup> on PET substrate and further grafting was continued with either PAA or PEI.

The films in the present study were previously discussed in the literature, usually for their growth behavior and morphology. There are some studies where the growth of PDADMAC/PSS pair was investigated in terms of the effect of solvent quality,<sup>33</sup> temperature,<sup>78</sup> ionic strength,<sup>62, 79</sup> and charge density,<sup>80</sup> etc. Even though the PDADMAC/PSS pair is more common in literature, it is also possible to find studies on the PDADMAC/PAA pair,<sup>32</sup> which we used. To the best of author’s knowledge, there are no studies on the adhesive strength of these samples via AFM. Instead, the peel-off test is quite common for the quantification of adhesive strength. The adhesion between two planar substrates coated with PDADMAC/PSS was investigated in a study by lap shear measurements.<sup>64</sup> In addition, PGMA anchored PET substrate grafted with either PAA or PEI was investigated in a study where the adhesive strength was quantified via peel-off test.<sup>63</sup>

## 5.2. Experimental section

### 5.2.1. Materials

For the preparation of thin polymer-treated films, poly(ethylene terephthalate) (PET, DuPont Teijin Films, Melinex S/142 Gauge) substrates were used. Polyions used in this study are poly(ethyleneimine) (PEI, 50% w/v,  $M_w$  of 600-1000 kg/mol), poly(allylamine hydrochloride) (PAH,  $M_w \sim 70$  kg/mol), poly(sodium 4-styrenesulfonate) (PSS, 30 % w/v,  $M_w \sim 200$  kg/mol), poly(acrylic acid) (PAA, 25 % w/v,  $M_w \sim 50$  kg/mol), poly-L-glutamic acid (PGA,  $M_w \sim 15$ -50 kg/mol), poly(glycidyl methacrylate) (PGMA, 10 % w/v in MEK,  $M_w \sim 25$  kg/mol), and poly(diallyldimethylammonium chloride) (PDADMAC, 20 % w/v,  $M_w \sim 200$ -350 kg/mol).

PE solutions were prepared either in water (milliQ reversed osmosis water, purity 18.2 ohms.cm) or methanol ( $M_w$  of 32.04 g/mol) or 2-butanone (Methyl Ethyl Ketone, MEK, Chromasolv for HPLC, 99.7%) using NaCl (purity  $\geq 99.0$  %) or NaBr ( $M_w$  of 102.89 g/mol). Except for PAA and PGMA (Polyscience Inc.), NaBr salt (J.T. Baker) and methanol (Fisher Scientific Inc.), all the chemicals were purchased from Sigma-Aldrich.

### 5.2.2. Layer-by-Layer Deposition Method

A variety of PE solutions were used to prepare polyelectrolyte multilayer (PEM) thin films. Prior to any deposition steps, PET substrate was air-plasma treated (PDC-32G, Harrick Plasma Cleaner) for 20 minutes. The deposition of layers took place in HMS<sup>TM</sup> Series Programmable Slide Container (Carl Zeiss, Inc.). The layer-by-layer (LbL) deposition of multilayers is a well-established method<sup>2</sup> where oppositely charged polyelectrolytes are consecutively deposited on the substrate.

PEI-PGA-PAH sample was prepared from PE solutions of 1.0 mg/ml containing 0.5 M NaBr. After each PE deposition (30 minutes), the layers were rinsed with water twice (2 minutes each) and then dried for 10 minutes.

PDADMAC-PSS-PAH sample was prepared the same way using 1.5 mg/ml PE concentration, containing 0.5 M NaCl. Likewise other samples, PDADMAC<sub>5</sub>PAA<sub>5</sub> was prepared according to LbL deposition method at a PE concentration of 1.0 mg/ml and 1.0 M NaCl.

### 5.2.3. Grafting Method

The samples were prepared by grafting method and PET thin films were used as substrates. The method was discussed in detail elsewhere.<sup>63</sup> Briefly, an air plasma-treated PET substrate (20 minutes) was immersed into PGMA solution (0.1% w/v in MEK) for 30 minutes and dried in oven at 120°C for 2 hours. PGMA anchored PET substrate was then immersed into PAA solution (1% w/v in methanol, 1.0 M NaCl) for 20 minutes and annealed at 100°C for 40 minutes. In another case, instead of PAA, PEI solution (1% w/v in methanol, 1.0 M NaCl) was used (20 minutes) at an annealing temperature of 80°C for an hour. A variety of samples were prepared by changing the deposition time of PGMA (30, 60, and 90 minutes) and the choice of PAA or PEI solution.

### 5.2.4. AFM Force Measurements

Atomic force microscopy, NanoScope IIIa (Dimension 3100, Veeco Metrology Inc., Santa Barbara, CA), was used to quantify the adhesive strengths of the resulted thin films. A colloidal silica probe (1  $\mu\text{m}$  SiO<sub>2</sub> particles) functionalized with COOH surface chemistry was purchased from Novascan Technologies, Inc. The spring constant of the probe was 14 N/m. Force

measurements were carried out in air at a controlled humidity level ( $\sim 45\%$  RH). Five measurements from one spot on the sample were taken and by moving the cantilever to ten different locations on the sample in both x and y directions, fifty measurements were obtained. The raw force curves were processed with the assistance of self-written MATLAB® and Microsoft Excel scripts.

### 5.3. Results and discussion

#### 5.3.1. Adhesive strength of thin films prepared by the LbL deposition method

LbL-deposition of polyelectrolyte multilayers is a common method for producing thin films at controlled thickness. The adhesive strength of the films was quantified using AFM, in which the interactions between the film surface and a functionalized colloidal probe were investigated. For two of the samples, a precursor layer of PEI or PDADMAC was deposited. The samples created in this way were PEI-PGA-PAH and PDADMAC-PSS-PAH. On the other hand, the third sample was prepared without a precursor layer and five bilayers were deposited (PDADMAC<sub>5</sub>PAA<sub>5</sub>). In the present study, bilayer refers to polycation/polyanion pairs and layer is either polycation or polyanion.

Typical force-separation curves are presented in Figure 5.1. For all samples, one adhesion peak was observed. The common problem for each of them was having noise on both retraction and approach curves over a wide range, even though the effect is not seen clearly in this chosen scale. Some indentation at approach part was seen for both PEI-PGA-PAH and PDADMAC-PSS-PAH (Figure 5.1 a, b); however, the indentation at approach curves was more pronounced for PDADMAC<sub>5</sub>PAA<sub>5</sub> (Figure 5.1 c). The observed phenomena can be partly attributed to noise. Also, it can be interpreted as strong attractive forces between PE chains and COOH functional group of the probe.

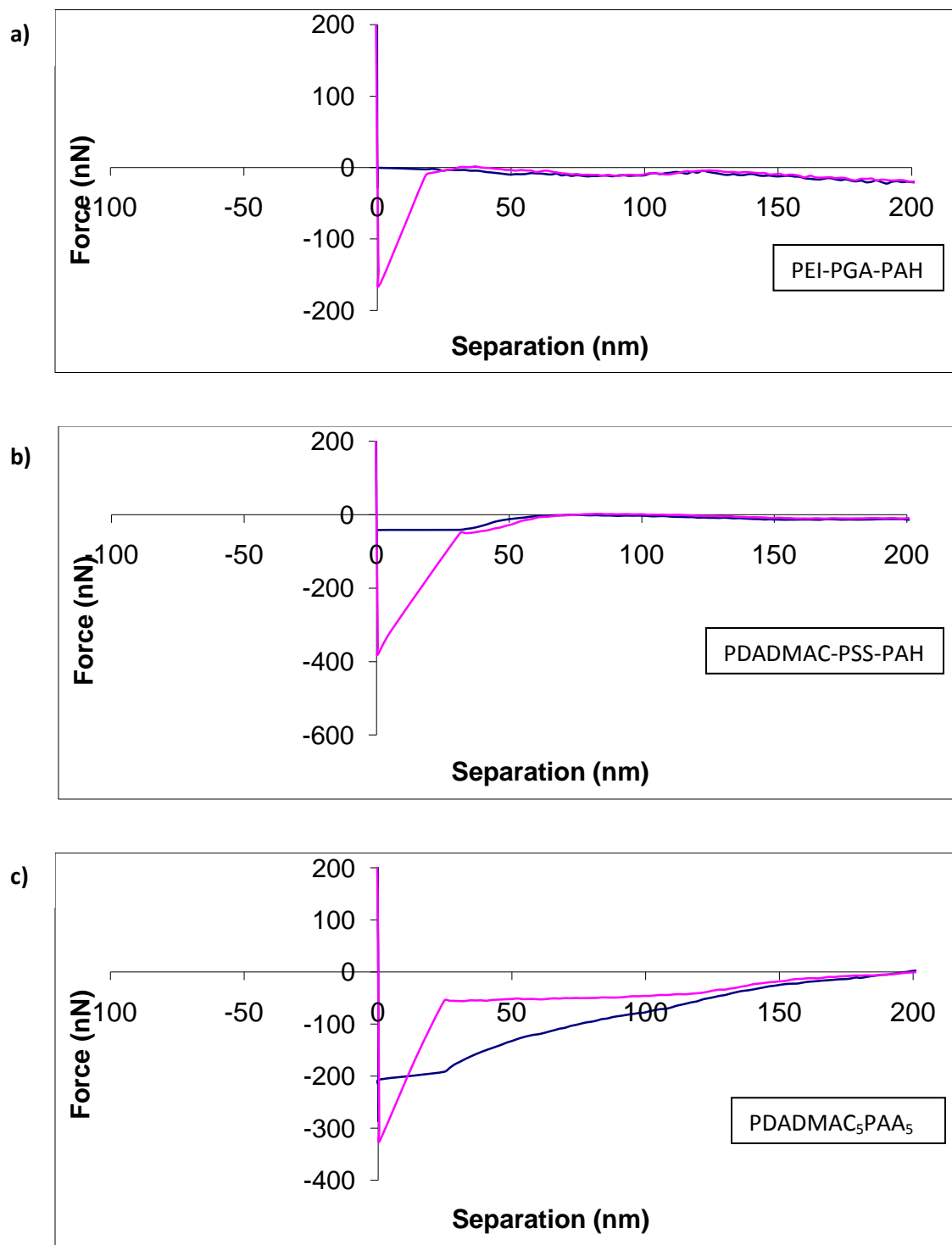


**Figure 5.1** Comparison of typical force-separation curves of a)PEI-PGA-PAH, b)PDADMAC-PSS-PAH, c)PDADMAC<sub>5</sub>PAA<sub>5</sub>.

The adhesion force distribution of each sample is compared in Figure 5.2. The frequency of adhesion forces of PDADMAC-PSS-PAH and PDADMAC<sub>5</sub>PAA<sub>5</sub> were close to each other at the observed adhesion force ranges. On the other hand, the frequency of adhesion force of PEI-PGA-PAH were higher compared to other samples' frequency at the lowest adhesion force range and lower at the higher adhesion force ranges.

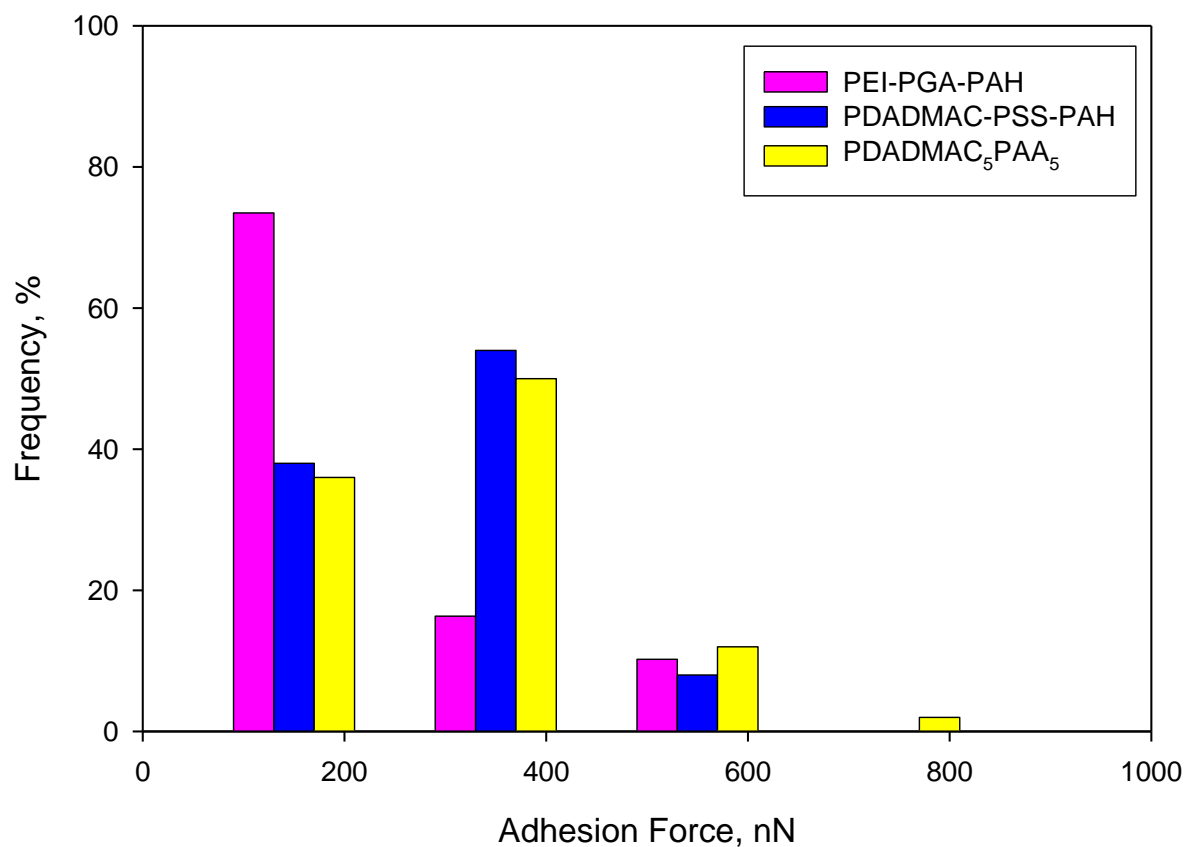


**Figure 5.2** Adhesion force distribution for samples PEI-PGA-PAH, PDADMAC-PSS-PAH, and PDADMAC<sub>5</sub>PAA<sub>5</sub>. Fifty measurements were collected for each sample at 45% RH using a functionalized colloidal silica probe.

Mean adhesion force values were obtained from fifty measurements and compared (Table 5.1). The lowest adhesive strength was observed for PEI-PGA-PAH. The mean adhesive strength of PDADMAC-PSS-PAH and PDADMAC<sub>5</sub>-PAA<sub>5</sub> was very close. These results show that not only the outermost layer of the thin film is important, but also the properties and features of the film are important at determining the adhesive strength. For PEI-PGA-PAH and PDADMAC-PSS-PAH, although the outermost layer was the same for the investigated interactions with a functionalized probe, the adhesive strengths differed. One can conclude that the choice of polyelectrolyte combinations plays an important role on the adhesive strength of the films. Anion-anion interactions were investigated for PDADMAC<sub>5</sub>PAA<sub>5</sub> while cation-anion interactions were present for the other two samples. The adhesive strength of PDADMAC<sub>5</sub>PAA<sub>5</sub> showed that the interactions between identical charges were as great as oppositely charged surface interactions. We obtained that competitive adhesive strength at the fifth bilayer. It is well established that the adhesion forces vary with a further deposition layer and the strength is usually low at the first layer deposition layer.<sup>52, 53</sup> Therefore, we believe that the adhesive strength at the first layer would be somewhat lower than 308.13 nN.

**Table 5.1** Comparison of mean adhesion forces for the samples.

Sample	Adhesion Force (nN)	
	mean	stdev
PEI-PGA-PAH	220.93	124.09
PDADMAC-PSS-PAH	303.24	115.58
PDADMAC <sub>5</sub> -PAA <sub>5</sub>	308.13	118.42

### 5.3.2. Adhesive strength of thin films prepared by the grafting method

PGMA was anchored to the PET substrate to modify the surface with the epoxy functionalities that would serve as reactive sites for the subsequent polymer attachments with functional groups such as carboxy and amino.<sup>63</sup> Burtovyy et al.<sup>63</sup> studied the grafting parameters (annealing temperature, and time, etc.) for PAA and PEI and the same values were used in the present study. Lower annealing temperature with a longer time (80°C & 1 hour) was used for PEI grafting compared to PAA grafting (100°C & 40 minutes). The reasons for these chosen parameters were related to PEI's lower glass transition temperature ( $T_g \sim 13^\circ\text{C}$ )<sup>81</sup> and the different reactivity of amino and carboxy groups towards the epoxy functionality.

For the ease of discussion, the samples will be called in a series of PGMA 1-6. Samples called PGMA 1, PGMA 2, and PGMA 3 were prepared at PGMA grafting times of 30, 60, and 90 minutes, respectively, with a subsequent PAA grafting. Similarly, PGMA 4, PGMA 5 and

PGMA 6 were prepared at an increased deposition time of PGMA and a further grafting of PEI (Table 5.2).

**Table 5.2** Grafted thin films prepared with a different choice of PGMA grafting time and a polyelectrolyte for the subsequent grafting.

Sample	Grafting time of PGMA anchoring layer (min)	Polyelectrolyte for subsequent grafting
PGMA 1	30	PAA
PGMA 2	60	PAA
PGMA 3	90	PAA
PGMA 4	30	PEI
PGMA 5	60	PEI
PGMA 6	90	PEI

The adhesive strength of the samples was determined by their interactions with a functionalized colloidal probe via AFM. Subsequent polymer attachments to the modified PET substrate resulted in different functional groups at the outermost layer that interact with the probe. While identical charge interactions were investigated for PGMA 1 through 3, oppositely charged interactions took place at the investigations for PGMA 4 through 6.

The adhesive strength of the samples was quantified by the lowest point of the adhesion peaks from the retraction curves. For all samples, only one single peak was observed. However, the peaks were in a different behavior than our earlier observations for PEM thin films (Chapters I and II). For this reason, we chose a sample from the previous chapters that would represent the

typical adhesion peak behavior and compared with a typical retraction curve of PGMA series. The comparison of retraction curves from PGMA 1-6 series and PEM thin film can be seen in Figure 5.3. The common property of the adhesion peaks for LbL deposited PEM thin films was a single sharp peak (Figure 5.3 a). However, there were many problematic curves obtained for PGMA series. The most pronounced problem was twisting of the adhesion peak at the lowest point (Figure 5.3 b). We believe that this problem is related to AFM: Probably the limit of position sensitive photodetector was exceeded at some point and the deflection was collected as constant at these conditions. Furthermore, approach curves seemed to be different than those for PEM thin films; very huge indentations were observed for PGMA series. The reasons for such these differences are not known yet and need to be further investigated. However, one thing is clear that both retraction and approach curves of grafted films behaved differently than those LbL deposited PEM films so far (Chapters I and II).

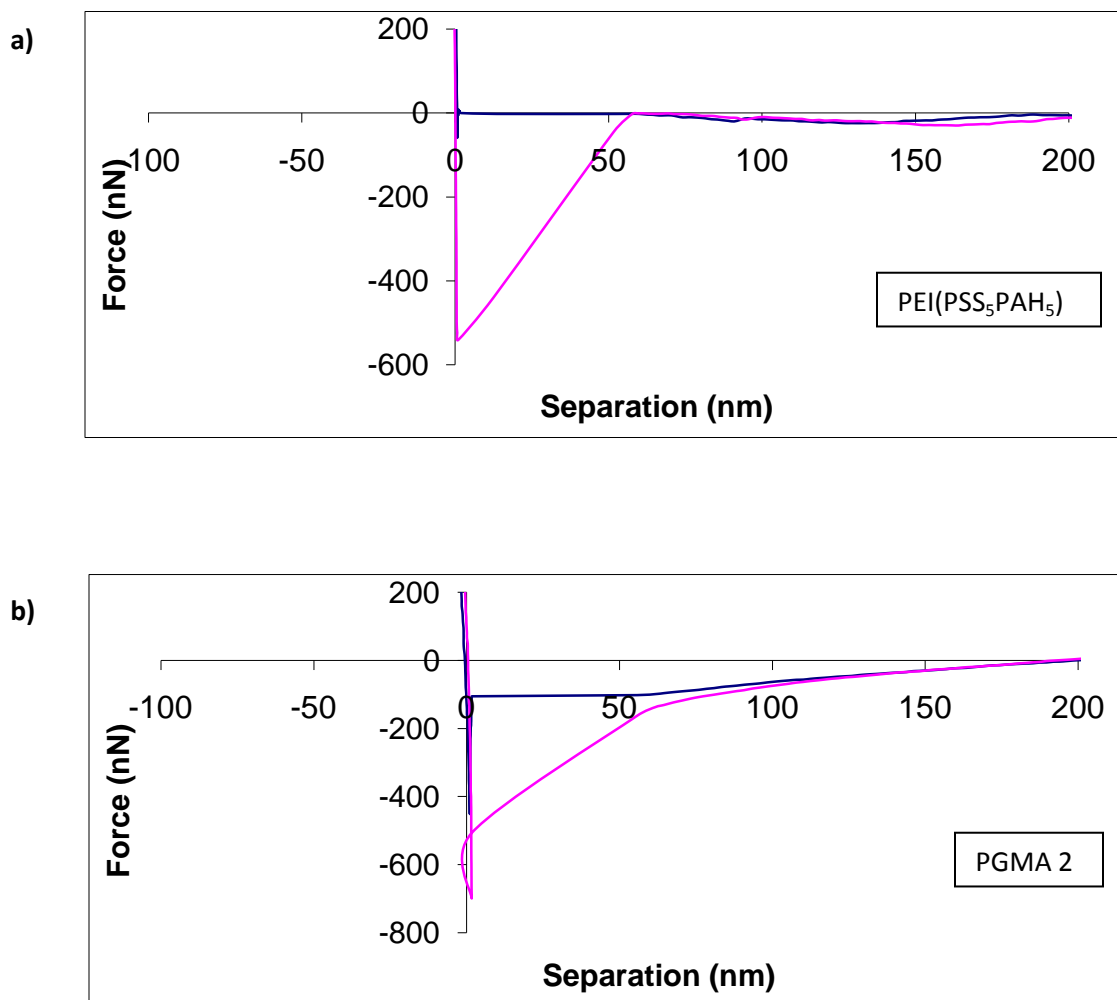


**Figure 5.3** Comparison of typical force-separation curves of a) PEM thin film [PEI(PSS<sub>5</sub>PAH<sub>5</sub>), 1.0 M NaCl], with problematic curves observed for PGMA series, b) PGMA 2.

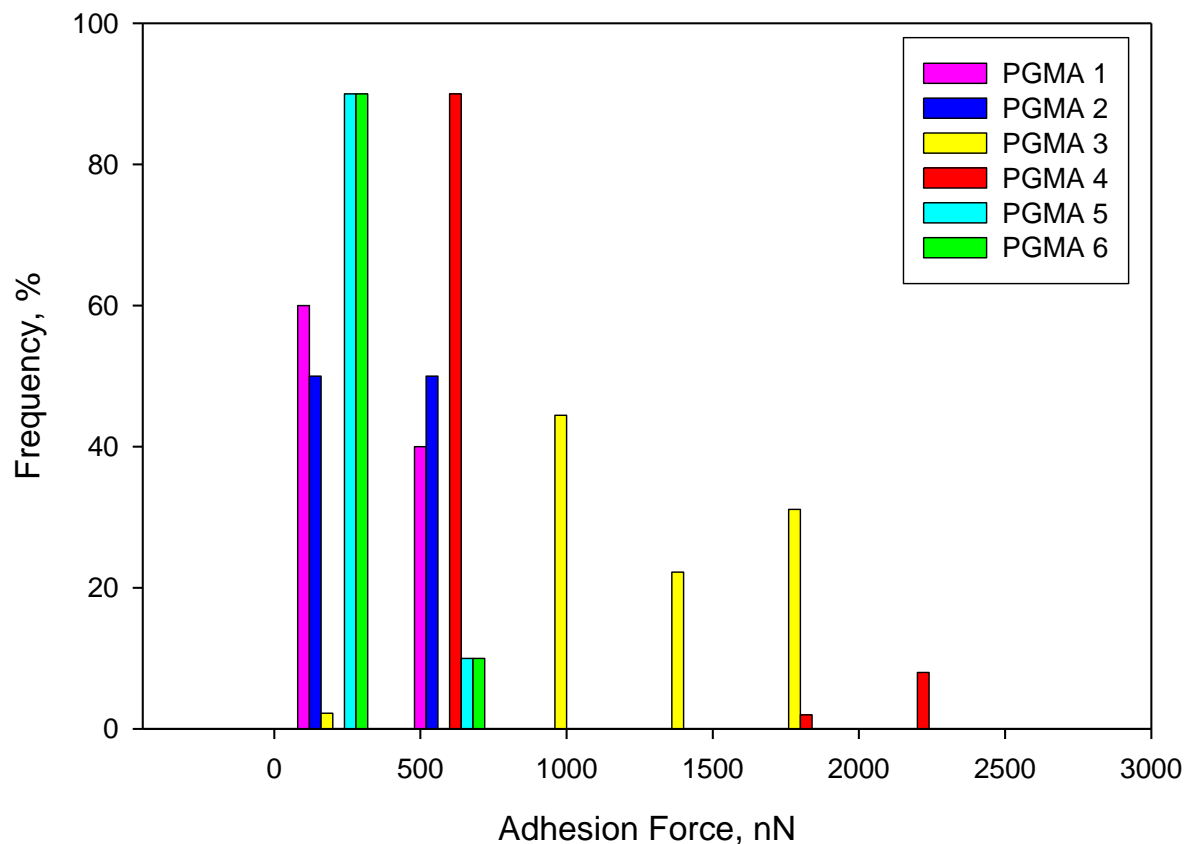


**Figure 5.4** Adhesion force distribution for samples PGMA 1 through PGMA 6. Fifty measurements were collected for each sample at 45% RH using AFM and functionalized colloidal silica probe.

Two parameters at the sample preparation conditions played an important role on the adhesive strength of the samples: PGMA grafting time and the choice of polyelectrolyte solution for the further grafting. PGMA grafting time had a pronounced effect for the samples prepared from PAA solution (Figure 5.4). Adhesion forces were distributed at closer values for PGMA 1 and PGMA 2 while PGMA 3 exhibited very high adhesion forces, further from those samples' distribution. The adhesion forces of PGMA 3 were generally around 1000-1800 nN. Increasing

the grafting time did not help to improve the adhesive properties of films prepared from PEI solution. The distribution of adhesion forces for PGMA 5 and PGMA 6 was almost the same. On the other hand, PGMA 4 showed higher adhesion forces compared to PGMA 5 and PGMA 6. Some percentage of the adhesion forces of PGMA 4 was as great as 2000 nN. From the comparison of all the samples, one can see that the greatest adhesive forces were obtained mainly for PGMA 3 and partly for PGMA 4.

The mean adhesion forces were compared for all the samples (Table 5.3). PGMA grafting time of 90 minutes and PAA grafting (PGMA 3) exhibited the greatest adhesive strength. Then the second large adhesion force was obtained for PGMA 4 where a deposition time of 30 minutes and PEI grafting took place. Other than these samples, the rest showed pretty average adhesion forces.

**Table 5.3** Comparison of mean adhesion forces for PGMA series.

Sample	Adhesion Force (nN)	
	mean	stdev
PGMA 1	449.21	146.43
PGMA 2	398.83	209.06
PGMA 3	1358.64	378.28
PGMA 4	724.01	449.85
PGMA 5	255.12	111.73
PGMA 6	214.44	121.72

The discrepancy on the adhesive strengths of PGMA 1-3 and PGMA 4-6 was noticed. The thin films prepared with a subsequent grafting of PAA exhibited much greater adhesive strength than those prepared with PEI subsequent grafting, except for PGMA 1 versus PGMA 4. These results can be attributed to the different reactivity of carboxy and amino groups towards the epoxy group of PGMA at the defined conditions. As a consequence, the films are resulted in different structures and properties.

The permeability of PGMA anchored PET membranes with a subsequent grafting of either PAA or PEI were investigated in a study.<sup>63</sup> The PGMA modified membrane with further polymer grafting had lower permeability due to the decreased size of pores. However, the test showed that the grafted polymers were present on the membrane surface and they did not block the pores. The adhesive strength of PGMA anchored PET membranes and unmodified PET membranes were compared using peel-off test.<sup>63</sup> Higher adhesion strength ( $\sim 20$  N/m) was obtained for the membranes modified with PGMA anchoring layer than those for the unmodified membranes. Our results could not be compared directly to the adhesive strength obtained via peel-off test since the techniques are different and investigate the interactions at different scales. However, we also concluded that the sample prepared via 'grafting to' method had a greater strength than those PEM thin films.

In summary, the greater adhesive strength was obtained for a grafted film (PGMA 3) rather than LbL film. This might be attributed to the existence of polymer brushes on the surface that interact with the probe.

## 5.4. Conclusions

In the present study, the adhesive strength of thin films was investigated using AFM and a functionalized colloidal probe. The films were prepared via either LbL deposition method or grafting. The mean adhesive strength of PEI-PGA-PAH, PDADMAC-PSS-PAH, and PDADMAC<sub>5</sub>PAA<sub>5</sub> was pretty close and it was 220.93, 303.24, and 308.13 nN, respectively. From this first section, it was concluded that even one layer deposition could be enough for the desired adhesive strength by a right choice of PE combination. In addition, the adhesive strength of PDADMAC<sub>5</sub>PAA<sub>5</sub> showed that the interactions between identical charges were as great as oppositely charged surface interactions.

Furthermore, grafting method was successfully applied on PET substrates with PGMA anchoring and further grafting of PAA or PEI. The adhesive strength of PGMA series was dependent on the PGMA grafting time and the choice of PE for the subsequent grafting. PGMA 3 (PGMA grafting time of 90 minutes, PAA grafting) showed the highest adhesion force at 1358.64 nN among the series.

Comparison of all the samples showed that the greatest adhesive strength was obtained for a grafted film. This was attributed to the existence of polymer brushes on the surface. Moreover, in this chapter, the scope of research on adhesion forces was expanded studying different samples and techniques.

## 6. Chapter IV: The Effect of Relative Humidity on the Adhesion Force Measurements

### 6.1. Introduction

Atomic force microscopy (AFM) is a great tool to probe the interactions between a tip and a sample at high resolution and at various environments such as ambient condition, liquid, or vacuum, and etc. The magnitude of adhesive forces can be different for different working environments: Adhesion forces obtained in a liquid environment are typically 1 or 2 orders of magnitude less than the ones in air.<sup>82</sup> Even the results obtained in air can differ due to capillary forces in very humid conditions. The control of humidity plays an important role when the molecular interactions are probed. There are several studies conducted on the effect of relative humidity (RH) on adhesion forces.<sup>67, 83-85</sup>

It is well established that capillary forces become significant at high RH values. There is a disagreement on the dependence of adhesion forces on RH for the studies on mica.<sup>84</sup> While some studies suggested that adhesion was affected by RH as low as 25-30%,<sup>86</sup> others showed that this effect was significant at ~80%.<sup>87</sup>

In the present study, we performed adhesion force measurements on clean glass slides at both low (24% RH) and high RH values (45% and 50% RH). We studied the effect of RH on the adhesion force measurements. The present study helped us to determine the best conditions to work at while conducting force measurements in air. Furthermore, a comparison was made for the adhesion forces of PEI(PSS/PAH) samples at 28% and 42% RH.

## 6.2. Experimental Section

### 6.2.1. Preparation of Samples

Glass slides (Corning® Glass Microslides, precleaned) were cleaned according to this protocol: Slides were immersed in 3:1 (v/v) HCl/HNO<sub>3</sub> solution for 30 minutes and rinsed with ultrapure water. Further, the slides were treated with piranha solution (7:3 (v/v) H<sub>2</sub>SO<sub>4</sub>/H<sub>2</sub>O<sub>2</sub>) for 30 minutes. Prior to AFM force measurements, the clean glass slides were dried with a stream of N<sub>2</sub> gas. HCl (12.1 M or N) and HNO<sub>3</sub> (68% in aq) were purchased from EMD Chemicals Inc. H<sub>2</sub>SO<sub>4</sub> (96.9% in aq) and H<sub>2</sub>O<sub>2</sub> (35% in aq) were purchased from Fischer Scientific Inc. and Alfa Aesar, respectively.

PEI(PSS/PAH) samples were prepared according to layer-by-layer deposition method, as discussed in previous chapters. Instead of PET substrate, glass slides were used for the fabrication of thin films. After a precursor layer of PEI, 20, 40, or 60 bilayers of PSS/PAH were deposited on the glass substrates, respectively.

### 6.2.2. AFM Force Measurements

Atomic force microscopy, NanoScope IIIa (Dimension 3100, Veeco Metrology Inc., Santa Barbara, CA), was used to quantify the adhesion forces. For each sample, 25 force measurements were carried out at five different spots where 5 cycles were collected from each. Stiff cantilevers with a spring constant of 20-80 N/m (Veeco, TESPA) were used for the force measurements. The raw force curves were processed using MATLAB® and Microsoft Excel scripts.

In our AFM room, the humidity was usually around 25% or less and sometimes even higher. The variation of humidity was inevitable, so that we decided to test the effect of humidity on the adhesion forces. For this reason, we chose three different RH levels; one was the typical relative humidity obtained in the AFM room, 24% RH. Another humidity levels were chosen as 45% and 50% RH. To adjust the humidity in the AFM room, a humidifier (Air O Swiss) was used. We conducted 3 sets of experiment at each determined RH and collected 25 force measurements from each.

### **6.3. Results and Discussion**

#### **6.3.1. Effect of humidity on the adhesion forces of clean glass slides**

We performed force measurements on a clean glass slide at various relative humidity (RH) values. The adhesion forces obtained at 24% RH were at a considerably broad range, 400-3000 nN (Figure 6.1). Even though the distribution of adhesion forces was almost at the same range, the percentages of those values differed between each set of experiment. Then we moved on the second humidity level, which was 45% RH. The distribution of adhesion forces was at a relatively lower range compared to the results from 24% RH (Figure 6.2). The adhesion forces varied between 200 nN and 900 nN. Except 20% of data in experiment 1, the adhesion forces in each experiment set were in a close proximity.

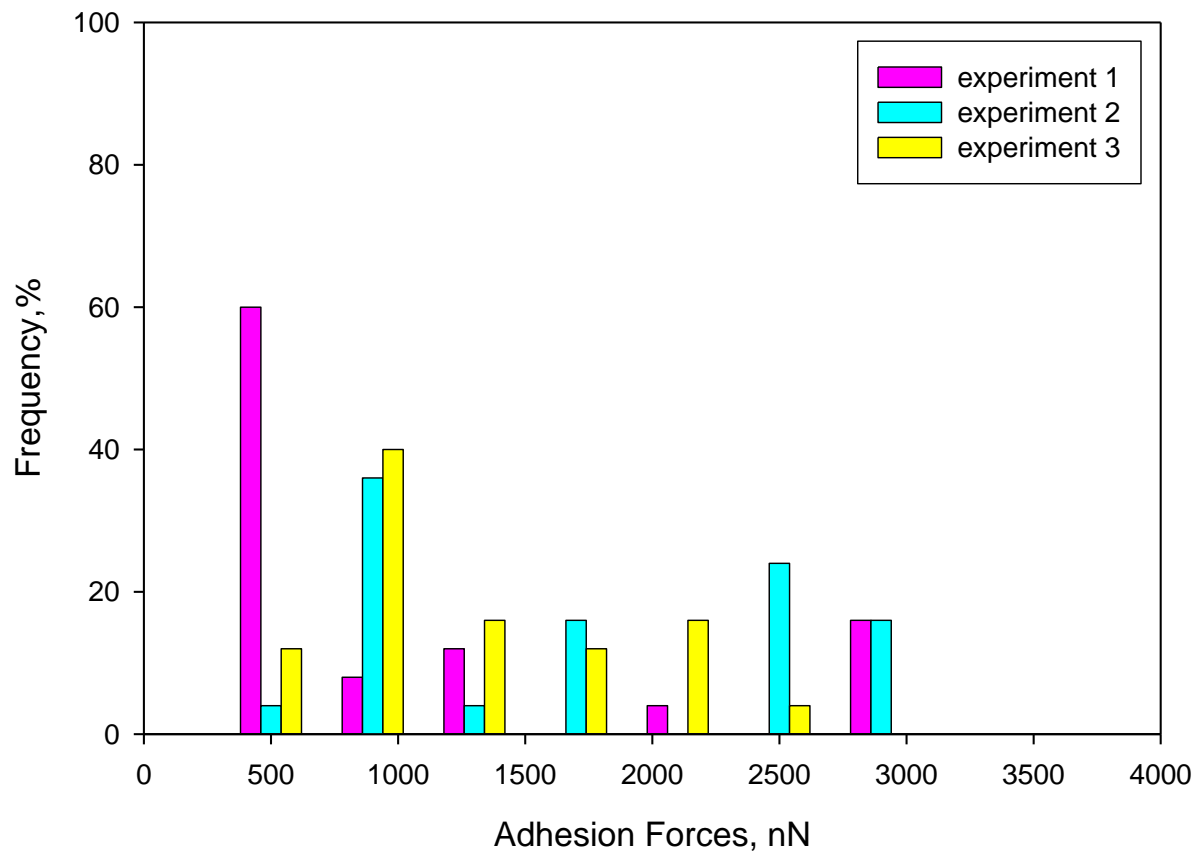


**Figure 6.1** Adhesion force distribution for a clean glass slide at 24% RH. Twenty-five force measurements were collected per experiment.

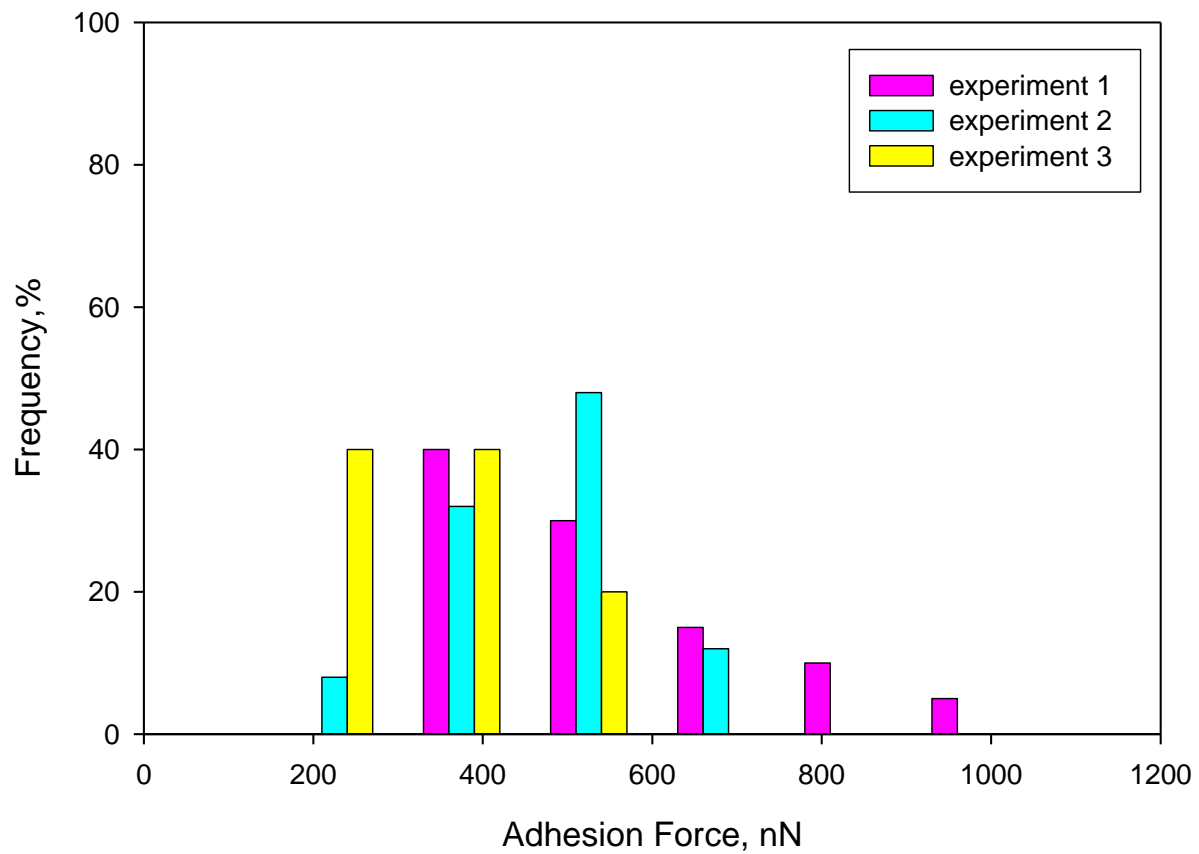


**Figure 6.2** Adhesion force distribution for a clean glass slide at 45% RH. Twenty-five force measurements were collected per experiment.

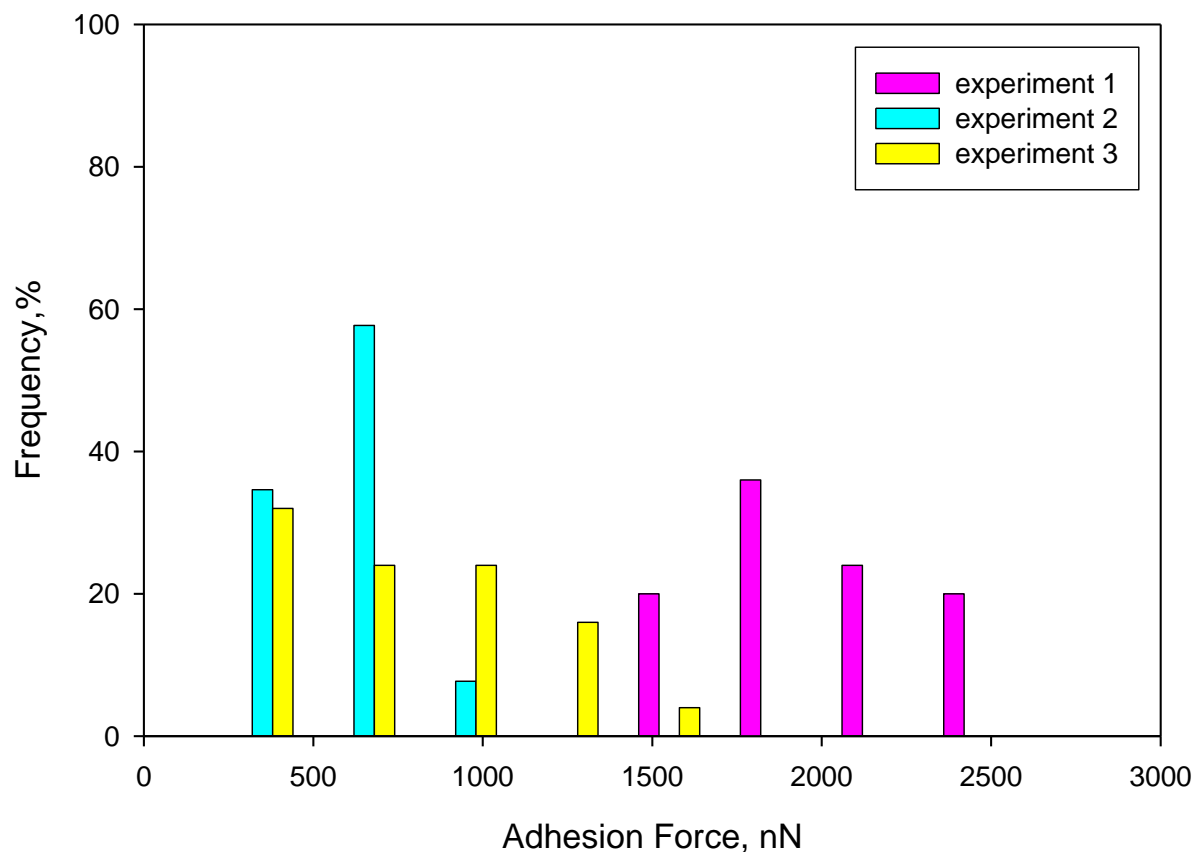


**Figure 6.3** Adhesion force distribution for a clean glass slide at 50% RH. Twenty-five force measurements were collected per experiment.

However, the scenario was a little bit different for 50% RH. The adhesion force distribution for each set of experiments was in a different range with some overlapping on experiments 2 and 3. The adhesion forces obtained in experiment 1 were much higher than experiments 2 and 3. Furthermore, we continued to analyze the adhesion forces by comparing the retraction curves. We selected ten force measurements out of twenty-five in each set of experiment and compared them. We were interested in the behavior of adhesion peaks where the reproducibility of those peaks was the criteria. At 24% RH, the reproducibility of the adhesion

peaks was not good, since many variations were observed considering thirty force curves (Figure 6.4). The variation was much less pronounced in 45% RH and 50% RH (Figures 6.5 and 6.6). Among high relative humidity results, 45% RH exhibited slightly better reproducibility (Figure 6.5). Most of the force curves accumulated at one spot and the number of variations much lesser.

Combining the results from both adhesion force distribution and retraction curves, we concluded that it was more reliable to work at 45% RH. Thio et al.<sup>58</sup> also briefly mentioned setting the relative humidity to a constant value while performing force measurements using AFM in air. They stated that a variation of typical relative humidity values (20-35%) in the lab conditions led to cases of unwanted electrostatic potential forces. For this reason, they performed AFM force measurements at room temperature, 45% RH. Higher humidity levels are risky since capillary force effects can be significant, however they tend to occur above 65% RH.<sup>59</sup>

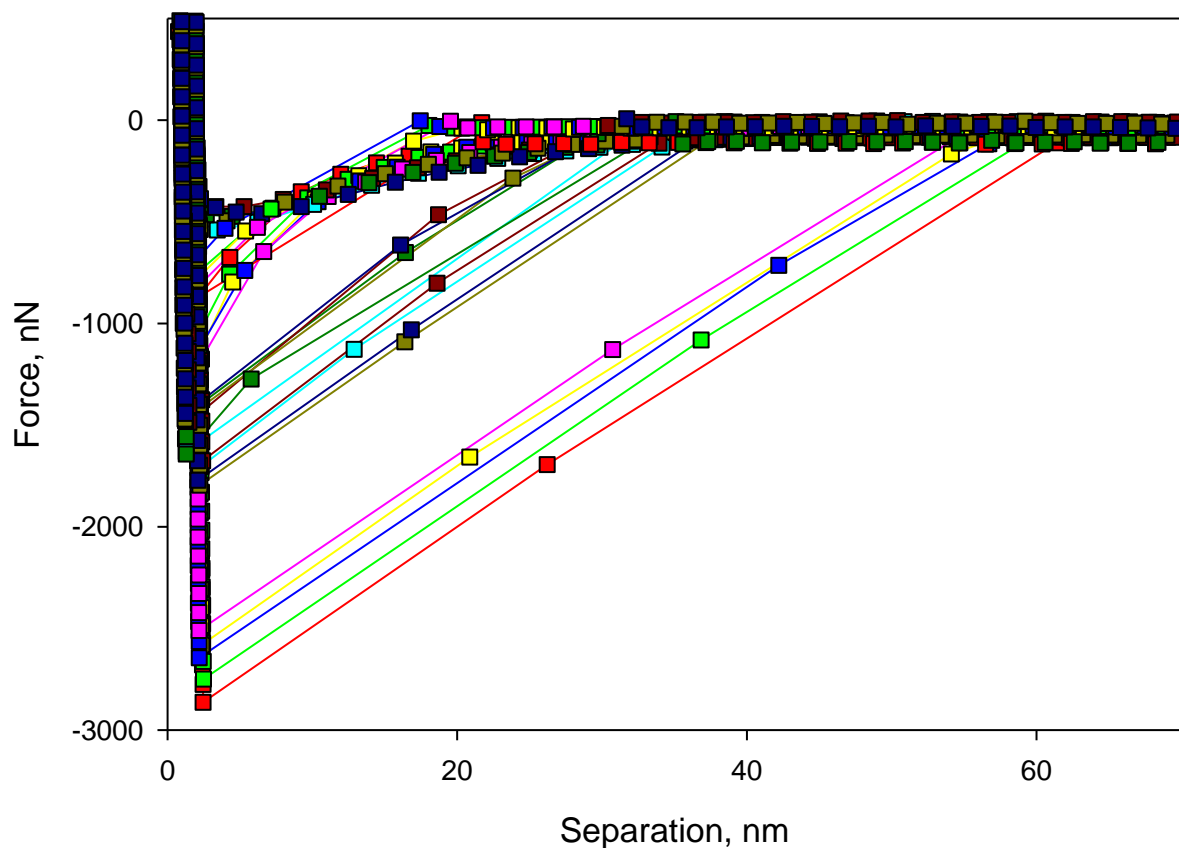


**Figure 6.4** Retraction curves of a clean glass slide at 24% RH. Ten out of twenty-five force measurements from each set of experiment were selected and compared by their retraction part. From one to ten, each force curve was represented with a different color. The order of representation of each color was same for each set of experiment, resulting the same color to be used three times.

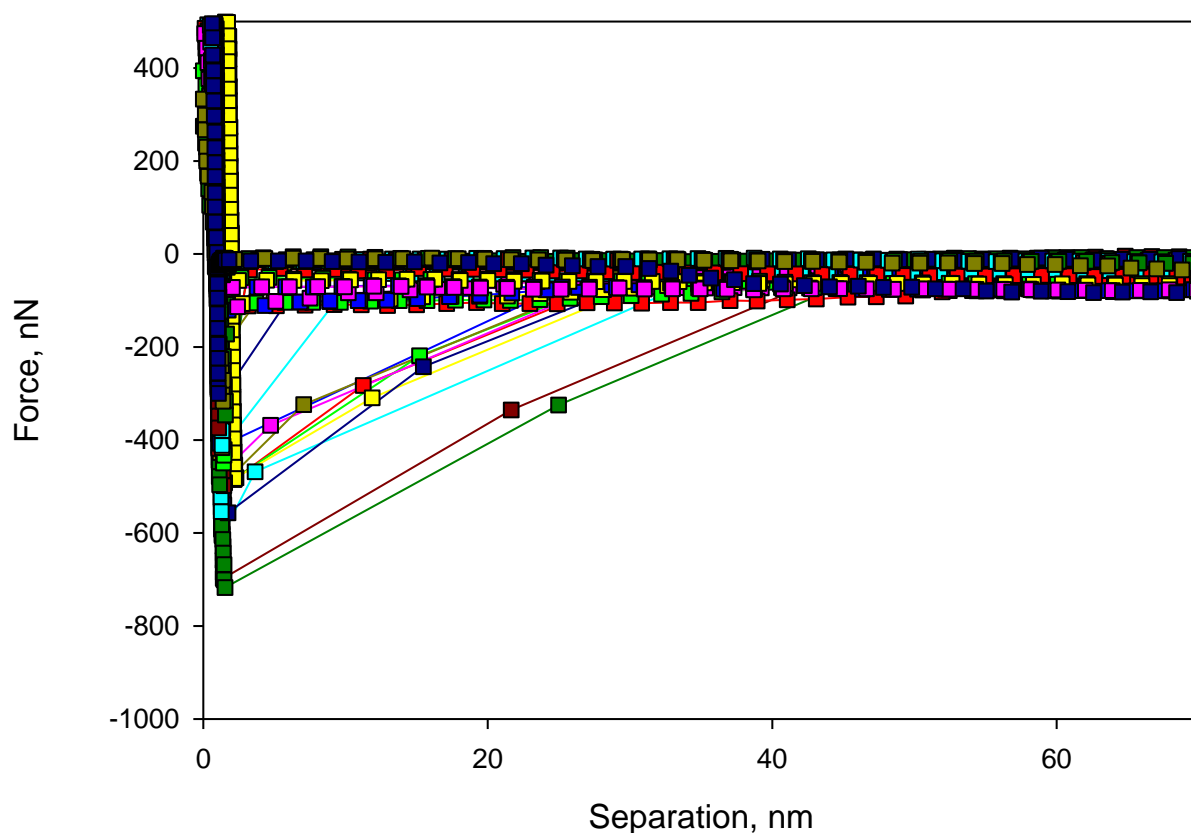


**Figure 6.5** Retraction curves of a clean glass slide at 45% RH. Ten out of twenty-five force measurements from each set of experiment were selected and compared by their retraction part. From one to ten, each force curve was represented with a different color. The order of representation of each color was same for each set of experiment, resulting the same color to be used three times.

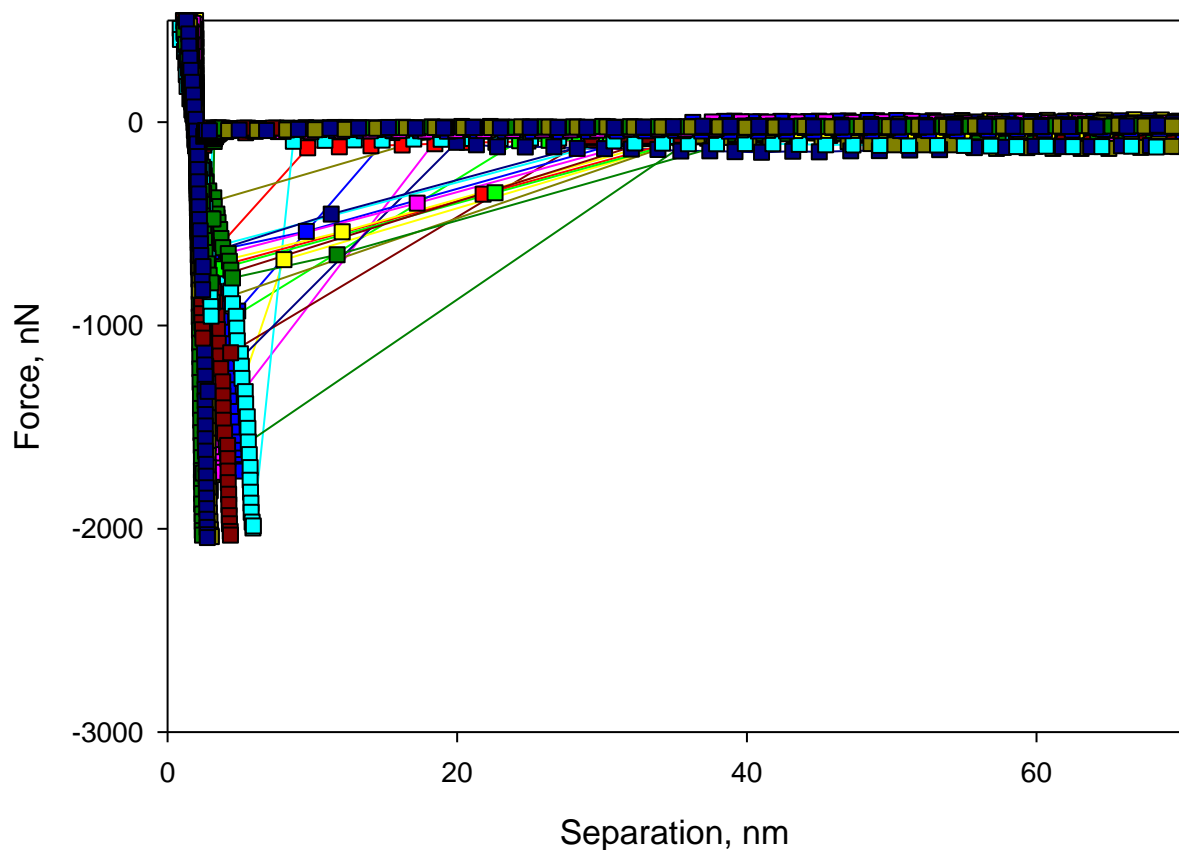


**Figure 6.6** Retraction curves of a clean glass slide at 50% RH. Ten out of twenty-five force measurements from each set of experiment were selected and compared by their retraction part. From one to ten, each force curve was represented with a different color. The order of representation of each color was same for each set of experiment, resulting the same color to be used three times.

### 6.3.2. Effect of humidity on the adhesion forces of PEI(PSS/PAH)

Another study on the effect of relative humidity was carried on PEI(PSS<sub>x</sub>PAH<sub>x</sub>) samples where x varied as 20, 40, and 60. AFM force measurements were performed at both 28% and 42% RH. Adhesion force distribution of each sample can be seen in Figure 6.7. Except for PEI(PSS<sub>20</sub>PAH<sub>20</sub>) at 28% RH, the adhesion forces were low and accumulated at a very narrow range (Figure 6.7, a). While adhesion forces of 20 bilayers reached to ~900 nN, those were only around 200 nN for 40 and 60 bilayers. On the other hand, broader adhesion force distribution at a considerably larger adhesion values were obtained at 42% RH, for the same samples (Figure 6.7, b). This time, adhesion forces at as great as 600 nN could be obtained for 40 and 60 bilayers. It was also evident from the mean adhesion values that higher adhesion forces were obtained at 42% RH (Table 6.1). The observed phenomenon shows that it is very important to control the humidity while performing force measurements in air. Even though we are confident that capillary forces are not significant at the studied RH values, variations on adhesion forces are inevitable at different humidity levels which can be a problem while determining the adhesive strength of samples.

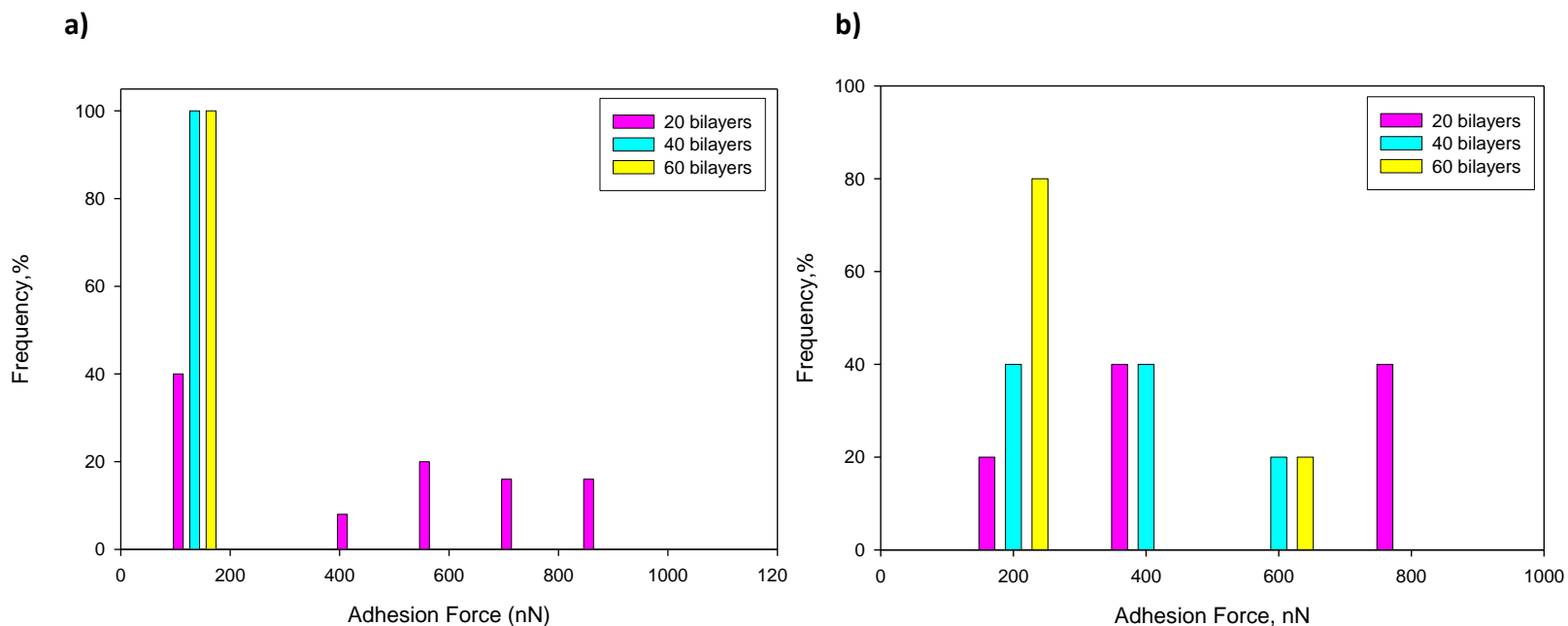


**Figure 6.7** Adhesion force distribution for PEI(PSS<sub>20</sub>PAH<sub>20</sub>), PEI(PSS<sub>40</sub>PAH<sub>40</sub>), and PEI(PSS<sub>60</sub>PAH<sub>60</sub>) at a) 28% RH, and b) 42% RH. Each color represents different sample. Twenty-five measurements were obtained for each sample.

**Table 6.1** Mean adhesion forces for PEI(PSS/PAH) at different humidity levels.

Number of bilayers	Adhesion force (nN) at 28% RH		Adhesion force (nN) at 42% RH	
	mean	stdev	mean	stdev
20	452.95	305.80	493.40	250.84
40	154.47	27.36	364.52	166.59
60	102.05	21.82	282.87	141.26

## 6.4. Conclusions

The effect of relative humidity on the adhesion forces was investigated using AFM in air at room temperature and various humidity levels. Force measurements were performed at both low and high relative humidity values and the adhesion forces were compared. First, clean glass slide was used on which 3 sets of force measurements were performed at 24%, 45%, and 50% RH. Both adhesion force distribution and retraction curves were analyzed in detail for better comparison. The reproducibility of adhesion forces was the criteria and the results from 45% RH exhibited the best case; there were not many variations on the retraction curves and the distribution of adhesion forces for each set of experiment was at a close proximity. 45% RH was also safe to work at since the capillary force becomes significant above 65% RH.<sup>59</sup> Furthermore, the effect of relative humidity on the adhesion forces of PEI(PSS<sub>x</sub>PAH<sub>x</sub>) samples was compared, where x was 20, 40, and 60. Adhesion force distribution varied for 40 and 60 bilayers at different humidity levels (28% and 42% RH) while relatively close adhesion force values was obtained for 20 bilayers. Comparison of mean adhesion forces showed that the adhesive strengths were higher at 42% RH. Evident from the first section, the discrepancy on adhesion forces at different RH values resulted from the change of the working environment. To conclude, controlling the relative humidity is very important while conducting force measurements under ambient conditions, since one can predict different adhesive strengths of the sample.

### 7. Conclusions and Future Work

The adhesive strength and morphology of PEMs were investigated using AFM throughout this study. It was acknowledged that the properties of PEMs were governed by several parameters such as the choice of polycation/polyanion pair, the ionic strength of the PE solution, salt type used during the build-up process, etc. We showed that not only the properties of the PEMs played an important role in the determination of their adhesive strength, but in addition, the properties of the environment where the interactions were being probed were also important. Since all experiments were conducted at room temperature in air, humidity was strictly controlled at all times. The choice of probe was also an important parameter in the determination of adhesive strength. We demonstrated the dependence of adhesion forces on 3 different types of colloidal silica probes. Ultimately, we attempted to show the effect of several different variables on the adhesion forces in order to substantiate understanding of the interactions between PEM-covered surfaces probed by this AFM and colloidal probe technique. A brief summary of the results discussed in each chapter follows.

In Chapter I, we studied the interactions between oppositely charged surfaces, comprised of a positively charged outermost layer of PEMs and a negatively charged colloidal probe, using AFM under ambient conditions at 45% relative humidity (RH). We investigated the effect of ionic strength and salt type on the adhesion forces, morphology, and roughness of PEI(PSS/PAH) PEMs at the 5<sup>th</sup> and 10<sup>th</sup> bilayers. The samples prepared from NaCl and NaF salts showed the greatest adhesive strength. The highest adhesion force was 489.12 nN which was for PEI(PSS<sub>10</sub>PAH<sub>10</sub>) sample prepared from 0.5 M NaF salt. On the other hand, the poorest adhesive strength was observed for the samples prepared from NaBr salt. We showed that by tuning the

## Conclusions and Future Work

---

salt type, concentration and deposition number, it was possible to fabricate PEM thin films with the desired adhesive strength and roughness.

In Chapter II, we studied the effect of probe on the adhesive strengths of PEM thin films using 3 different types of probes. The adhesive strengths of PEI(PAA<sub>5</sub>PAH<sub>5</sub>) were always greater than those of PEI(PSS<sub>6</sub>PAH<sub>6</sub>). The highest adhesive strength, 2209.76 mN/m, was obtained for PEI(PAA<sub>5</sub>PAH<sub>5</sub>) with a bare probe. On the other hand, the lowest adhesive strengths were obtained with functionalized probes. In addition, we found a correlation between the pull-off force magnitude (nN) and range (nm). Greater adhesive strengths were always obtained at larger pull-off forces. To conclude, we demonstrated the dependence of adhesive forces on the choice of probe as well as the properties of the sample. Considering the series of probes used in this study, we were able to show the interactions between two PEM-covered surfaces.

In Chapter III, we studied the adhesive strengths of thin films prepared via the LbL deposition technique and ‘grafting to’ method. Different PEs and PE combinations not studied in previous chapters were used. The measured adhesive strengths of LbL deposited samples, namely PEI-PGA-PAH, PDADMAC-PSS-PAH, and PDADMAC<sub>5</sub>PAA<sub>5</sub>, were in close proximity, 220.93, 303.24, and 308.13 nN, respectively. The results showed that even one layer deposition was good enough to obtain sufficient adhesive strength with the correct choice of PE combination. Furthermore, great adhesive strength (1358.64 nN) was obtained for PGMA 3 prepared via the ‘grafting to’ method. PGMA grafting time and the choice of PE for the subsequent grafting played an important role in the PGMA series. The high adhesive strength obtained via the ‘grafting to’ method was attributed to the polymer brushes on the sample surface.

## Conclusions and Future Work

---

In Chapter IV, we investigated the effect of relative humidity (RH) on the adhesion force measurements using AFM in air. For this reason, clean glass slides were used as substrates and force measurements were performed at 24%, 45%, and 50% RH settings in which 3 sets of experiments were carried out. From the comparisons of adhesion force distribution and retraction curves, it was concluded that 45% RH was the best setting: the distribution of each set of experiments were at a close proximity and there were not many variations on the retraction curves. As a consequence of this uniformity the results at this humidity level were the most stable and reproducible. Furthermore, the importance of relative humidity was reinforced by comparing adhesive strengths at 28%RH and 42%RH for the samples of PEI(PSS/PAH) at 20<sup>th</sup>, 40<sup>th</sup>, and 60<sup>th</sup> bilayers.

To conclude, we succeeded in preparing PEM thin films with great adhesive strength: as high as ~2000 mN/m. For further research in this study, we suggest that the spray method be used instead of the dipping method for the fabrication of PEMs. We believe that the spray method would save substantial time in the preparations of samples. Even higher multilayer numbers can be achieved at more convenient times.

In addition, it would be interesting to conduct experiments on polyanion-terminated samples and study the interactions between negatively charged surfaces systematically, as in Chapter II. For instance, the effect of different probe types on the adhesion force measurements in the case of PEI(PAA<sub>6</sub>PAH<sub>5</sub>) and/or PEI(PSS<sub>6</sub>PAH<sub>5</sub>) PEMs would give a strong basis of comparison with the results of Chapter II. With this comparison, one would be well equipped to determine the role of electrostatic interactions on the measured adhesive strengths. Moreover, a detailed study with an emphasis on the modeling of adhesion forces can help to determine the contribution of each type of forces and shed some more light on these results.

## Conclusions and Future Work

---

The current state of Polyelectrolyte Multilayer research is expansive and further development of the field appears promising. PEMs and LbL deposition technique are of great interest to polymer science and the field has been rapidly expanding in many application areas. For instance, interest in biodegradable polyelectrolytes such as poly(L-glutamic acid) (PGA), poly(L-lysine) (PLL), hyaluronan (HA) etc. has been increasing since these PEs were demonstrated to allow creation of biomimetic architectures. Biodegradable polyelectrolytes are also strong candidates for various biomedical applications such as in drug delivery, tissue engineering, etc. Due to the flexibility of incorporation of any type of material to the fabrication of LbL deposited thin films, the field will continuously expand and more products will find their places in the market.

### 8. References

1. Decher, G.; JD, H.; J, S., Buildup of ultrathin multilayer films by a self-assembly process
3. Consecutively alternated adsorption of anionic and cationic polyelectrolytes on charged surfaces. *Thin Solid Films* **1992**, 210, 831-835.
2. Decher, G., Fuzzy Nanoassemblies: Toward Layered Polymeric Multicomposites. *Science* **1997**, 277, 1232-1237.
3. Blodgett, K. B., *J. AM. CHEM. SOC.* **1934**, 56, 495.
4. Iler, R. K., Multilayers of colloidal particles *Journal of Colloid and Interface Science* **1966**, 21, 569-594.
5. Decher, G.; Schmitt, J., Fine-tuning of the film thickness of ultrathin multilayer films composed of consecutively alternating layers of anionic and cationic polyelectrolytes. *Prog. Colloid Polym. Sci.* **1992**, 89, 160-164.
6. Hammond, P. T., Form and Function in Multilayer Assembly: New Applications at the Nanoscale *Adv. Mater.* **2004**, 16, 1271-1293.
7. Decher, G.; Schlenoff, J. B., *Multilayer Thin Films: Sequential Assembly of Nanocomposite Materials*. Wiley-VCH: Weinheim, Germany, 2003.
8. Bertrand, P.; Jonas, A.; Laschewsky, A.; Legras, R., Ultrathin polymer coatings by complexation of polyelectrolytes at interfaces: suitable materials, structure and properties. *Macromol. Rapid Commun* **2000**, 21, 319-348.
9. Decher, G. *An Introduction to Polyelectrolyte Multilayers*; Institut Charles Sadron: Strasbourg.

## References

---

10. Schlenoff, J. B., Retrospective on the Future of Polyelectrolyte Multilayers. *Langmuir* **2009**, *25*, 14007-14010.
11. Claesson, P. M.; Dedinaite, A.; Rojas, O. J., Polyelectrolytes as adhesion modifiers. *Advances in Colloid and Interface Science* **2003**, *104*, 53-74.
12. Zhang, J.; Pelton, R.; Wagberg, L.; Rundlof, M., The effect of charge density and hydrophobic modification on dextran-based paper strength enhancing polymers. *Nordic Pulp and Paper Research Journal* **2000**, *15*, 440-445.
13. Lvov, Y.; Ariga, K.; Onda, M.; Ichinose, I.; Kunitake, T., Alternate Assembly of Ordered Multilayers of SiO<sub>2</sub> and Other Nanoparticles and Polyions. *Langmuir* **1997**, *13*, 6195-6203.
14. Lvov, Y.; Decher, G.; Sukhorukov, G., Assembly of thin films by means of successive deposition of alternate layers of DNA and poly(allylamine). *Macromolecules* **1993**, *26*, 5396-5399.
15. Picart, C.; Lavalle, P.; Hubert, P.; Cuisinier, F. J. G.; Decher, G.; Schaaf, P.; Voegel, J.-C., Buildup Mechanism for Poly(L-lysine)/Hyaluronic Acid Films onto a Solid Surface. *Langmuir* **2001**, *17*, 7414-7424.
16. Correa-Duarte, M. A.; Kosiorek, A.; Kandulski, W.; Giersig, M.; Liz-Marzan, L. M., Layer-by-Layer Assembly of Multiwall Carbon Nanotubes on Spherical Colloids. *Chem. Mater.* **2005**, *17*, 3268-3272.
17. Wong, J. E.; Gaharwar, A. K.; Müller-Schulte, D.; Bahadur, D.; Richtering, W., Dual-stimuli responsive PNiPAM microgel achieved via layer-by-layer assembly: Magnetic and thermoresponsive. *Journal of Colloid and Interface Science* **2008**, *324*, 47-54.

## References

---

18. Sukhorukov, G. B.; Donath, E.; Davis, S.; Lichtenfeld, H.; Caruso, F.; Popov, V. I.; Mohwald, H., Stepwise Polyelectrolyte Assembly on Particle Surfaces: a Novel Approach to Colloid Design. *Polym. Adv. Technol.* **1998**, *9*, 759-767.
19. Sukhorukov, G. B.; Donath, E.; Lichtenfeld, H.; Knippel, E.; Knippel, M.; Budde, A.; Mohwald, H., Layer-by-layer self assembly of polyelectrolytes on colloidal particles. *Colloids and Surfaces A: Physicochem. Eng. Aspects* **1998**, *137*, 253-266.
20. Izquierdo, A.; Ono, S. S.; Voegel, J.-C.; Schaaf, P.; Decher, G., Dipping versus Spraying: Exploring the Deposition Conditions for Speeding Up Layer-by-Layer Assembly. *Langmuir* **2005**, *21*, 7558-7567.
21. Ladhari, N.; Hemmerlé, J.; Ringwald, C.; Haikel, Y.; Voegel, J.-C.; Schaaf, P.; Ball, V., Stratified PEI-(PSS-PDADMAC)<sub>20</sub>-PSS-(PDADMAC-TiO<sub>2</sub>)<sub>n</sub> multilayer films produced by spray deposition *Colloids and Surfaces A: Physicochemical and Engineering Aspects* **2008**, *322*, 142-147.
22. Schlenoff, J. B.; Dubas, S. T.; Farhat, T., Sprayed Polyelectrolyte Multilayers. *Langmuir* **2000**, *16*, 9968-9969.
23. DeLongchamp, D.; Hammond, P. T., Layer-by-Layer Assembly of PEDOT/Polyaniline Electrochromic Devices. *Advanced Materials* **2001**, *13*, 1455-1459.
24. DeLongchamp, D. M.; Kastantin, M.; Hammond, P. T., High-Contrast Electrochromism from Layer-By-Layer Polymer Films. *Chem. Mater.* **2003**, *15*, 1575-1586.
25. Lee, D.; Rubner, M. F.; Cohen, R. E., All-Nanoparticle Thin-Film Coatings. *Nano Lett.* **2006**, *6*, 2305-2312.

## References

---

26. Picart, C.; Schneider, A.; Etienne, O.; Mutterer, J.; Schaaf, P.; Egles, C.; Jessel, N.; Voegel, J.-C., Controlled Degradability of Polysaccharide Multilayer Films In Vitro and In Vivo. *Adv. Funct. Mater.* **2005**, 15, 1771-1780.
27. Berg, M. C.; Zhai, L.; Cohen, R. E.; Rubner, M. F., Controlled Drug Release from Porous Polyelectrolyte Multilayers. *Biomacromolecules* **2006**, 7, 357-364.
28. Sun, Y.; Zhang, X.; Sun, C.; Wang, B.; Shen, J., Fabrication of ultrathin film containing bienzyme of glucose oxidase and glucoamylase based on electrostatic interaction and its potential application as a maltose sensor. *J. Macromol. Chem. Phys.* **1996**, 197, 147-153.
29. Laurent, D.; Schlenoff, J. B., Multilayer Assemblies of Redox Polyelectrolytes. *Langmuir* **1997**, 13, 1552-1557.
30. Cheng, J. H.; Fou, A. F.; Rubner, M. F., Molecular self-assembly of conducting polymers *Thin Solid Films* **1994**, 244, 985-989.
31. Laschewsky, A.; Mayer, B.; Wischerhoff, E.; Arys, X.; Bertrand, P.; Delcorte, A.; Jonas, A., A new route to thin polymeric, non-centrosymmetric coatings *Thin Solid Films* **1996**, 284, 334-337.
32. Elzbienciak, M.; Kolasinska, M.; Warszynski, P., Characteristics of polyelectrolyte multilayers: The effect of polyion charge on thickness and wetting properties. *Colloids and Surfaces A: Physicochem. Eng. Aspects* **2008**, 321, 258-261.
33. Dubas, S. T.; Schlenoff, J. B., Factors Controlling the Growth of Polyelectrolyte Multilayers. *Macromolecules* **1999**, 32, 8153-8160.
34. Notley, S. M.; Eriksson, M.; Wagberg, L., Visco-elastic and adhesive properties of adsorbed polyelectrolyte multilayers determined in situ with QCM-D and AFM measurements. *Journal of Colloid and Interface Science* **2005**, 292, 29-37.

## References

---

35. Kolasinska, M.; Krastev, R.; Warszynski, P., Characteristics of polyelectrolyte multilayers: Effect of PEI anchoring layer and posttreatment after deposition. *Journal of Colloid and Interface Science* **2007**, 305, 46-56.
36. Kolasinska, M.; Warszynski, P., The effect of nature of polyions and treatment after deposition on wetting characteristics of polyelectrolyte multilayers. *Applied Surface Science* **2005**, 252, 759-765.
37. Wong, J. E.; Zastrow, H.; Jaeger, W.; Klitzing, R. v., Specific Ion versus Electrostatic Effects on the Construction of Polyelectrolyte Multilayers. *Langmuir* **2009**, 25, 14061-14070.
38. Elzbiaciak, M.; Zapotoczny, S.; Nowak, P.; Krastev, R.; Nowakowska, M.; Warszynski, P., Influence of pH on the Structure of Multilayer Films Composed of Strong and Weak Polyelectrolytes. *Langmuir* **2009**, 25, 3255-3259.
39. Trybała, A.; Szyk-Warszynska, L.; Warszynski, P., The effect of anchoring PEI layer on the build-up of polyelectrolyte multilayer films at homogeneous and heterogeneous surfaces. *Colloids and Surfaces A: Physicochem. Eng. Aspects* **2009**, 343, 127-132.
40. Lowack, K.; Helm, C. A., Molecular Mechanisms Controlling the Self-Assembly Process of Polyelectrolyte Multilayers. *Macromolecules* **1998**, 31, 823-833.
41. Poptoshev, E.; Schoeler, B.; Caruso, F., Influence of Solvent Quality on the Growth of Polyelectrolyte Multilayers. *Langmuir* **2004**, 20, 829-834.
42. Mermut, O.; Barret, C. J., Effects of Charge Density and Counterions on the Assembly of Polyelectrolyte Multilayers. *Journal of Physical Chemistry B* **2003**, 107, 2525-2530.
43. Klitzing, R. v., Internal structure of polyelectrolyte multilayer assemblies. *Phys. Chem. Chem. Phys.* **2006**, 8, 5012-5033.

## References

---

44. Ladam, G.; Schaad, P.; Voegel, J. C.; Schaaf, P.; Decher, G.; Cuisinier, F., In Situ Determination of the Structural Properties of Initially Deposited Polyelectrolyte Multilayers. *Langmuir* **2000**, *16*, 1249-1255.
45. Bosio, V.; Dubreuil, F.; Bogdanovic, G.; Fery, A., Interactions between silica surfaces coated by polyelectrolyte multilayers in aqueous environment: comparison between precursor and multilayer regime. *Colloids and Surfaces A: Physicochem. Eng. Aspects* **2004**, *243*, 147-155.
46. Wang, H.; Wang, Y.; Yan, H.; Zhang, J.; Thomas, R. K., Binding of Sodium Dodecyl Sulfate with Linear and Branched Polyethyleneimines in Aqueous Solution at Different pH Values. *Langmuir* **2006**, *22*, 1526-1533.
47. Claesson, P. M.; Poptoshev, E.; Blomberg, E.; Dedinaite, A., Polyelectrolyte-mediated surface interactions. *Advances in Colloid and Interface Science* **2005**, *114*, 173-187.
48. Cappella, B.; Dietler, G., Force-distance curves by atomic force microscopy. *Surface Science Reports* **1999**, *34*, 1-104.
49. Kappl, M.; Butt, H.-J., The Colloidal Probe Technique and its Application to Adhesion Force Measurements. *Part. Part. Syst. Charact.* **2002**, *19*, 129-143.
50. Drelich, J.; Tormoen, G. W.; Beach, E. R., Determination of solid surface tension from particle-substrate pull-off forces measured with the atomic force microscope. *Journal of Colloid and Interface Science* **2004**, *280*, 484-497.
51. Butt, H.-J.; Cappella, B.; Kappl, M., Force measurements with the atomic force microscope: Technique, interpretation and applications *Surface Science Reports* **2005**, *59*, 1-152.
52. Johansson, E.; Blomberg, E.; Lingstrom, R.; Wagberg, L., Adhesive Interaction between Polyelectrolyte Multilayers of Polyallylamine Hydrochloride and Polyacrylic Acid Studied Using Atomic Force Microscopy and Surface Force Apparatus. *Langmuir* **2009**, *25*, 2887-2894.

## References

---

53. Gong, H.; Garcia-Turiel, J.; Vasilev, K.; Vinogradova, O. I., Interaction and Adhesion Properties of Polyelectrolyte Multilayers. *Langmuir* **2005**, 21, 7545-7550.
54. Creton, C.; Kramer, E. J.; Hui, C. Y.; Brown, H. R., Failure mechanisms of polymer interfaces reinforced with block copolymers. *Macromolecules* **1992**, 25, 3075-3088.
55. Lingströma, R.; Wågberg, L.; Larsson, P. T., Formation of polyelectrolyte multilayers on fibres: Influence on wettability and fibre/fibre interaction *Journal of Colloid and Interface Science* **2006**, 296, 396-408.
56. Delcorte, A.; Bertrand, P., Adsorption of Polyelectrolyte Multilayers on Polymer Surfaces. *Langmuir* **1997**, 13, 5125-5136.
57. Chen, W.; McCarthy, T. J., Layer-by-Layer Deposition: A Tool for Polymer Surface Modification. *Macromolecules* **1997**, 30, 78-86.
58. Thio, B. J. R.; Meredith, J. C., Quantification of E. coli adhesion to polyamides and polystyrene with atomic force microscopy. *Colloids and Surfaces B: Biointerfaces* **2008**, 65, 308-312.
59. Podczecka, F.; Newton, J. M.; James, M. B., Influence of Relative Humidity of Storage Air on the Adhesion and Autoadhesion of Micronized Particles to Particulate and Compacted Powder Surfaces. *journal of colloid and interface science* **1997**, 187, 484-491.
60. Pericet-Camara, R.; Papastavrou, G.; Behrens, S. H.; Helm, C. A.; Borkovec, M., Interaction forces and molecular adhesion between pre-adsorbed poly(ethylene imine) layers. *Journal of Colloid and Interface Science* **2006**, 296, 496-506.
61. Carrière, D.; Krastev, R.; Schönhoff, M., Oscillations in Solvent Fraction of Polyelectrolyte Multilayers Driven by the Charge of the Terminating Layer. *Langmuir* **2004**, 20, 11465-11472.

## References

---

62. McAloney, R. A.; Sinyor, M.; Dudnik, V.; Goh, M. C., Atomic Force Microscopy Studies of Salt Effects on Polyelectrolyte Multilayer Film Morphology. *Langmuir* **2001**, *17*, 6655-6663.
63. Burtovyy, O.; Klep, V.; Turel, T.; Gowayed, Y.; Luzinov, I., Polymeric Membranes: Surface Modification by "Grafting to" Method and Fabrication of Multilayered Assemblies. In *2009*; Vol. 1016, pp 289-305.
64. Matsukuma, D.; Aoyagi, T.; Serizawa, T., Adhesion of Two Physically Contacting Planar Substrates Coated with Layer-by-Layer Assembled Films. *Langmuir* **2009**, *25*, 9824-9830.
65. Thio, B. J. R.; Meredith, J. C., Measurement of polyamide and polystyrene adhesion with coated-tip atomic force microscopy. *Journal of Colloid and Interface Science* **2007**, *314*, 52-62.
66. Chen, Y.-L.; Israelachvili, J. N., Effects of Ambient Conditions on Adsorbed Surfactant and Polymer Monolayers. *J. Phys. Chem.* **1992**, *96*, 1152-1160.
67. Chen, L.; Gu, X.; Fasolka, M. J.; Martin, J. W.; Nguyen, T., Effects of Humidity and Sample Surface Free Energy on AFM Probe#Sample Interactions and Lateral Force Microscopy Image Contrast. *Langmuir* **2009**, *25*, 3494-3503.
68. Nguyen, T.; Gu, X.; Chen, L. J.; Fasolka, M.; Briggman, K.; Hwang, J.; Martin, J. In *Mater. Res. Soc. Symp.*, 2005; 2005.
69. Noy, A.; Vezenov, D. V.; Lieber, C. M., Chemical Force Microscopy. *Annu. Rev. Mater. Sci.* **1997**, *27*, 381-421.
70. Adamczyk, Z.; Zembala, M.; Warszynski, P.; Jachimaska, B., Characterization of Polyelectrolyte Multilayers by the Streaming Potential Method. *Langmuir* **2004**, *20*, 10517-10525.

## References

---

71. Shiratori, S. S.; Rubner, M. F., pH-Dependent Thickness Behavior of Sequentially Adsorbed Layers of Weak Polyelectrolytes. *Macromolecules* **2000**, 33, 4213-4219.
72. Thomas, R. C.; Houston, J. E.; Crooks, R. M.; Kim, T.; Michalske, T. A., Probing Adhesion Forces at the Molecular Scale. *J. Am. Chem. Soc.* **1995**, 117, 3830-3834.
73. Singh, N.; Husson, S. M.; Zdyrko, B.; Luzinov, I., Surface modification of microporous PVDF membranes by ATRP *Journal of Membrane Science* **2005**, 262, 81-90.
74. Iyer, K. S.; Zdyrko, B.; Malz, H.; Pionteck, J.; Luzinov, I., Polystyrene Layers Grafted to Macromolecular Anchoring Layer. *Macromolecules* **2003**, 36, 6519-6526.
75. Ionov, L.; Zdyrko, B.; Sidorenko, A.; Minko, S.; Klep, V.; Luzinov, I.; Stamm, M., Gradient Polymer Layers by “Grafting To” Approach. *Macromol. Rapid Commun.* **2004**, 25, 360-365.
76. Brittain, W. J.; Minko, S., A Structural Definition of Polymer Brushes. *Journal of Polymer Science: Part A: Polymer Chemistry* **2007**, 45, 3505-3512.
77. Burtovyy, O.; Klep, V.; Chen, H.-C.; Hu, R.-K.; Lin, C.-C.; Luzinov, I., Hydrophobic Modification of Polymer Surfaces via “Grafting to” Approach *J. Macromol. Sci. Part B: Physics* **2007**, 46, 137-154.
78. Salomäki, M.; Vinokurov, I. A.; Kankare, J., Effect of Temperature on the Buildup of Polyelectrolyte Multilayers. *Langmuir* **2005**, 21, 11232–11240.
79. Guzman, E.; Ritacco, H.; Rubio, J. E. F.; Rubio, R. G.; Ortega, F., Salt-induced changes in the growth of polyelectrolyte layers of poly(diallyldimethylammonium chloride) and poly(4-styrene sulfonate of sodium). *Soft Matter* **2009**, 5, 2130-2142.
80. Voigt, U.; Jaeger, W.; Findenegg, G. H.; Klitzing, R. v., Charge Effects on the Formation of Multilayers Containing Strong Polyelectrolytes. *J. Phys. Chem. B* **2003**, 107, 5273-5280.

## References

---

81. Guo, Q., Miscible blends containing a crystallizable component: poly(vinyl alcohol)/poly(ethyleneimine). *macromolecular rapid communications* **1995**, 16, 785-791.
82. Weisenhorn, A. I.; Hansma, P. K.; Albrecht, T. R.; Quate, C. F., Forces in atomic force microscopy in air and water. *Appl. Phys. Lett.* **1989**, 26, 2651-2653.
83. Eastman, T.; Zhu, D.-M., Adhesion Forces between Surface-Modified AFM Tips and a Mica Surface. *Langmuir* **1996**, 12, 2859-2862.
84. Sedin, D. L.; Rowlen, K. L., Adhesion Forces Measured by Atomic Force Microscopy in Humid Air. *Anal. Chem.* **2000**, 72, 2183-2189.
85. Fuji, M.; Machida, K.; Takei, T.; Watanabe, T.; Chikazawa, M., Effect of Wettability on Adhesion Force between Silica Particles Evaluated by Atomic Force Microscopy Measurement as a Function of Relative Humidity. *Langmuir* **1999**, 15, 4584-4589.
86. Hu, J.; Xiao, X.-D.; Ogletree, D. F.; Salmeron, M., Imaging the Condensation and Evaporation of Molecularly Thin Films of Water with Nanometer Resolution *Science* **1995**, 268, 267-269.
87. Thundat, T.; Zheng, X.-Y.; Chen, G. Y.; Sharp, S. L.; Warmack, R. J.; Schowalter, L. J., Characterization of atomic force microscope tips by adhesion force measurements. *Appl. Phys. Lett.* **1993**, 63, 2150-2152.

## Appendices

### Appendix A: Support File for Chapter I

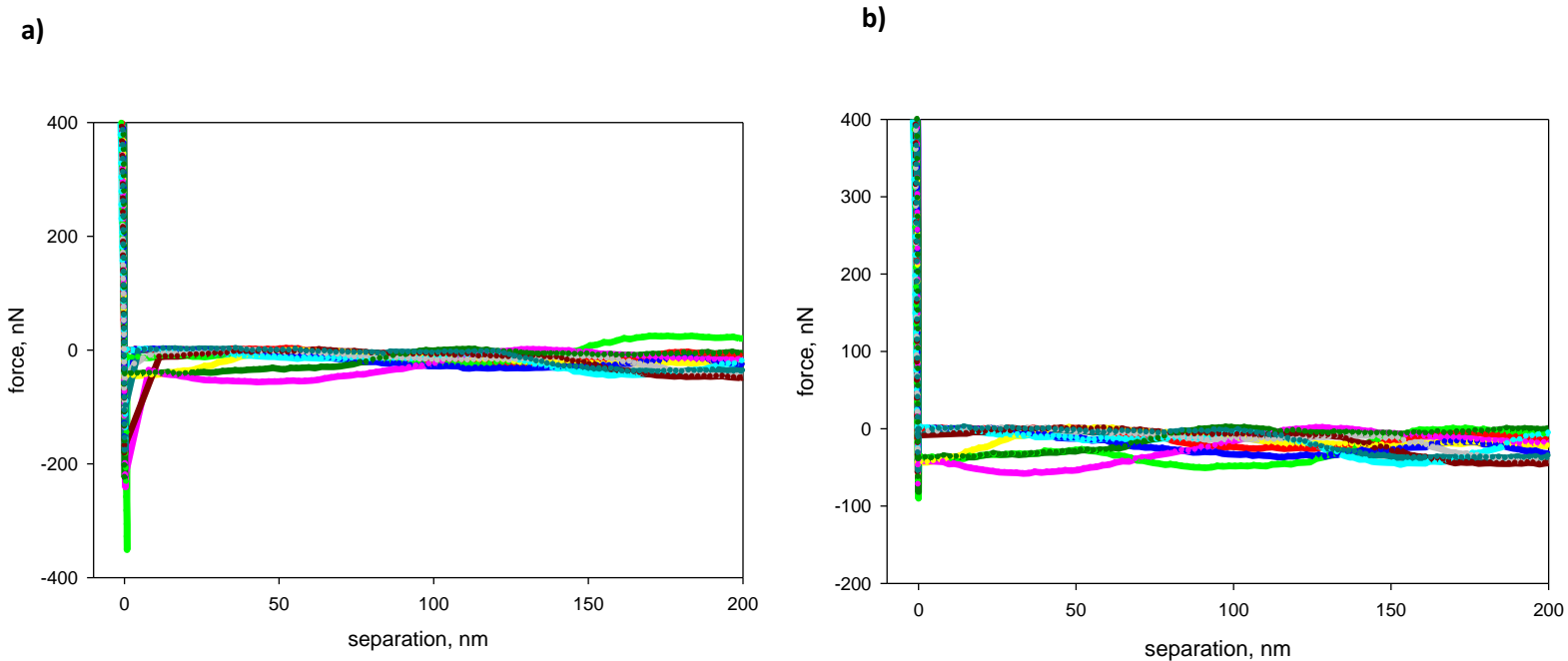


**Figure 9.1** Typical force-separation curves for PEI(PSS<sub>5</sub>PAH<sub>5</sub>) prepared at 0.5 M NaBr ionic strength a) retraction curves, b) approach curves.

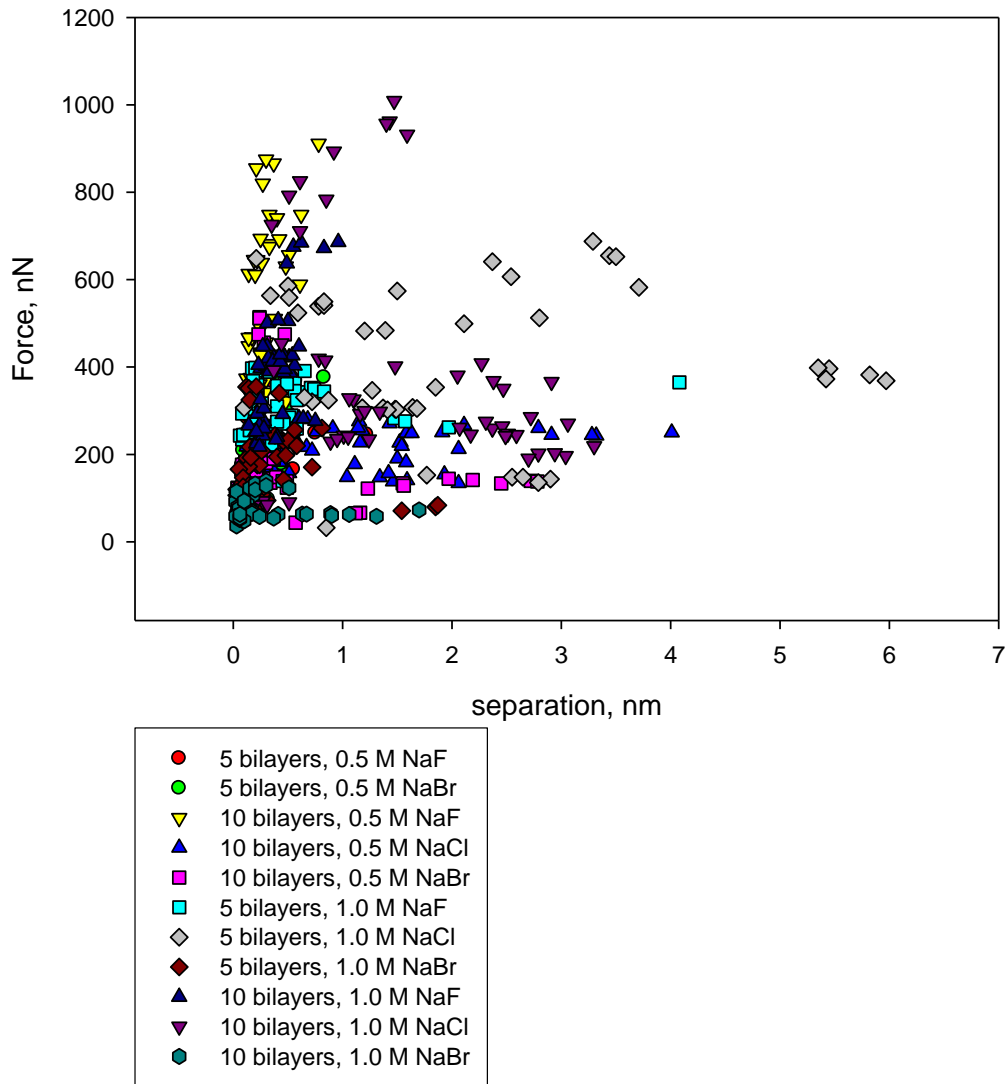


**Figure 9.2** Force versus separation data for all the samples.

**Appendix B: Support File for Chapter II**

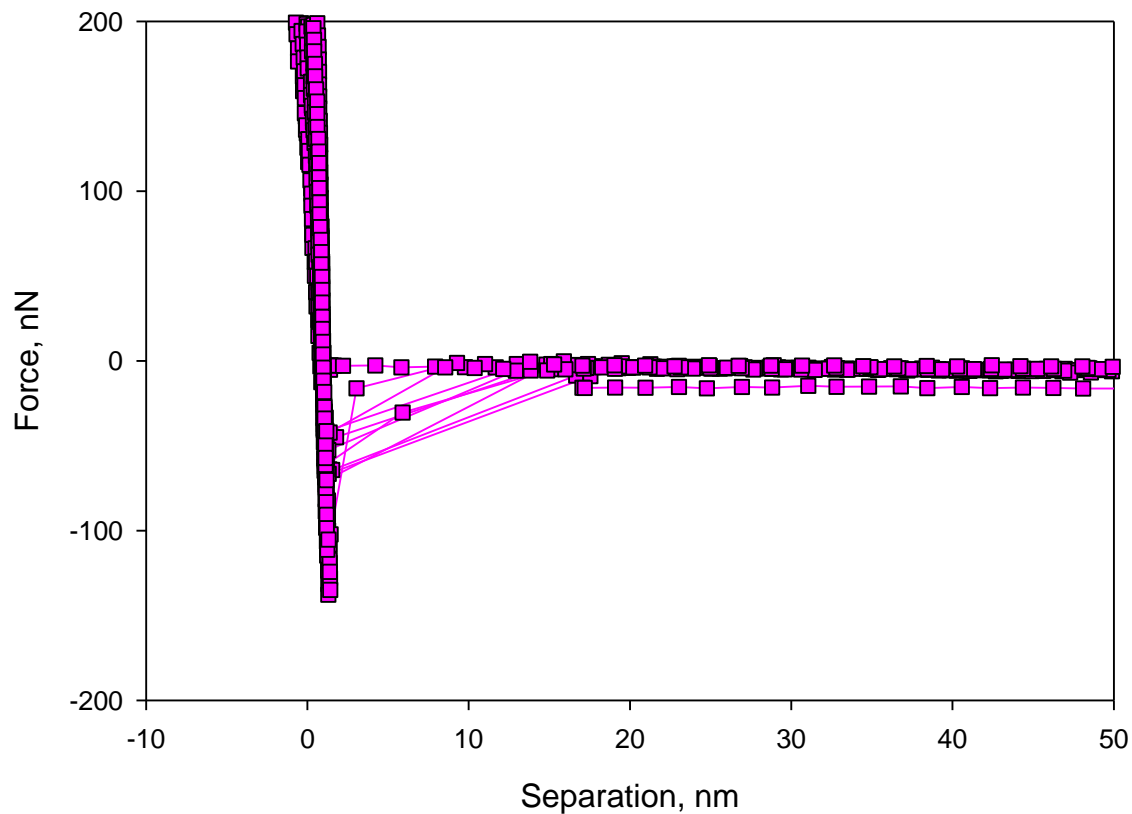


**Figure 9.3** Force-separation curves for PEI(PAA<sub>5</sub>PAH<sub>5</sub>) prepared at 0.5 M NaCl. The measurements were collected at 45% RH with a colloidal silica probe functionalized with COOH surface chemistry. This figure is zoomed-in version of Figure 4.3. Ten force curves, five being from the same spot, were represented upon retraction.

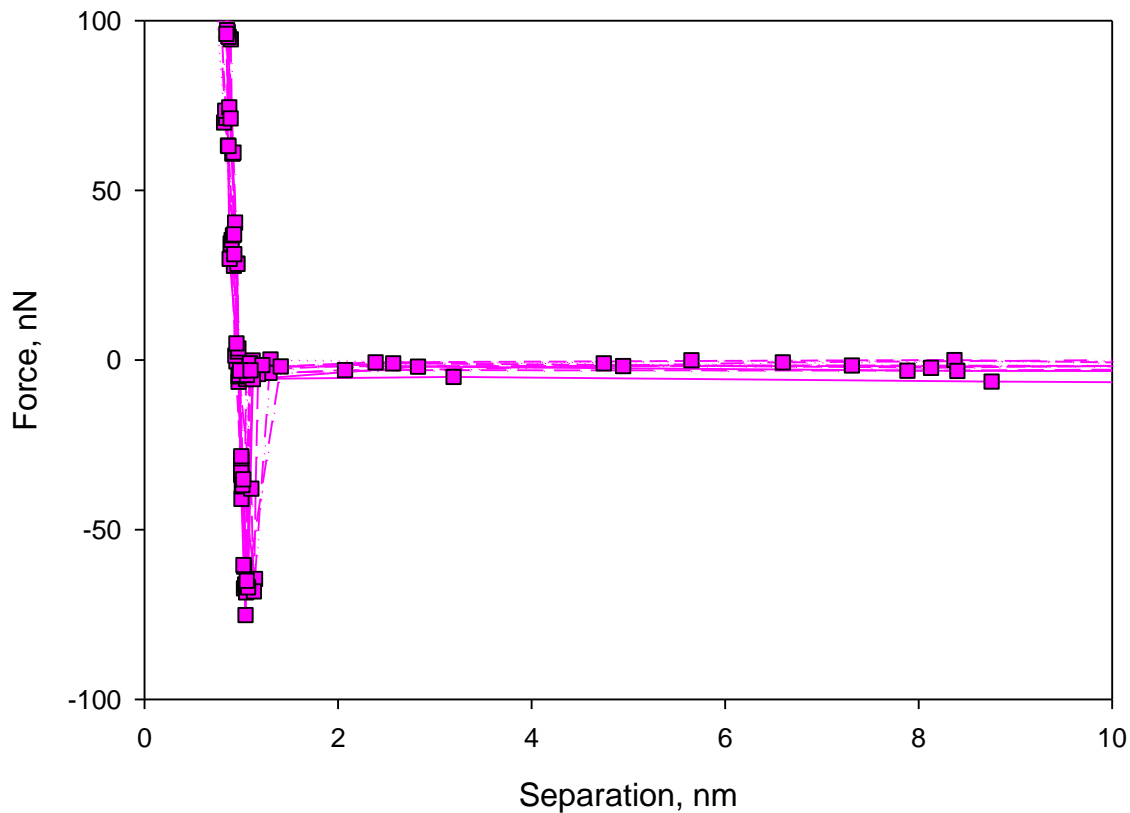


**Figure 9.4** Force-separation curves for PEI(PSS<sub>6</sub>PAH<sub>6</sub>) prepared at 0.5 M NaCl. The measurements were collected at 45% RH with a colloidal silica probe functionalized with COOH surface chemistry. This figure is zoomed-in version of Figure 4.8. Ten force curves, five being from the same spot, were represented upon retraction.